Barbara Rupp

Photochemical Crosslinking for Tailoring Properties of Polymers

PhD Thesis

Dissertation

Zur Erlangung des akademischen Grades eines Doktors der
Naturwissenschaften eingereicht an der
Technischen Universität Graz

Betreuer: Univ.-Doz. Dipl. Ing. Dr. techn. Christian Slugovc
Institut für chemische Technologie von Materialien (ICTM)

Graz, im Februar 2010

STATUTORY DECLARATION

I declare that I have authored this thesis independently, that I have not used other than the declared sources / resources, and that I have explicitly marked all material which has been quoted either literally or by content from the used sources.

…………………………   …………………………………………..

date   (signature)

Dedicated to my parents

Acknowledgement

Abstract

The presented work focus on the photochemical cross-linking of polymers. The goals of the particular projects of this study and the different polymers used, request various photochemical reactions. Polyethylene oxide e.g. is cross-linked via the hydrogen abstraction mediated by a photoinitiator and the recombination of the consequently formed macromolecular radicals, while in other tasks the cross-linking step is done by a cross-linking agent.

The networks formed suite various purposes: in one case the crystallisation of the polymer is avoided due to the network and in other cases the crosslinked polymers are used as photoresist or simply as materials with enhanced mechanical properties.

The methods introduced show a high potential for different applications, which range from battery technology and nano technology to modifications of biodegradable polymers.

Kurzfassung

Die vorliegende Arbeit konzentriert sich auf das photochemische Vernetzen von Polymeren. Die Zielsetzungen in den jeweiligen Schwerpunkten und die verwendeten Polymere erfordern den Einsatz verschiedener Photoreaktionen. So werden zum einen Polyethylenoxidketten via Photoinitiator-induzeierte Protonenabstraktion und der anschließenden Rekombination der entstandenen Radikale vernetzt, während in anderen Projekten mit verschiedenen photochemisch aktiven Vernetzungsreagenzien gearbeitet wird. Die daraus resultierenden makromolekularen Netzwerke dienen unterschiedlichen Zielsetzungen: Wird so in einem Fall das Auskristallisieren des Polymers verhindert, wird in anderen Fällen das Polymer als Photolack verwendet oder die mechanische Stabilität erhöht.

Die hier vorgestellten Methoden zeigen ein vielfältiges Anwendungspotential. Vom Einsatz in der Batterietechnologie über Nanotechnologie bis hin zur Modifizierung von biologisch abbaubaren Polymeren zeigt das Vernetzen der Polymere viel versprechende Ergebnisse.

INDEX

1. General introduction

The history of radiation curing technology begins in 1946 with a patent for a UV-cured ink based on unsaturated polyesters in styrene. In the 1950s theoretical discussions were published and in the early 1960s the first commercial applications of this technology in coatings appeared.[1] With further development of the radiation sources and new photoactive substances the market expanded fast. Especially the applicability of acrylates for a large number of coatings or the like forced the growth of this branch of industry. Nowadays the spectrum of applications is broad and ranges from photoinduced polymerisations via photografting to laser ablation. Another example is an application in the imaging area in the printing industry and microelectronics: relief images for microcircuits[2] in electronics, printing plates or UV-curable inks[3] are state of the art today.

The advances over other usual (e.g. thermal) treatments are rapid through-cure, low energy requirements, room-temperature treatments, non-polluting and solvent free formulations and low costs.[4,5]

The focus of this work presented is on photochemical crosslinking of various polymers. The used photochemical reactions as well as the targets and applications are versatile: the cross-linking via hydrogen abstraction is used for lowering the crystallinity of polyethylene oxide and enhancing the mechanical stability. In other projects the thiol-ene reaction is the tool for cross-linking polynorbornenes or polyoxazolines for enhancing the mechanical and the chemical stability. The network building step for polyhydroxy alkanoates is done via a cross-linking agent as well as in the examples before for mechanical stabilisation.

Partial the systems can be used as negative resists for surface modifications and imprinting or for conservation of special shapes of self assembled structures, as can be seen in chapter 5.

UV curing is a well established technology with a high potential for new developments. Herein known photo-reactions for new applications are introduced.

---

[1] J.P. Fouassier, J.F. Rabek, *Radiation curing in Polymer science and technology Volume 1 fundamentals and methods*, Elsevier science publisher ltd, **1993.**

[2] Feit, E. D., C Wilkins Jr., *Polymer Materials for Electronic Applications*, American Chemical Society, Washington, DC, USA, **1982.**

[3] Jäckel, K.P., *Prog Org. Coatings*, **1988** *16*, 355-370.

[4] Pappas, S. P., *UV-Curing : Science and Technology*, Technology Marketing Corp., Stamford, CT, USA, **1978** and **1985.**

[5] Roffey, C. G., *Photopolymerization of Surface Coatings*, J. Wiley, New York, USA **1982.**

2. Theory

2.1. Photochemistry in polymer sciences

2.1.1. Basic principles of Photochemistry[6,7]

Light is a part of the electromagnetic radiation which is referred to several classes: UV (200 – 400 nm), the visible (400 – 700) and the near IR (700 – 1000 nm). A particular radiation is defined by its energy and hence characterized by frequency,

$$E = h\nu$$

With E is energy, h is the planck's constant and ν is the frequency.

A molecule in its ground state (S_0) can absorb a quantum of radiation which leads to an energetically exited state (S_1). Based on this state there are a few fundamental processes occurring consequently. These conversions are usually presented by the Perrin – Jablonski diagram[1]:

Fluorescence: $S_1 \longrightarrow S_0 + h\nu$

Internal conversion: $S_1 \longrightarrow S_0 + kT$

Intersystem crossing: $S_1 \longrightarrow T_1$

From the triplet state T_1 the following processes occur in the majority of cases:

Phosphorescence: $T_1 \longrightarrow S_0 + h\nu$

Intersystem crossing: $T_1 \qquad S_0 + kT$
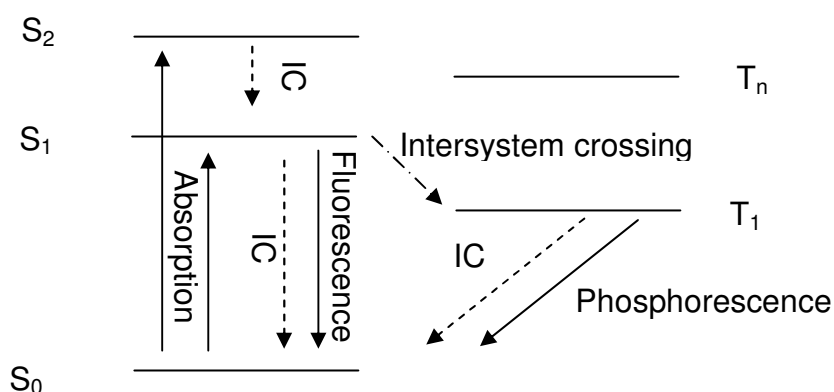
Fig 2-1:Perrin-Jablonski diagramm

[6] Turro, N. J., *Modern Molecular Photochemistry*. Benjamins, New York, USA, **1978**.
[7] Wayne, R. P., *Principles and Applications of Photochemistry*, Oxford Science and Publications, Oxford, UK, **1982**.

Many photochemical reactions originating from the triplet state generate radicals. These reactions are used within photoinitiators as shown in the following section.

2.1.2. Photoinitiators[1]

In principle a polymer photoreaction consists of a chain reaction resulting from the irradiation of an initiator generating a radical or cationic species.

$$M \xrightarrow{h\nu} M\bullet \quad\quad \text{or} \quad\quad M \xrightarrow{h\nu} M^+$$

In general the direct formation of a reactive species on the monomer (respectively oligomer or polymer) by light absorption is not efficient and the presence of an initiator is necessary.

$$I \xrightarrow{h\nu} {}^1I^* \longrightarrow {}^3I^* \longrightarrow R\bullet \xrightarrow{M} RM\bullet$$
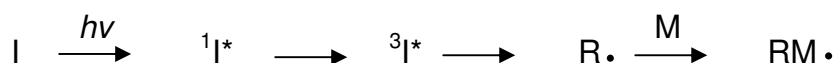
Various reaction pathways of the initiators are known:

Norrish typ I photoscission:
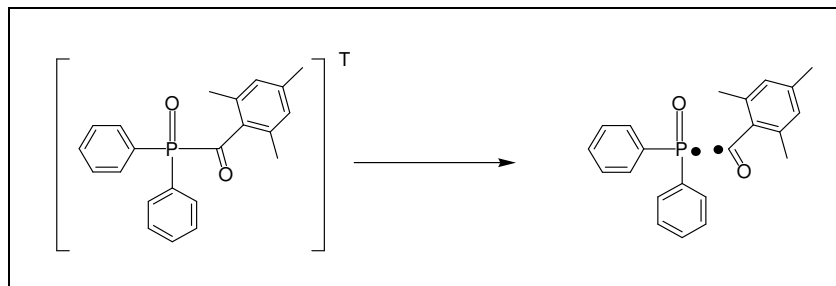
Fig 2-2: Scheme of the Norrish typ I photoscission

Hydrogen abstraction from nπ* state:
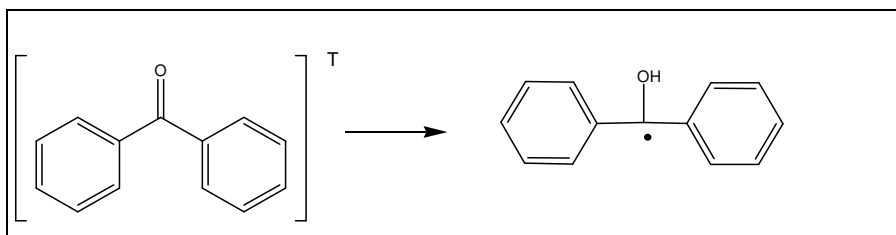
Fig 2-3: Scheme of the hydrogen abstraction from nπ* state

Further frequent reactions are electron transfer reactions leading to a charge transfer complex.

2.1.3. Photocrosslinking processes

In general photocrosslinking[8,9] processes are the crosslinking of macromolecular chains through a photochemical mechanism.
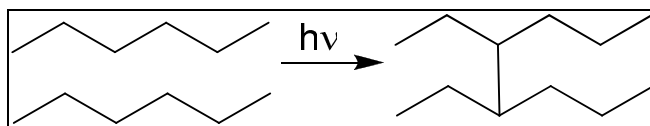
Fig 2-4 scheme of the crosslinking of macromolecular chains.

One way of photochemical crosslinking works as follows[10]: the photoinitiator generates after UV-light exitation radicals and subsequently radical reactions in the polymer matrix (e.g. hydrogen abstraction). This leads to crosslinks between to macromolecular chains. In precense of oxygen, hydroperoxides are easily generated. In this case the photoinitiator acts as donor and transfers the energy absorbed to the peroxides. The latter undergo radical homolytic cleavage and the formed alkoxy macroradicals lead to ether type crosslinks.

2.1.3.1. Photocycloadditions

This type of reaction is a well known system. The most prominent examples are polyvinyl-cinnamate derivatives, chalcone type compounds, bis-maleimides and cyclised polyisoprenes.[11,12,13] In these reactions e.g. a cyclobutane ring is formed by the dimerisation double bonds due to UV curing.
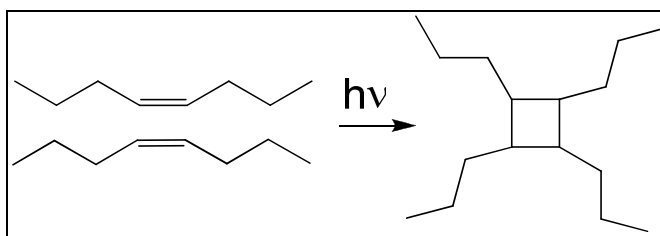
Fig 2-5: Scheme of a cycloaddition of doublebonds to form a cyclobutane

---

[8] Green G. E., Stark B.P., Zahir S. A., *J. Macromol.Sci.* (Rev. Macromol. Chem.) **1981-82** *C21* (2) 187.
[9] Meier K., Zweifel, H.J., *J. Photochem.*, **1986** *35*, 353-366.
[10] J. A. Bousquet, J. P. Fouassier, *Polym. Degrad. Stabil.*, **1983** *5*, 113-133.
[11] Reiser, A., *J. Chem. Phys.*, **1980** *77*, 469-482.
[12] Finter, J., Lohse F., Zweifel H., *J. Photochem.*, **1985** *28*, 175-185.
[13] Hasagawa, M., *Comprehensive Polymer Science*. Pergamon Press, **1989**

The reactions are usually sensitised to extend the sensitivity of the system.

2.1.3.2. Thiol-ene reaction

Polymers with reactive double bonds can react with multifunction thiols and form networks. These systems work by a free radical addition of thiols to the available double bonds.[14] The crosslinking reaction can occur directly with a suitable wavelength or in the presence of photoinitiators.[15]
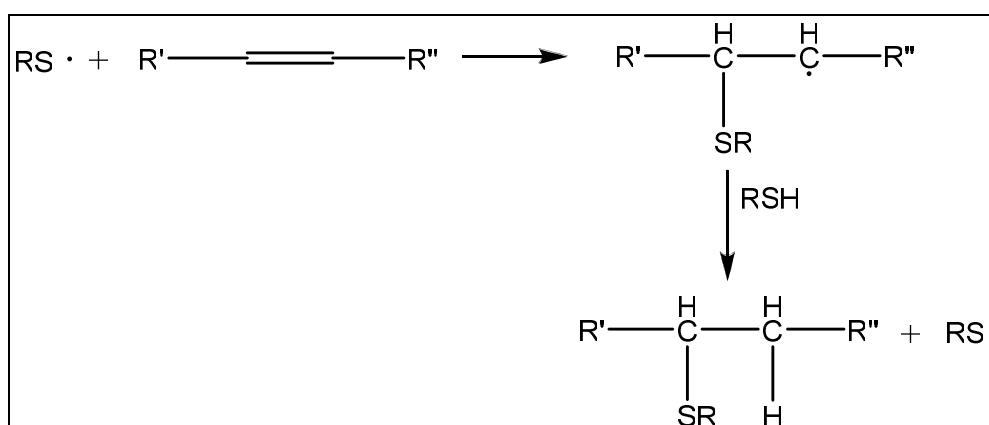
Fig 2-6: Scheme of the thiol-ene reaction pathway

In contrast to most other radiation-induced reactions the thiol-ene addition is not inhibited by oxygen, as the peroxy radicals are also capable of substracting hydrogen from a thiol.[16]

A further advantage is the tolerance of this reaction versus numerous functional groups (except double bonds). This offers the possibility to use the thiol-ene reaction for "click"-chemistry and thus lead to the creation of functional polymers via a facile and efficient route.[17,18]

[14] Hoyle C.E., Lee T. Y, Roper T., *J. Polym. Sci. Part A*, **2004** *42* (21), 5301 – 5559.

[15] Cramer N. B.; Davies T.; O'Brein A. K.; Bowman C. N., *Macromolecules* **2003**, *35*, 5361-5365.

[16] J.P. Fouassier, J.F. Rabek, *Radiation curing in Polymer science and technology Volume 4 fundamentals and methods*, Elsevier science publisher ltd **1993**.

[17] David, R. L. A., Kornfield J. A., *Macromolecules* **2008**, 41, 1151 - 1161.

[18] Gress, A., Volkel A., Schlaad H., *Macromolecules* **2007**, *40*, 7928 – 7933.

2.2. Battery technology

The field of Lithium-battery technology is expanding for many years now and is still growing. The applications are versatile and so are the requests on the performances of the differing battery-systems. Batteries using Lithium as negative electrode material attract attention because of their high specific energy and the strong negative potential of the lithium-electrode. These properties yield this technology to their potential application in small electronic devices, electric vehicles and many more applications.[19,20]

2.2.1. Solid Electrolytes for Lithium-batteries

Rechargeable lithium polymer batteries (LPBs) using polymer electrolytes in solid state offer many advantages compared with liquid electrolytes, such as easy handling during fabrication processes and better safety properties. But the main drawback of these electrolytes (at the moment) is the low ionic conductivity at room temperature. This handicap is limiting the performance of polymer batteries.[21]

In recent years many polymers have been tested as well as other improvements such as small molecular solvents as additives (for example propylene carbonate), various kinds of conducting salts and inorganic fillers like SiO_2.[22]

Ionic liquids are room temperature molten salts. In general, they are consisting of an organic cation and an inorganic anion.[23] They have attracted the attention of chemists because of their properties such as being non- volatile, non-flammable and conductive. Therefore the interest has also increased in the possible use of this type of liquid in energy storage devices.[24,25]

---

[19] W.A. van Schalkwijk, B. Scrosati, *Advanced in Lithium-Ion Batteries*, Kluwer Academic/Plenum Publisher, **2002**.

[20] G-A Nazri, G. Pistoia, *Lithium Batteries*, Kluwer Academic/Plenum Publisher, **2004**.

[21] B. Scorsati, *Applications of Electroactive Polymers*, Chapman & Hall, **1993**.

[22] Stephan, A. M., *European Polymer Journal* **2006**, *42*(1) 21-42.

[23] R.D.Rogers, K.R. Seddon , Eds., *Ionic Liquids- Industrial Application to Green Chemistry*; ACS Symposium Series 818; Oxford University Press **2002**.

[24] Adam, D. *Nature* **2000**, *407*, 938.

[25] M.J. Earle, K.F. Seddon, *Pure Appl. Chem.* **2000**, *72*, 1391,.

A composite of polymers and ionic liquids to form a solid electrolyte could combine the advantages of both of these materials and lead to a save battery with good performance, using green chemistry, as discussed in chapter 2.2.2.

2.2.2. Polyethylene oxide based electrolytes in combination with ionic liquids

In the field of polymer-electrolytes, polyethylene oxide (PEO) is the most intensively studied system[26,27,28]

For high molecular weight samples (M_w ~ $4*10^6$) the glass transition temperature (T_g) has been determined as between -65 and -60°C and the melting point (T_m) as 65°C. These values are changing with a decrease of the molecular weight, up to a T_g = -17°C and T_m ~ 66°C for a molecular weight of 6000. This maximum can be explained in terms of the percentage of crystalline material present in PEO, which is highest at a molecular weight of about 6000.[29]

Dry PEO-based electrolytes without any further solvent or additive show very low ionic conductivity in the range of 10^{-8} to 10^{-4} Scm^{-1} at temperatures between 40 and 100°C. The transport of the ions is controlled by the motion of the polymer chains as shown in Fig 2-7. Crystalline regions of the PEO do not contribute to the conductivity and ion transport only occurs in the amorphous regions of the polymer. For this reason the crystallization of the PEO reduce the mobility of the chains and in succession the ionic conductivity.

[26] Song, J. Y., Wang Y. Y., *Journal of Power Sources* **1999**, *77*(2) 183-197.
[27] Appetecchi, G. B., J. H. Shin, *Journal of Power Sources* **2005***, 143*(1-2): 236-242.
[28] Shin, J. H., W. A. Henderson, *Journal of the Electrochemical Society* **2005**, *152*(5): A978-A983.
[29] Fiona M. Gray, *Solid Polymer Electrolytes*, VCH Publishers, **1991**.
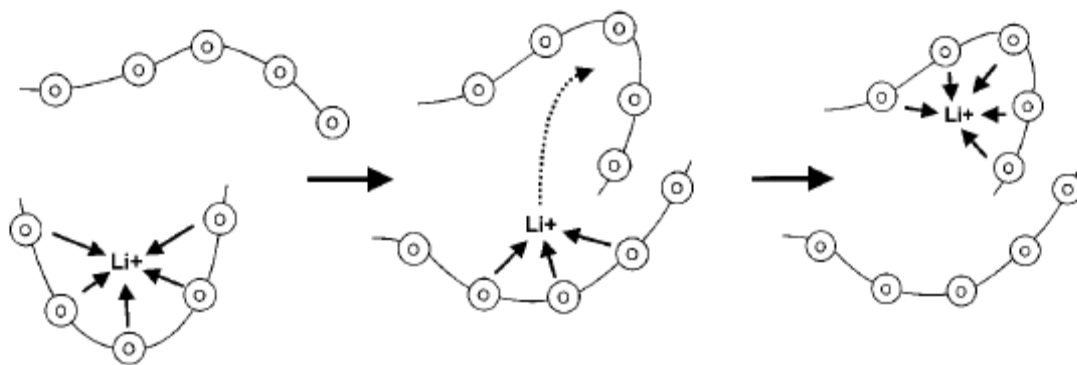
Fig 2-7: Ion motion in polymer host[30]

As reported by Shin *et al.*[31] the addition of room temperature molten salts can enhance the ionic conductivity to 10^{-3} Scm^{-1} at 40°C and forms in the appropriate mole ratio a freestanding polymer electrolyte film. The ionic liquid used is called *N*-methyl-*N*-butylpyrrolidiniumbis(trifluoromethan-sulfonyl)imide ($PYR_{14}TFSI$) because of its large electrochemical stability window in the used potential range and also because of the good conductivity. The phase behavior $PYR_{14}TFSI$ combined with a conducting salt is known.[32] It is not toxic and like other ionic liquids it is non-volatile and non-flammable.

The critical composition of the electrolyte (as well containing the conducting salt Li-TFSI) is 10 mol monomeric units PEO + 1 mol conducting salt + 1 mol ($PYR_{14}TFSI$). From this base on the research for the improvement of this separator in chapter 3 was started.

[30] Meyer, W. H., *Advanced Materials* **1998**, *10*(6), 439.
[31] Shin, J. H., W. A. Henderson, *Journal of the Electrochemical Society* **2005***, 152*(5), A978-A983.
[32] Henderson W.A., Passerini S., *Chemistry of Materials* **2004.**, *16,* 2881-2885.

2.3.   Ring opening metathesis polymerisation (ROMP)

Olefin metathesis is a popular and useful reaction with many facets.[33] In general the reaction pathway works via the coordination of the metal-carbene bond to an available double bond of an olefin, resulting in a [2+2]-cycloaddition and consequently a metalcyclobutane-complex as intermediate product. With the following retro-[2+2]-reaction, the only irreversible step in this mechanism, the desired metathesis product is obtained. This, so called dissociative mechanism was first reported by Chauvin and co-workers in 1971.[34,3536]
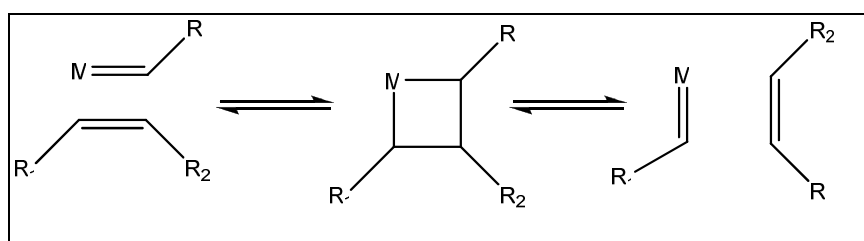
Fig 2-8: Mechanism of olefin metathesis

Common known examples for olefin metathesis are cross metathesis (CM), ring closing metathesis (RCM), ring opening cross metathesis (ROCM), ring rearrangement metathesis (RRM), ene-yne metathesis, ring-expansion metathesis, ring-closing alkyne metathesis (RCAM) and acyclic diene metathesis polymerisation.[37,38,39,40,41]

In the following, this chapter will focus on ring opening metathesis polymerisation (ROMP). This reaction cuts in tree parts: initiation, propagation and termination as shown in Fig 2-9.

The diversity of monomers applicable for ROMP and the broad variety of initiators developed, brought this method to an outstanding and important polymerisation tool. The reaction and the target macromolecule can be influenced by

[33] Slugovc, C., *Macromol. Rapid Commun* **2004**, *25*, 1283-1297.
[34] Herisson, J.-K, Chauvin, Y., *Macromol. Chem*. **1971**, *141*, 161.
[35] Dias E. L., Nguyen S. T., Grubbs R. H., J*. Am. Chem. Soc.* **1997**, *119*, 3887.
[36] Sanford, M. S., Love J.A., Grubbs R.H., *J. Am. Chem. Soc* **2001**, *123*, 6543-6554.
[37] T. M. Trnka, R. H. Grubbs, *Acc. Chem. Res*. **2001**, *34*, 18.
[38] M. R. Buchmeiser, *Chem. Rev*. **2000**,*100*, 1565-1604.
[39] A. Fürstner, *Angew. Chem. Int. Ed*. **2000**, *39*, 3012-3043.
[40] M. E. Maier, *Angew. Chem. Int. Ed*. **2000**, *39*, 2073-2077.
[41] R. R. Schrock, *Tetrahedron* **1999**, *55*, 8141-8153.

the poll of the monomer and the initiator, as well by the chosen solvent, additives and reaction conditions.[33]

Initiation:
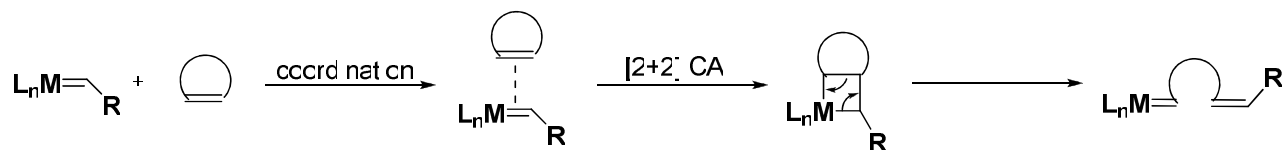
Propagation:

Termination:

Fig 2-9: Mechanism of ROMP[42]

The most prominent monomers used in ROMP are cyclobutene, cyclopentene, cyclooctene, norborenes and dicyclopentadien. The release of ring strain provides the main driving force that is required to overcome the unfavourable entropy change in polymerisation. [43] That is why the norbornene with a quite high ring strain undergoes the polymerisation reaction more readily than e.g. a cyclohexene.

In case of the initiators, the invention of transition metal catalysts opens up new ways of polymerisations. The used initiator in this work is a ruthenium based catalyst with coincident high functional group tolerance and high reactivity.[44]

Living polymerisation in combination with the conveniences of the ruthenium based catalyst and a reactive monomer offers a multitude of advantages[43]: control over molecular weight, narrow molecular weight distribution, the possibility to synthesise advanced macromolecular architectures as well as functionalized polymers with well-ordered structures.

[42] Dissertation, Christina Lexer, *Towards functionalized Ring Opening Metathesis Polymers*, Graz University of Technology, **2009**.
[43] Grubbs, R.H., *Handbook of metathesis, Volume 3*, Wiley-VCH, Weinheim, **2003**.
[44] Trnka, T.M., Grubbs R.H., *Acc. Chem. Res.* **2001**, *34*, 18-29.

2.4.   Microwave assisted polymerisation

The first commercial microwave ovens were introduced in the 1950s and in the 1980s the first serious experiments in scientific laboratories began. About ten years ago special microwave equipment for e.g. applications in food chemistry came into operation and soon after that pharmaceutical industry was to benefit from this new technology.[45]
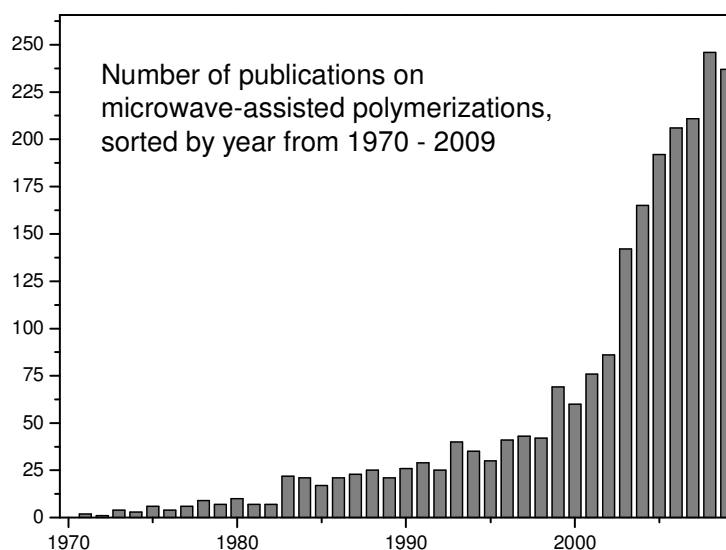
Fig 2-10: Number of publication on microwave-assisted polymerizations, sorted by year[46]

Nowadays many academic labs take advantage of the conveniences of microwave technology, e.g.: accurate control of temperature and pressure, the possibility to drive the reaction to give one or other of the products[47], in some cases the abdication of solvents[48] and the direct heating of the reaction mixtures, without heating the vessel and consequently speeding up the reaction.

Also for polymer chemistry these advantages have been recognized and utilized for example the step-growth polymerizations of amides and imides, free and controlled radical polymerizations and ring opening polymerizations.[49] For the

---

[45] Adam, D., *Nature* **2003***, 421*, 571-572.
[46] Resutl from the search „*Microwave and Polymerization*" in the SciFinder database on January 18th **2010**
[47] Stuerga, D., Gonon, K., Lallemant M., *Tetrahedron* **1993**, *49*, 6229 -6234.
[48] Varna, R.S., *Pure. Appl. Chem.* **2001***, 73*, 193 -198.
[49] Wiesbrock, F., Hoogenboom R., Schubert U. S., *Macromol. Rapid Commun.* **2004**, *25*, 1739-1764.

majority of polymerization reactions a significant increase in reaction speed can be determined under microwave irradiation, compared to conventional heating methods, originating from thermal effects (higher temperature). In some cases the better performance of the reaction under microwave irradiation, results in the selective excitation of one of the educts involved, e.g. ions or metals which absorb the irradiation. Microwave-assisted polymerizations are a powerful tool for the synthesis of polymers with shortened reaction times, higher yields, enhanced selectivity and environmentally friendly.

3. Polymer Electrolyte for Lithium Batteries based on photochemically crosslinked Poly(ethylene oxide) and Ionic Liquid

Abstract

Polymer / ionic liquid composites were investigated as solvent-free electrolytes for lithium batteries. Ternary electrolytes based upon poly(ethylene oxide), a ionic liquid and a conducting salt were UV-crosslinked with benzophenone as photoinitiator.

Cross-linking leads to an increase in mechanical stability of the PEO composites. This straight-forward process provides a way to increase the content of ionic liquid and thus to raise ionic conductivity without loosing in mechanical stability. Impedance measurements showed that the ionic conductivity of the composites is not affected by the UV-curing process. Moreover, the UV-curing process causes a decrease in the degree of crystallinity in the PEO composites which contributes to an increase in ionic conductivity. The present work is related to safety issues of lithium batteries.

3.1. Introduction

Solvent-free polymer electrolytes are of immediate interest for rechargeable lithium batteries. This is related to safety issues since volatile organic electrolytes (e.g. propylene carbonate) can incinerate in case of malfunction of the Li battery (e.g. thermal run-away). Poly(ethylene oxide) (PEO), an inert polymer, belongs to the most intensively studied materials for this purpose. The fact that PEO builds complexes with Li salts [50] and displays both thermal as well as interfacial stability [51] makes PEO a promising candidate as polymer electrolyte. However, at room temperature the ionic conductivity of Li salts dissolved in PEO is limited because the highly symmetrical repeating units in PEO tend to crystallize. Crystalline regions in PEO (m.p. approx. 65 °C [52]) are not available for ion transport, and conductivity is therefore limited to the amorphous regions of PEO (glass transition temperature T_g approx. -55 °C [52]). One approach towards an increased conductivity of PEO/Li salt composites can be a reduction in crystallinity of the polymer matrix, e.g. by statistical copolymerization of ethylene oxide (EO) with propylene oxide (PO). However, although block copolymers of EO and PO are marketed on a technical scale, statistical EO-PO copolymers are hardly available.

Ionic liquids (IL) or so-called "room temperature molten salts" have attracted considerable interest as an alternative to organic solvents. Consisting of an organic cation and an inorganic anion, ionic liquids have several advantages over organic solvents: high chemical and thermally stability, non-flammability, negligible vapour pressure and in some cases high electrochemical stability and hydrophobicity [53,54,55]. These properties make ionic liquids attractive candidates for numerous applications, e.g. solvents in preparative chemistry and electrolytes in lithium batteries.

Only a few years ago, the combination of a polymer and an ion conducting, electrochemically stable ionic liquid has been explored as a polymer-based

[50] Wright P V. *Br Polym J* **1976**, *7*, 319.
[51] Shin J-H, Henderson W A, Passerini S. *J Electrochem Soc* **2005**; *152(5)*, A978-983.
[52] Nijenhuis A J, Colstee E, Grijpma D W, Pennings A, *J. Polymer* **1996**; *37,* 5849.
[53] Wasserscheid P, Keim W. *Angew Chem Int Ed* **2000**, *39*, 3772.
[54] Earle M J, Seddon K R. *Pure Appl Chem* **2000**, *72,* 1391.
[55] Anderson J L, Ding J, Welton T, Armstrong D W., *J Am Chem Soc* **2002**, *124*, 14247.

electrolyte in lithium ion batteries[56,57]. PEO, a conducting salt (lithium bis(trifluoromethansulfonyl) imide; LiTFSI) and a ionic liquid (*N*-methyl-*N*-butylpyrrolidinium (trifluoromethansulfonyl) imide; $PYR_{14}TFSI$) were mixed and processed at elevated temperatures under dry conditions. By this process, ternary composites PEO / IL / LiTFSI / with high ionic conductivity were obtained in the form of thin films. No solvent was used in the process. However, the increase in conductivity (compared to binary systems PEO/Li salt) is still limited, as the mechanical stability of the composites is poor when the content of ionic liquid exceeds a certain limit. It has been reported that for ternary composites PEO / IL / LiTFSI this limit is in the range 10 / 1 / 1 (by mole). At higher contents of ionic liquid, soft and gelly materials are obtained which are difficult to process on an industrial scale. Until today this has been seen as a serious limitation to the use of ionic liquids in PEO based electrolytes.

The present work aims at a solution to this problem. Our approach is based upon crosslinking of PEO in the presence of conducting salts and ionic liquids. By this method, the mechanical stability of the ternary composite can be increased. Consequently, higher fractions of ionic liquid can be employed in the polymer electrolyte, which results in higher ionic conductivities while maintaining a sufficient mechanical stability of the electrolyte foils.

In the following, first results on the UV induced crosslinking of PEO and measurements of the thermal properties and the ionic conductivity of PEO / IL / Li salt composites are presented. This work is a contribution to the development of safe lithium ion batteries which can be operated without the use of volatile and combustible electrolyte liquids.

---

[56] Shin J-H, Henderson W A, Passerini S., *Electrochem Comm* **2003**, *5*, 1016.
[57] Brandrup J, Immergut, E H, Grulke E A, Polymer Handbook, 4th edition. Chichester: John Wiley & Sons; **2003**.

3.2. Experimental

3.2.1. Materials

Benzophenone (purum) was bought from Fluka and used without further purification. PEO (Union Carbide, WSR 301, M_w = 4.000.000 g mol^{-1}) was dried *in vacuo* at 50°C for 48h. The conducting salt LiTFSI was obtained from 3M, the ionic liquid PYR$_{14}$TFSI was provided by ENEA (Italy). Both substances were dried *in vacuo* at 110°C for 24h.

3.2.2. Preparation and characterisation of the samples

In pre-experiments the ability of the PEO to undergo the cross-linking reaction was determined. First the pure polymer was tested with benzophenone as photoinitiator in CH_2Cl_2, second the reaction was tested in a PYR$_{14}$TFSI environment.

LiTFSI and benzophenone were dissolved in PYR$_{14}$TFSI by slight heating (50°C). Afterwards, PEO was added and the mixture was kept for 24 hours at 40°C. The amounts of LiTFSI, benzophenone, ionic liquid and PEO are given in the section Results and Discussion. Composite foils were prepared from this mixture by hot-pressing between two sheets of poly(ethylene terephthalate) (Mylar). Hot-pressing was done at 70°C for 5 min, and foils of approx. 150µm thickness were obtained.

For UV illumination of the sample foils a mercury lamp (EFOS Novacure N 2000-A) was used. Polychromatic irradiation was carried out at a sample temperature of 70 °C which is above the melting point of the crystalline regions of PEO. There was no need to remove the Mylar foils prior to UV irradiation because Mylar is transparent at wavelengths > 300 nm, where the n-π* transition of benzophenone is excited.

For determining the degree of cross-linking in PEO, sol/gel analysis was performed as described in the following. PEO containing benzophenone (5 wt.-%) was prepared by dissolving PEO and benzophenone in chloroform. From this solution, films were spin-cast onto CaF_2 plates and dried in vacuo. The film thickness was in the range of a few micrometers. After taking an FTIR spectrum of the PEO layer (absorbance mode), the CaF_2 plate was illuminated with UV light under inert gas conditions (N_2). The sample was then immersed in dichloromethane for 1 hr

(development). After drying in vacuo, another FTIR spectrum was taken. From the difference in absorbance at the ether band at 1100 cm^{-1} the residual film thickness (i.e. the insoluble fraction W) was calculated.

PEO samples containing both ionic liquid and benzophenone were prepared by dissolving benzophenone at 50°C in the ionic liquid and then PEO was added. The sample composition was 57 parts of PEO, 43 parts of IL and 5 parts of benzophenone (by weight). From these PEO samples, films of approx. 150 µm thickness were prepared by hot-pressing between Mylar foils. The samples were thermostatted at 70°C and UV illuminated under inert gas conditions (N$_2$). After UV irradiation, the PEO samples were weighed and subsequently immersed in dichloromethane for 1 hr (development). After drying in vacuo (24 hr at 40°C) the samples were weighed again. The gel fraction W was calculated from the mass of the extracted PEO sample divided by the mass of the original PEO sample and expressed in %. The values of W are corrected for the amount of IL added.

Differential scanning calorimetry (DSC) measurements were run with a Netzsch DSC 204 instrument in a temperature range from -80°C to 90°C (inert gas conditions). The heating rate was 10 K min^{-1} at a N$_2$ flow rate of 20 ml/min. Scanning electron microscopy (SEM) pictures were taken on a JOEL JWS-7515 wafer inspection system with an acceleration voltage of 5 kV. Impedance measurements to analyze the ionic conductivity of the electrolyte were performed by sandwiching the electrolyte between two stainless steel electrodes in a Swagelok-type cell. The measuring system IM5d (Zahner Messsysteme) was used. Impedance spectra were recorded in a frequency range from 1Hz to 2 MHz and the AC oscillation amplitude was set to 5 mV.

3.3.   Results and discussion

3.3.1. Pre-experiments

When looking for a convenient way to induce cross-linking of a polymer, radiation induced processes can be considered. For polyethylene oxide it has been reported that ionizing radiation (β, γ) causes chain fragmentation and concomitant cross-

linking. The radiation chemical yields for fragmentation (G(s)) and cross-linking (G(x)) depend on the physical state of the polymer (solid, dissolved) and on the temperature[58]. In most cases chain fragmentation predominates and the average molar mass of PEO is lowered when this material is exposed to radiation. Indeed, ionizing radiation is used to adjust the average molar mass of (high molecular) PEO to lower values. However, the photochemical crosslinking of solid PEO can be achieved with benzophenone as photoinitiator[58,59]. After UV excitation of the benzophenone to a n,π^* triplet state, hydrogen abstraction from the PEO chain proceeds as depicted in Figure 1.
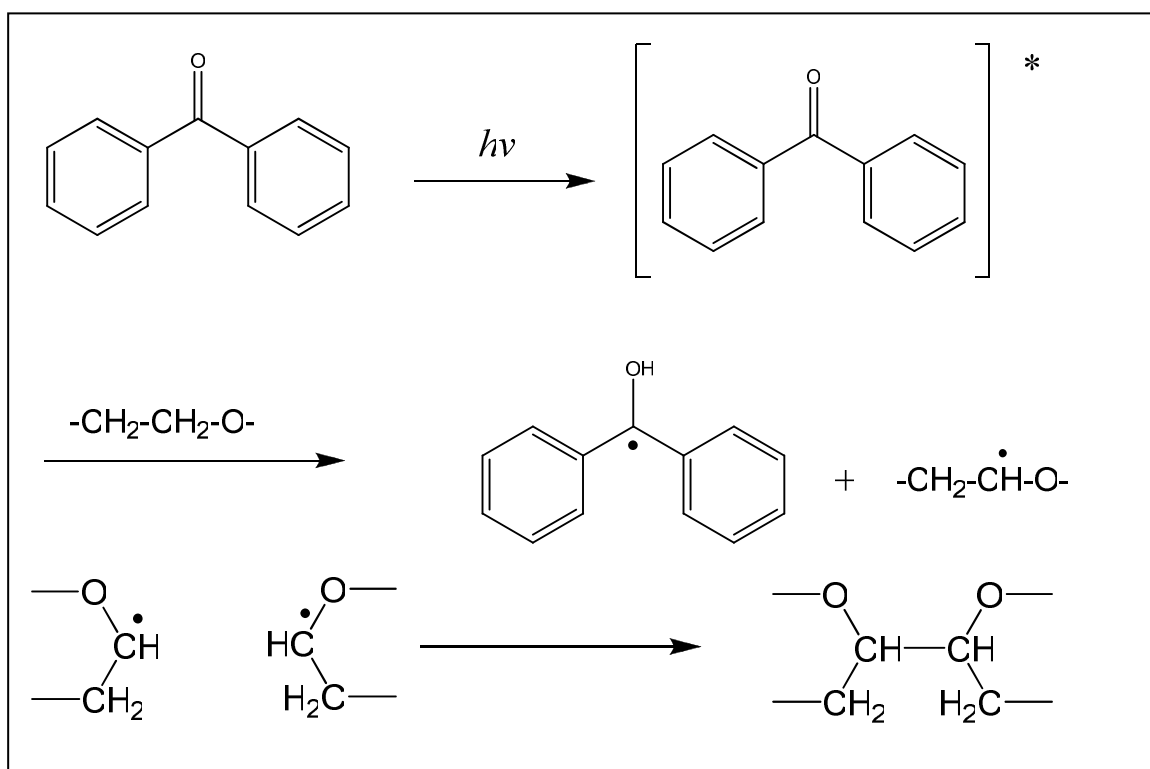

Fig 3-1: Crosslinking of poly(ethylene oxide) by UV irradiation in the presence of benzophenone as photoinitiator

The PEO macroradicals then generate the desired network by recombination.

[58] Doytcheva M, Dotcheva D. *J Appl Polym Sci* **1997**, *6,* :2299-2307.

[59] Doytcheva M, Stamenova R, Zvetkov V, Tsvetanov Ch B*., Polymer* **1998**; *39*, 6715.

3.3.2 Photochemical crosslinking

Experiments with thin films of PEO (a few µm thickness) containing 5 wt.-% of benzophenone showed that an insoluble (gel) fraction W = 80% can be achieved by photo-crosslinking under inert gas conditions. For determining the gel fraction FT-IR spectra have been measured (once after the illumination and once after the development step) and compared as described above. As reference the ether band at 1100 cm^{-1} was chosen because of the high intensity of this stretching vibration. The residual film thickness after the development (i.e. the insoluble fraction W) was calculated due to the intensity of the band at 1100 cm^{-1}.
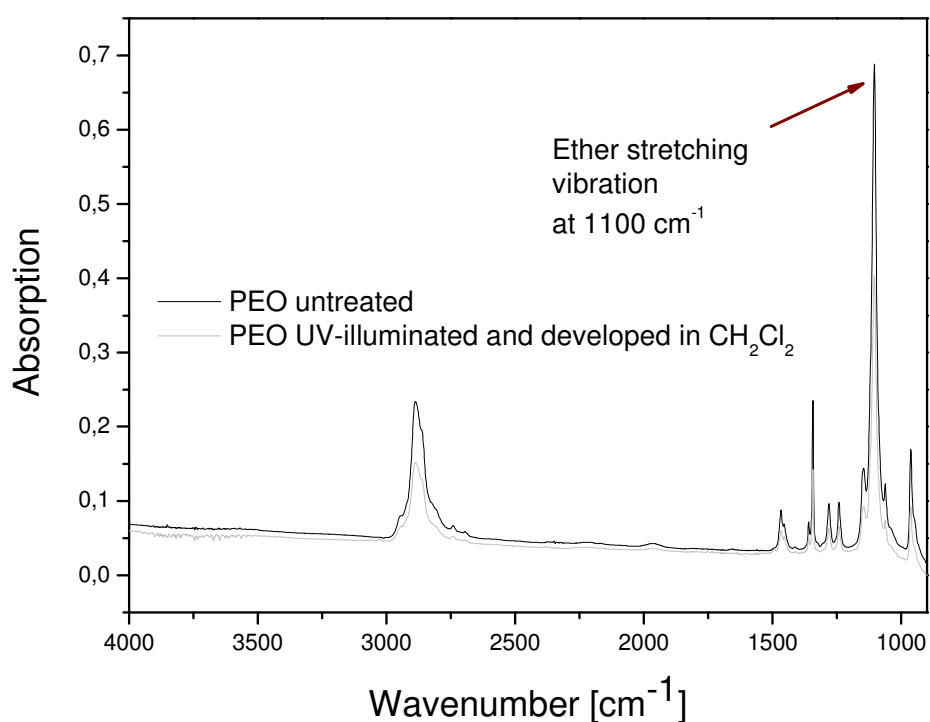

Fig 3-2: FT-IR spectra of PEO befor and after UV-illumination and development

This procedure has been repeated for several illumination durations. The calculated insoluble fractions have been plotted against the time of irradiation. In this way we obtained the so called Sol-Gel-curve of this system.
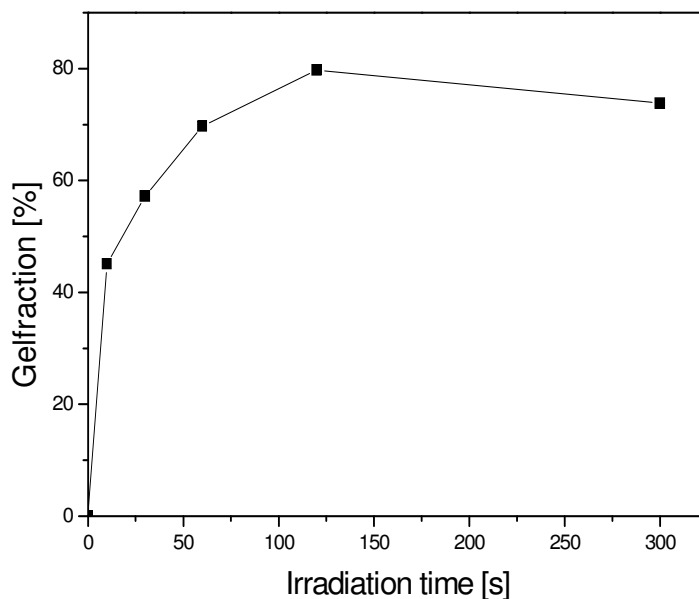
Fig 3-3: Sol-Gel-curve of spincoated PEO

Apart from benzophenone also 2,6-bis(4-azidobenzylidene)-4-methylcyclohexanone has been used as photoinitiator for the cross-linking step. In the FTIR spectra of these experiments the decomposition of the azide group can be easily observed.


$$RN_3 + h\nu \longrightarrow RN^{\cdot \cdot} + N_2$$
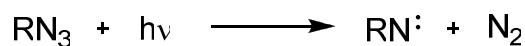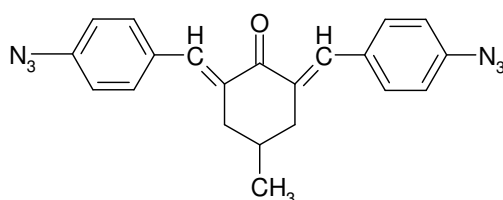
Fig 3-4: 2,6-bis(4-azidobenzylidene)-4-methylcyclohexanone and the photochemical decomposition of the azide group

The cross-linking worked as fast and efficient as with benzophenone and is an appropriate alternative. In particular to avoid the side products of the reaction with benzophenone where compounds with OH groups can be generated.

- 30 -
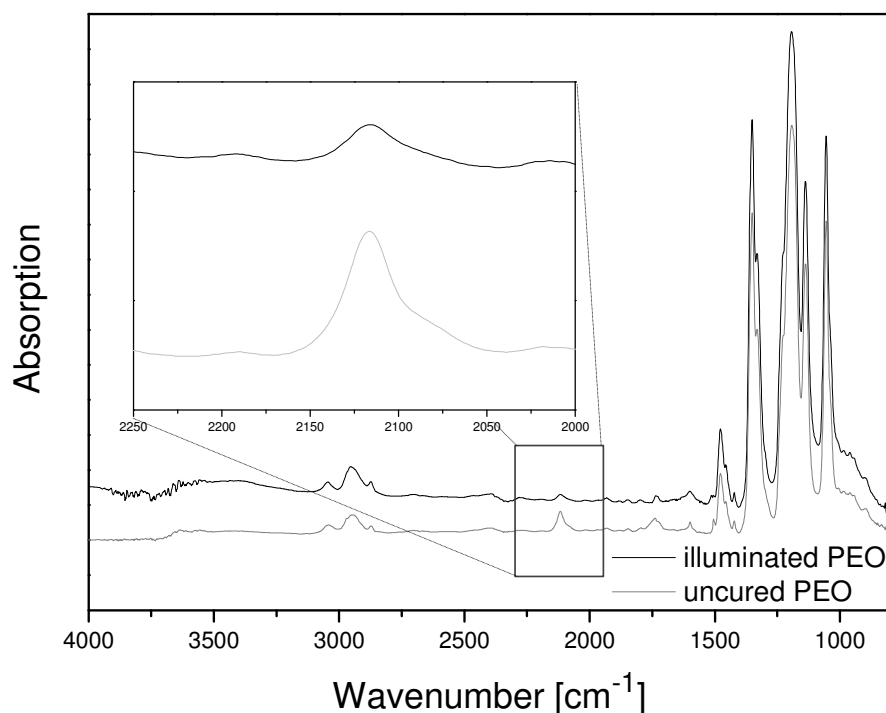
Fig 3-5: Illumination of PEO with a bisazide as photoinitiator and especially the decrease of the azide band at 2120 cm⁻¹ after illumination.

In a next series of experiments the crosslinking of binary PEO / IL composites was investigated. *N*-methyl-*N*-butylpyrrolidinium (trifluoromethansulfonyl) imide (PYR$_{14}$TFSI) was employed as IL. PEO composites containing 57 parts of PEO, 43 parts of IL and 5 parts of benzophenone (by weight) were prepared as films (150 μm thickness) between Mylar foils and irradiated with a medium pressure mercury lamp. Mylar is transparent for wavelengths > 300 nm, where the PEO matrix does not absorb at all. At the 365 nm line of the Hg spectrum, only benzophenone absorbs (ε_{365} = 58 l mol⁻¹ cm⁻¹). For the ionic liquid PYR$_{14}$TFSI, negligible absorbance was found at 365 nm (ε_{365} = 0.042 l mol⁻¹ cm⁻¹). Thus we could avoid to remove the Mylar foil before illumination and simplified the procedure because the inert atmosphere was so already given.
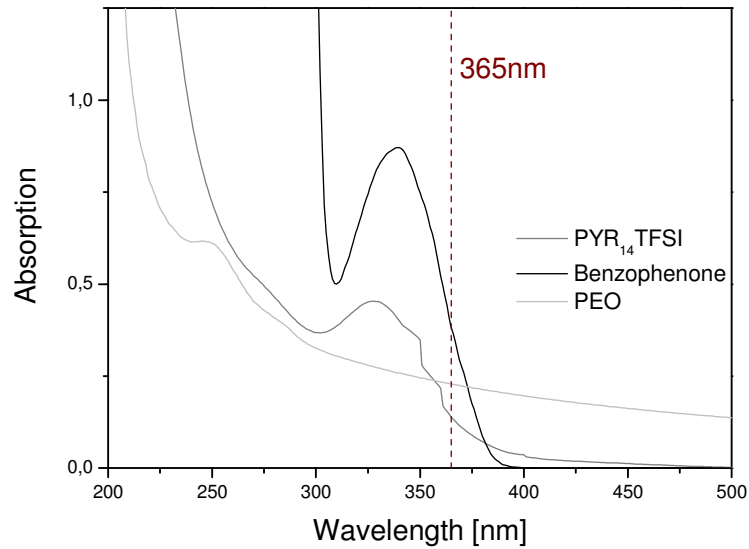
Fig 3-6: UV-Vis-spectra of PEO, benzophenone and PYR$_{14}$TFSI

Figure 1-5 shows the sol/gel curve which was recorded for these composites. It is found that also in this case the insoluble fraction W amounts to 80%. Prolonged UV irradiation then leads to lower values of W which indicates fragmentation reactions.
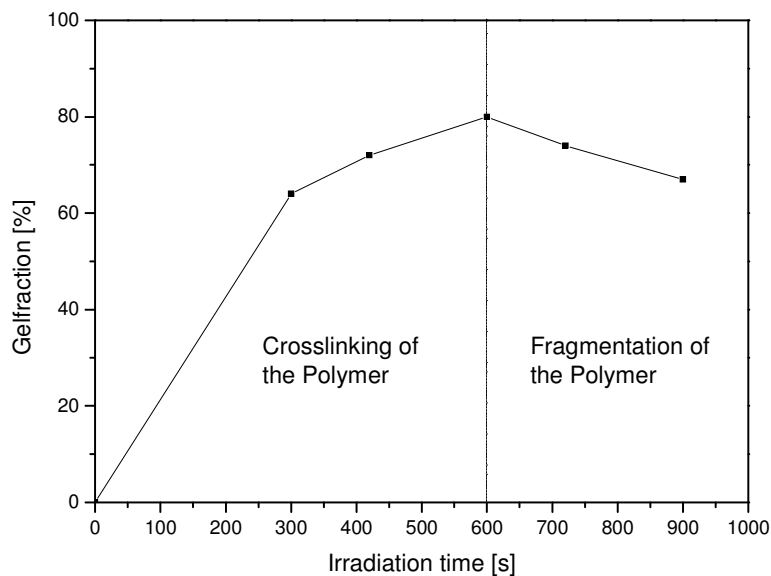

Fig 3-7 Photocrosslinking of PEO / IL composites which contain 57 parts of PEO, 43 parts of IL and 5 parts of benzophenone (by weight). The insoluble fraction W is plotted as a function of the irradiation time

FTIR spectra of the cross-linked (and thoroughly extracted) PEO films did not display any signals typical of the ionic liquid *N*-methyl-*N*-butylpyrrolidinium (trifluoromethansulfonyl) imide (PYR$_{14}$TFSI). This indicates that the IL does not participate in the photo-crosslinking reaction and is not covalently attached to the PEO matrix after UV irradiation.

In Fig 1-6 the mechanical properties of the PEO/IL composites before and after illumination are illustrated. Without the illumination step the composite is very brittle. It is obvious that due to the treatment the flexibility is enhanced enormously.
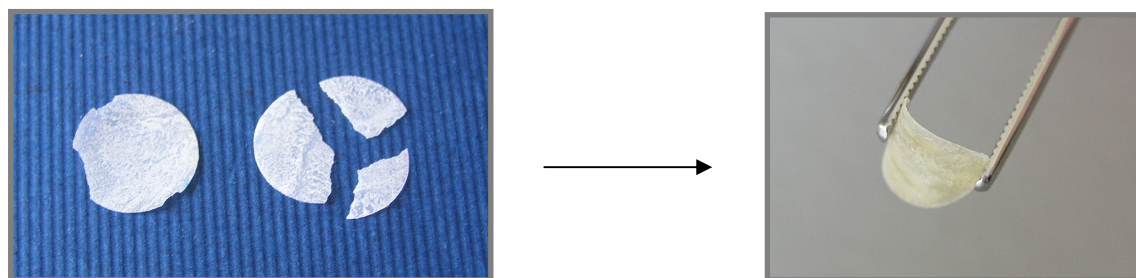

Fig 3-8: PEO / IL composites before and after illumination

In another series of experiments the cross-linking of ternary PEO composites containing both the ionic liquid (PYR$_{14}$TFSI) and the conducting salt LiTFSI was assessed. Also composites PEO / PYR$_{14}$TFSI / LiTFSI can be photo-cross-linked with benzophenone (5 wt.-%, with respect to PEO) as evidenced by sol/gel analysis. The addition of the salt LiTFSI did not exert any adverse effects on the progress of the cross-linking reaction.

The mechanical stability of the PEO composites was investigated. With non-cross-linked composites, the limiting composition for mechanically stable films is approx. PEO / / PYR$_{14}$TFSI / LiTFSI ~ 10 / 1 / 1 (by mole). At higher IL contents (e.g. 10 / 2 / 1) very sticky materials are obtained which cannot be processed as films at ambient temperature. It was found that UV cross-linking significantly improves the mechanical stability of these composites. To give an example, Figure 1-7 displays the photograph of a non-treated sample and a photo-crosslinked film with the composition PEO / PYR$_{14}$TFSI / LiTFSI ~ 10 / 2 / 1 (by mole). The transparency of the samples after curing indicates low crystallinity. This will be assessed in the following section.
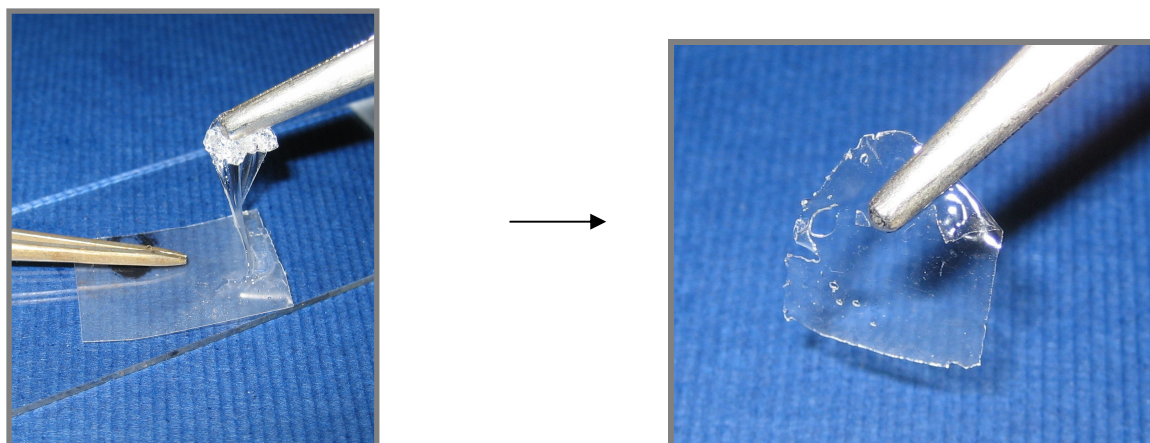
Fig 3-9: Free standing film of a composite PEO / PYR$_{14}$TFSI / LiTFSI = 10 / 2 / 1 (by mole) produced by UV crosslinking.

3.3.2. Thermal analysis

DSC measurements were undertaken to investigate the degree of crystallinity in the PEO composites. Most important, we wished to see to which degree crystallinity is influenced by UV crossllinking of PEO/IL composites. The changes in the thermal properties of PEO due to the addition of ionic liquids have already been studied by Shin et al.[51].

In Figure 1-8 the DSC traces (second heating runs) of ternary composites PEO / IL / Li salt are displayed. The DSC measurements were taken under N$_2$ at a heating rate of 10 K min^{-1}. Trace 1 and trace 3 refer to uncured PEO samples containing different ratios of ionic liquid (PEO / PYR$_{14}$TFSI / LiTFSI = 10 / 1 / 1 and 10 / 2 / 1, respectively), while trace 2 and trace 4 refer to UV cross-linked samples. In all samples a glass transition in the temperature range between -70 and -55 °C can be observed. It is also seen that the melting point of the crystalline PEO fraction shifts from M$_p$ = 41°C (10 / 1 / 1 sample) to M$_p$ = 36°C for the 10 / 2 / 1 sample which contains a larger fraction of ionic liquid. The melting points are significantly lower than that of neat PEO (approx 55°C). As a result of UV cross-linking, this endothermal signal disappears for both composite samples. From this we conclude that the UV cross-linking process, which is carried out at 70°C well above the melting point of PEO, leads to a significant reduction of the crystalline fraction. With respect to ionic conductivity, this would be beneficial as conductivity is restricted to the amorphous regions of PEO.
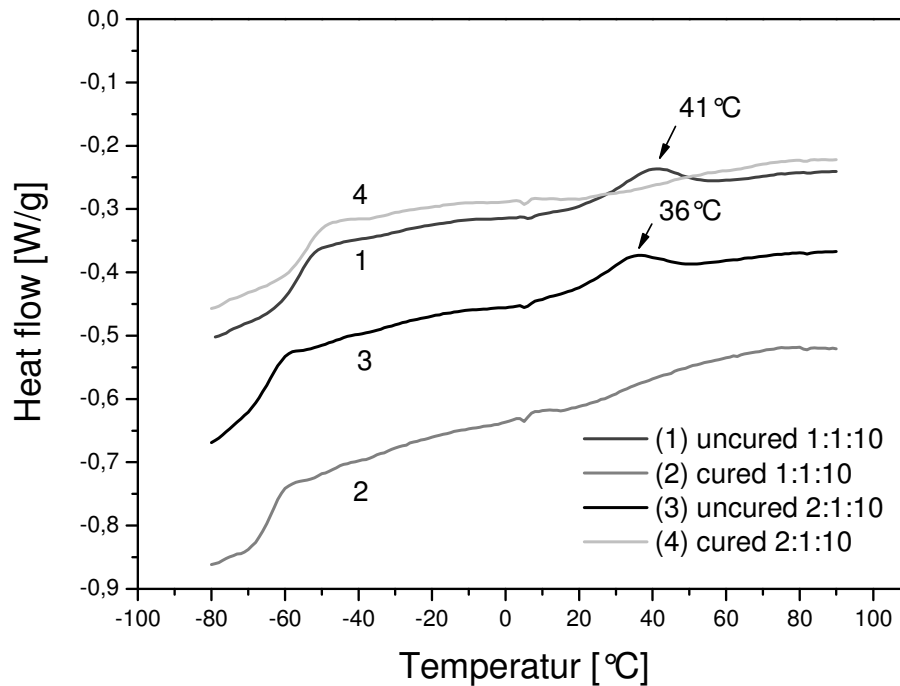
Fig 3-10: Thermal analysis (DSC) of composites of PEO, PYR$_{14}$TFSI and LiTFSI. Trace (1): molar ratio 10 / 1 / 1 prior to UV-curing; trace (2): molar ratio 10 / 1 / 1 after UV-curing; trace (3): molar ratio 10 / 2 / 1 prior to UV-curing; trace (4): molar ratio 10 / 2 / 1 after UV-curing.

3.3.3 SEM pictures

This result is backed by scanning electron microscopy. SEM images of the cross-linked ternary polymer electrolyte (10 / 2 / 1 sample) were taken at 5 kV acceleration voltage. There was no further coating of the sample (to avoid contaminations) and so a higher acceleration voltage have destroyed the sample, melted the PEO of the sample respectively. The SEM micrograph in Figure 1-9 indicates that the ternary electrolyte is homogenous. No crystalline domains are discernible in this sample.
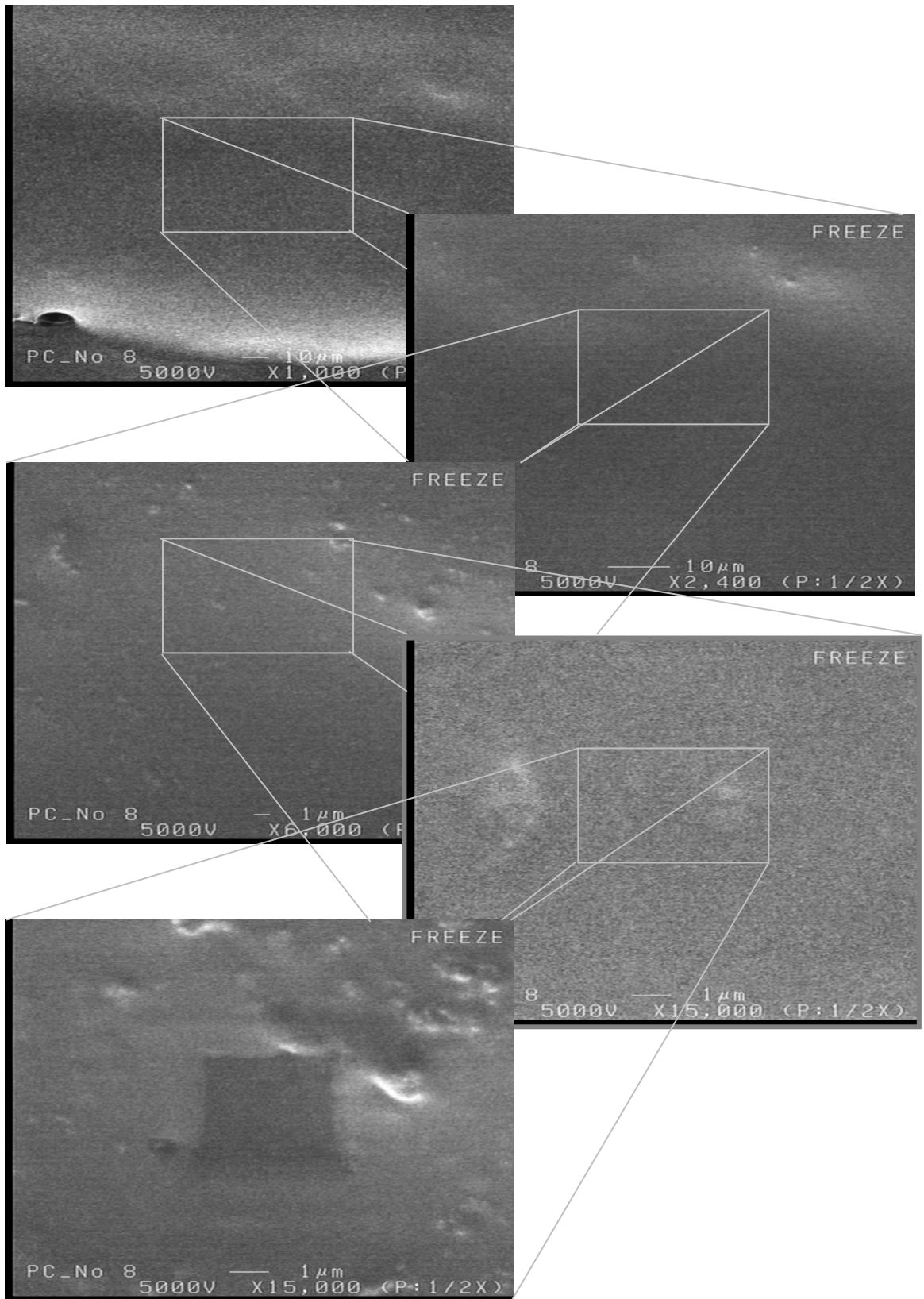
Fig 3-11: SEM micrographs of a UV crosslinked composite PEO / PYR$_{14}$TFSI / LiTFSI = 10 / 2 / 1 (by mole) in various magnifications.

3.3.4 Impedance measurements

The ionic conductivity of the ternary systems with different contents of ionic liquid was measured by AC impedance spectroscopy. Following the equation

$$s = t * (A * R)^{-1}$$

where t is the thickness of the sample (in cm), A is the area of the sample (in cm^2) and R is the ohmic impedance (in Ω), the ionic conductivity s ($S\ cm^{-1}$) was determined. Polymer electrolytes with the composition PEO / PYR$_{14}$TFSI / LiTFSI = 10 / 1 / 1 and 10 / 2 / 2 were prepared as foils, cross-linked by double-faced UV illumination, and subjected to impedance measurements over a temperature range from 25 to 80 °C. Figure 1-10 displays the ionic conductivity of the composites as a function of temperature (Arrhenius plot). As expected, the ionic conductivity of both composites drops at decreasing temperature.

The conductivity data obtained for the UV-cross-linked 10 / 1 / 1 composite are compared to reference data taken from the literature[60]. These literature data refer to a non-cross-linked composite containing PEO, PYR$_{14}$TFSI and LiTFSI at a molar ratio 10 / 1 / 1. The comparison shows that the conductivity of the cross-linked sample is virtually equal to its non-cross-linked counterpart in the temperature region 20 – 50 °C. At higher temperatures (up to 80 °C), the cross-linked composite displays 10 - 20% higher conductivity than the non-cross-linked composite. It is interesting to see that UV cross-linking does not affect the ionic conductivity of the composite, although the mobility of ions is expected to be lower in a polymeric network. Obviously, the lower degree of crystallinity in the UV-cured composite compensates and even over-compensates for the effects of cross-linking on ion mobility.

Comparing the cross-linked composites (10 / 1 / 1 and 10 / 2 / 1, respectively) it is seen that ionic conductivity increases with the content of ionic liquid. This effect is most pronounced at elevated temperatures. At 80 °C, ionic conductivity is approx. twice as high for the 10 / 2 / 1 sample.

---

[60] Kim G-T, Appetecchi G, Alessandrini F, Passerini S., *J Power Sources* **2007**;*171*, 861-869.
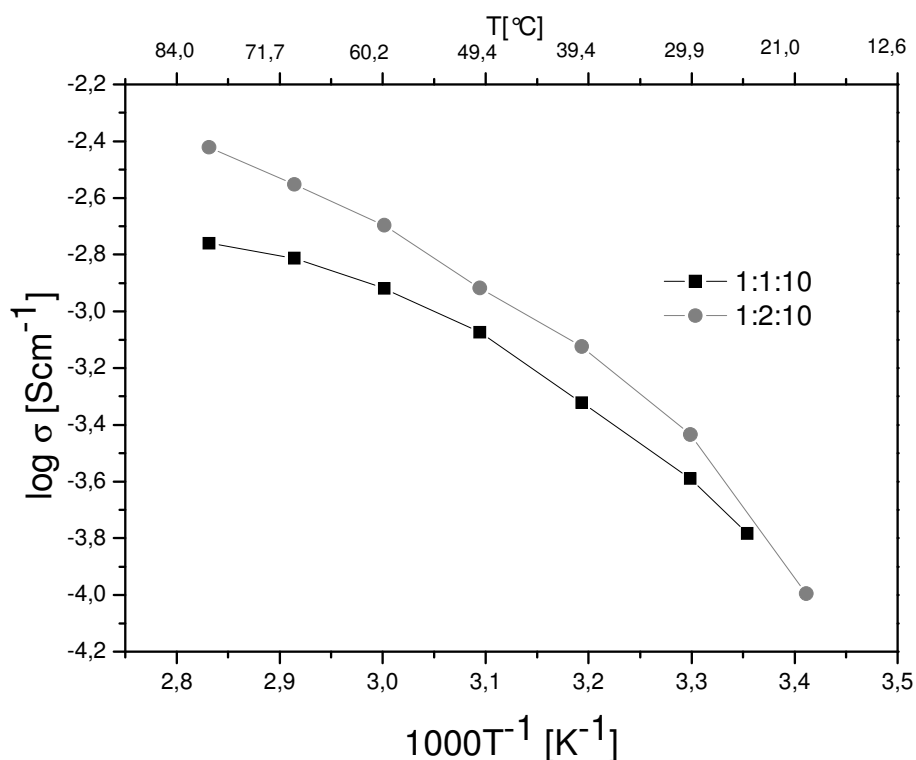
Fig 3-12: Ionic conductivity (log scale) of PEO / PYR$_{14}$TFSI / LiTFSI composites as a function of inverse temperature (Arrhenius plot). (■) molar ratio 10 / 1 / 1 (crosslinked); (●) molar ratio 10 / 2 / 1 (crosslinked).

3.4   Conclusion

A new type of solvent-free electrolyte for lithium batteries has been developed, which is based upon photochemically cross-linked composites of polyethylene oxide (PEO), ionic liquid (PYR$_{14}$TFSI) and a conductive lithium salt (LiTFSI). Using benzophenone as photoinitiator, a PEO gel fraction of 80% can be obtained. Prolonged UV irradiation leads to a degradation of the network (chain scissoring) and the gel fraction decreases.

UV cross-linking results in a mechanical stabilisation of the PEO / PYR$_{14}$TFSI / LiTFSI composites. This provides a way to increase the content of ionic liquid in such composites without loosing in mechanical stability. While uncured samples containing PEO, PYR$_{14}$TFSI and LiTFSI at a molar ratio 10 / 2 / 1 are gelly liquids, stable foils are obtained after performing the photo-curing step. By this way, the handling and processing of such composites is facilitated which is beneficial for technical processes.

The ionic conductivity of the composites is not affected by the UV-curing process. The lower degree of crystallinity in these samples (over)compensates for the effect of network formation on the mobility of ions. A careful optimization of the electrolyte concerning the ratio of PEO / ionic liquid / lithium salt may result in even higher values of ionic conductivity.

3.5 Acknowledgements

4. UV cross-linking of short chain length polyhydroxyalkanoates

Abstract

Short chain length (scl) Poly(3-hydroxyalkanoate)s (PHAs) were cross-linked with 2,6-bis(4-azidobenzylidene)-4-methylcyclohexanone. Due to the properties and mechanism of the cross-linking agent it was not necessary to add functional groups in the polymer chain for the network building. The procedure of polymer synthesis as well as the cross-linking step are easy, cheap and more effective than known photochemical systems for PHAs. Further the ability of the system to work as a negative resist for photolithographic applications was tested. As medium for the development CH_2Cl_2 was used. The results proof the suitability of biodegradable scl-PHAs for microlithography.

4.1 Introduction

Poly(3-hydroxy alkanoate)s are a class of polyesters, first time detected by Lemoigne[61] in 1926. They differ in the multitude of monomers, which can be incorporated in the polymers. Biosynthesized by a large number of bacteria, they serve as carbon and energy reserves.[62,63]

The composition of PHA is mainly dependent on two factors: first of the enzymatic specificity of the organism used and second of the carbon substrate provided to the bacteria.

In fact the potential production of different PHAs seems to be limited by the availability and costs of chemicals which can provide as precursor substrates to the bacteria, rather than by the substrate range of PHA synthesis[64].

Their potential application as bioplastics in medical devices and tissue engineering and their biodegradability draw a lot of attention. But also their synthesis from renewable carbon sources, based on agriculture of even industrial wastes makes PHAs so fascinating.[65,66]

The properties of these polyesters are similar to those of some polyolefines like polyethylene or polypropylene and can be fabricated in production processes such as batch, semi batch or continuous fermentation. In applications in which they would pose a sure advantage, biodegradable polymers have not yet replaced conventional plastics in any significant way. This is due to the fact, that the production of petroleum based plastics is until now much more cost effective.[67]

The two general classes of the broad spectrum of PHAs are based on the size of their repeating units: Medium-chain-length polyhydroxyalkanoates (mcl-PHAs), which have a typical chain length of C6-C14 and short chain length polyhydroxy alkanoates (scl-PHAs) which have a chain length of C3-C6.[68]

In this work we focus on scl-PHAs. PHB-homopolymers are highly crystalline thermoplastic with a melting point around 180°C. PHB is often compared to polypropylene in its physical properties because they have similar melting point,

[61] Lemoigne, M., *Bull Soc. Chem. Biol.*, **1926**, *8*, 770-782
[62] Anderson AJ, Dawes EA. *Microbiol Rev* **1990**, *54* (4): 440-72
[63] Lenz R., Marchessault, R. *Biomacromolecules*, **2005**, *6* (1) 1-8
[64] Steinbüchel A., Valentin H., FEMS Microbiology Letters **1995**, *128*, 219-228
[65] Braunegg, G. J. *Biotechnology* **1998**, *65*, 127-161
[66] Ashby, R. *Biol. Macromolecules* **1998**, *23*, 61-72
[67] Nonato, R.V., Mantelatto P.E., Rossell C.E.V., *Appl. Microbiol Biotechnol*, **2001**, *57*, 1-5
[68] Kim, D.Y.; Kim, H.W.; Chung, M.G.; Rhee, Y.H. *J. Microbiol.* **2007**, *45*, 87-97.

degree of crystallinity and glass transition temperature. Anyway PHB is stiffer, more brittle and different in chemical properties.[69]

The incorporation of 3-hydroxyvaleric acid units in the PHB chain leads to a decrease in crystallinity, melting point and stiffness but an increase of toughness of the polymer.

For further decrease of the crystallinity of the copolymers and an enhancement of the mechanical properties a photochemical crosslinking step is proposed. Crosslinking of scl-PHAs is known in literature: for example chemically crosslinking via peroxides[70]. Moreover photochemical crosslinking of mcl-PHAs has been published previously[66,71,72]. In latter publications the network-building step was enabled by incorporation of additional functional groups into the polymer chain e.g. double bonds. The approach presented in this work is the use of scl-PHB-Vs, which are produced in a simple straight forward process and which are cross-linked via a photochemical active crosslinking agent, without further modifications of the polymer. The abdication of functional groups simplifies the production process of the PHA and contributes to cost efficiency in a future production.

4.2 Experimental

4.2.1 Materials

2,6-Bis(4-azidobenzylidene)-4-methylcyclohexanone (97%) was bought from Aldrich and used without further purification. The PHB copolymer (PHB-HV, L-132 18.25%-HV, 2008, Biocycle, Brazil) was purified two times as follows: A Soxhlet extraction in ethanol was made over night (approximately 24h) and then the residue was dried in vacuum oven.

The following data were obtained via gel permeation chromatography:

Number average molar mass M_n: 167.7 kDa

Weight average molar mass M_w: 334.2 kDa

---

[69] Holmes, P.A., *Phys. Technol.*, **1985**, *16*, 32-36.

[70] Gagnon, K.D., Lenz, R. W., Farris, R. J., Fuller R.C., *Polymer*, **1994**, *35* (20), 4358-4367

[71] Hazer, B., Demirel, S.I., Borcakli, M., Eroglu, M.S., Cakmak, M., Erman B., *Polymer Bulletin*, **2001**, *46*, 389-394.

[72] Kim, S.N., Shim S.C., Kim, D.Y., Rhee, Y.H., Kim, Y.B.,, *Macromol. Rapid Commun.*, **2001**, *22*, 1066-1071.

Polydispersity Index: 2.0

NMR data: δ (ppm) = 0.88 (0.55; t, 3·0.18 H = 0.54 H, $^3J_{H,H}$ = 6.9 Hz, H5),
1.26 (2.48; d, 3·0.82 H = 2.46 H, $^3J_{H,H}$ = 6.5 Hz, H4'),
1.57-1.64 (0.38; m, 2·0.18 H = 0.36 H, H4),
2.44-2.64 (2.05; m, 2·0.82 H + 2·0.18 H = 2 H, H2 und H2'),
5.12-5.18 (0.18; m (dd), 0.18 H, H3),
5.22-5.28 (0.83; m (dd), 0.82 H, H3').
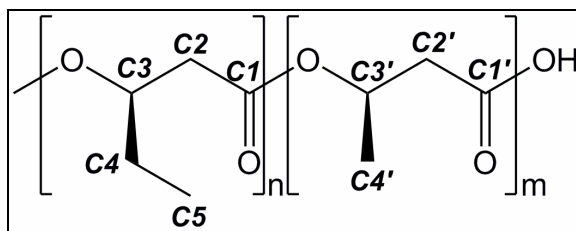
*Fig 4-1: Scheme of the PHA units*

4.2.2 Preparation and characterisation

For UV illumination of the samples a mercury lamp (EFOS Novacure from EXFO) was used. Polychromatic irradiation was carried out in Nitrogen atmosphere.

For determining the degree of crosslinking in PHB copolymer, sol/gel analysis was performed as described in the following. The PHB copolymer containing 2,6-bis(4-azidobenzylidene)-4-methylcyclohexanone (1, 3 and 5 wt.-% of the polymer) was prepared by dissolving PHB and the bisazide in chloroform. From this solution, films were spin-cast onto CaF_2 plates. The film thickness was in the range of a few micrometers. After taking an FTIR spectrum of the PHB layer (absorbance mode), the CaF_2 plate was illuminated with UV light under inert gas conditions (N_2). The sample was then immersed in dichloromethane for at least 15 minutes (development). After drying, another FTIR spectrum was taken. From the difference in absorbance at the ester band at 1724 cm^{-1} the residual film thickness (i.e. the insoluble fraction, also referred to as gel fraction W) was calculated.

The photolithographic imprinting was done as follows: The substrate was a glass plate with a layer of ITO (Indium Tin Oxide) and second layer of chrome. The last layer was the PHA-bisazide-system, applied by spin-coating. The patterning was obtained by illumination under a mask. Due to the development in dichloromethane

the non-crosslinked PHA was removed. Than an etching step was required to remove the chrome which was not covered by the remaining PHA.

4.3   Results and discussion

4.3.1 Photochemical crosslinking

When looking for a convenient way to induce cross-linking of a polymer, radiation induced processes can be considered. Frequently, high-energy radiation-induced intermolecular cross-linking of linear polymers does not occur very efficiently, because of low radiation chemical yields. Bisazid has been reported to react as cross-linking agent[73]. Due to reactive nitrenes that are formed after electronic excitation network formation occurs after insertion into the carbon hydrogen bonds of the polymer chains (fig. 1).
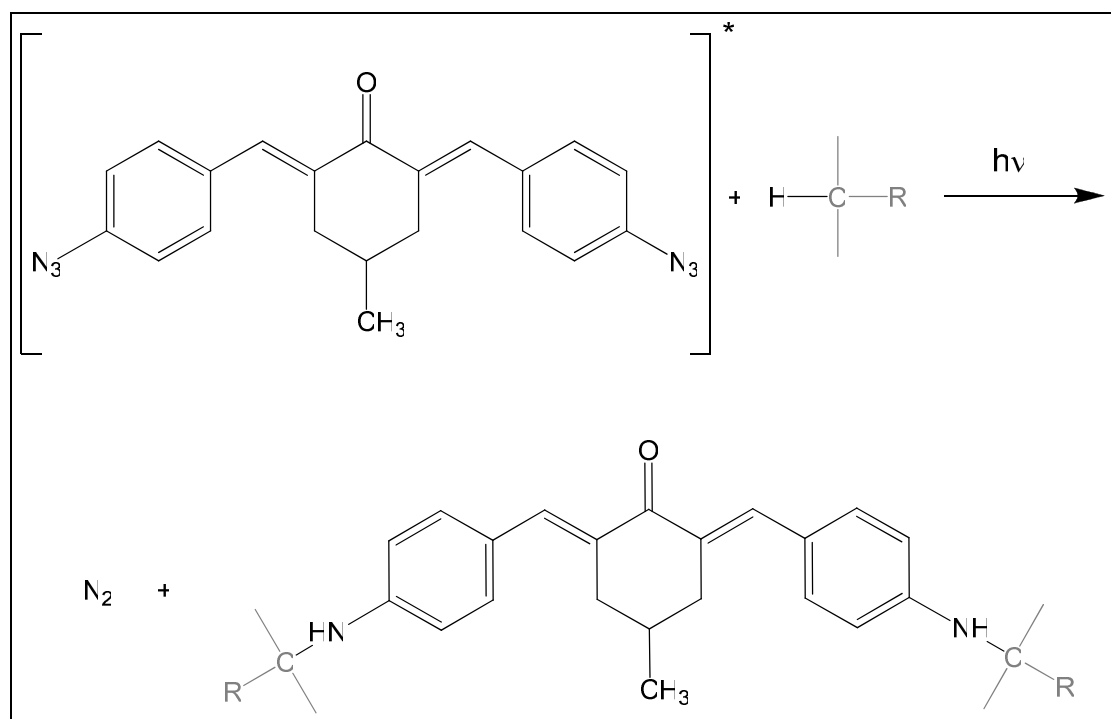
Fig 4-2: Cross-linking of carbon hydrogens by UV irradiation in the presence of 2,6-bis(4-azidobenzylidene)-4-methylcyclohexanone as photoinitiator and cross-linking agent

---

[73] J.P. Fouassier, J.F. Rabek, *Radiation curing in Polymer science and technology Volume 1 fundamentals and methods,* Elsevier science publisher ltd **1993**

The decomposition of the bisazide can also be easily observed in FTIR-spectra measured before and after illumination. The peak at 2118 cm⁻¹, which can be clearly assigned to the azid-group in the molecule, disappears completely after irradiation (fig Fig 4-3).
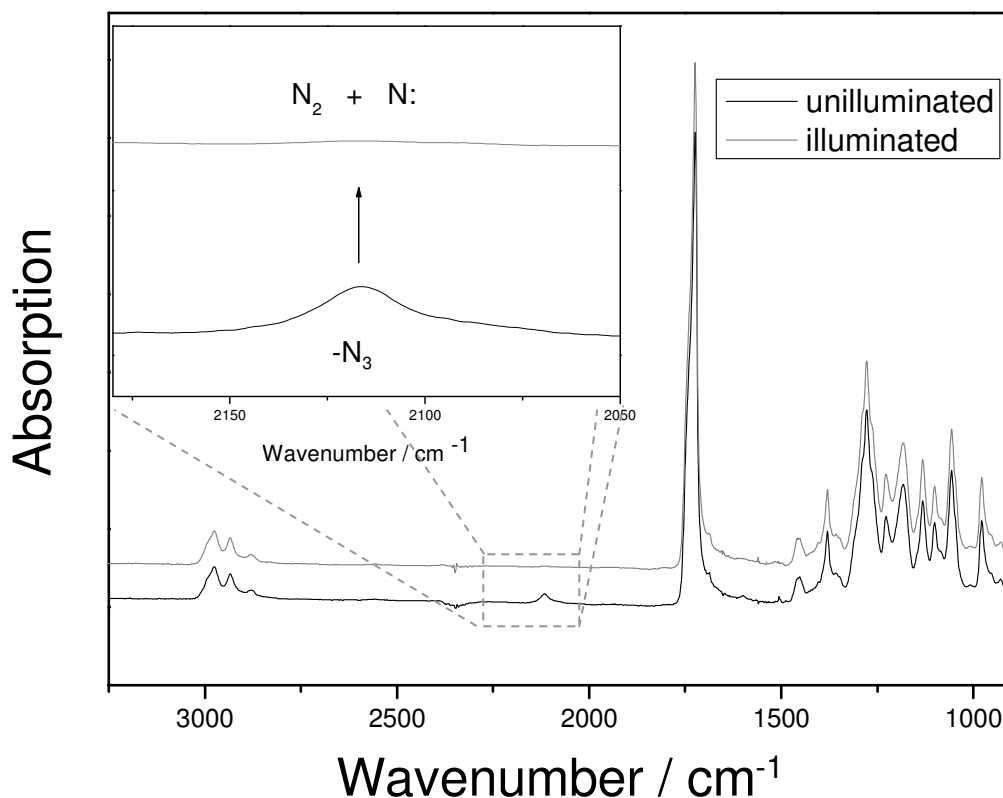
Fig 4-3: FTIR-spectra of the polymer-cross-linking-agent composition before and after illumination

By contrast the determination of the gel fraction was done by comparison of the ester peak at 1724 cm⁻¹ after illumination and after development according to the following equation:

$$Gelfraction(\%) = \frac{pht_1}{pht_0} \times 100 \qquad (1)$$

where pht_0 is the original peak-height of the ester band after the illumination and pht_1 the peak-height of the ester band after the development step.

Fig 4-4 – Fig 4-8 show the gel-fractions of PHA films illuminated for certain durations and with various concentrations of the bisazide.

1 weight-% of bisazide in the composition leads to a gel-fraction of about 70% after 30 s of illumination. With raising concentration of the cross-linking agent the cross-linking reaction occurs faster and the maximum of the gel-fraction rises up to curtly 80% with 2 weight-% of bisazide respectively more than 85% with 3 weight-%. Further enhancing of the concentration of the cross-linker leads as well to high gel-fractions of more than 90% but the maximum is reached after extended illumination durations.
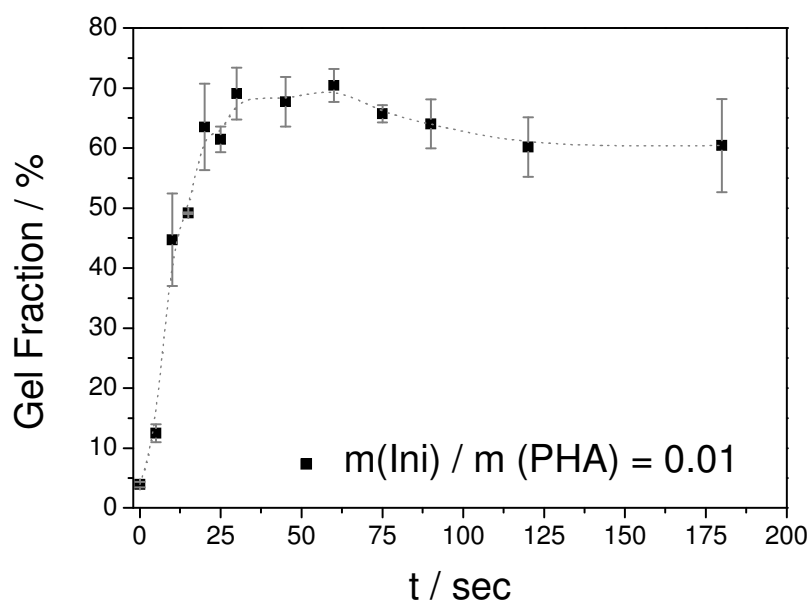
Fig 4-4: Photocrosslinking of PHA with 1 weight-% of bisazide. The insoluble fraction W is plotted as a function of the irradiation time.
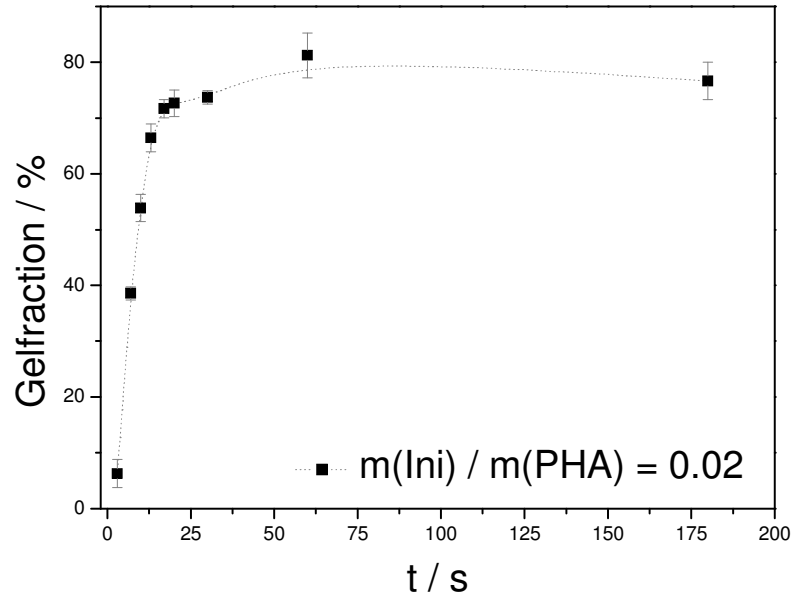
Fig 4-5: Photocrosslinking of PHA with 2 weight-% of bisazide. The insoluble fraction W is plotted as a function of the irradiation time.
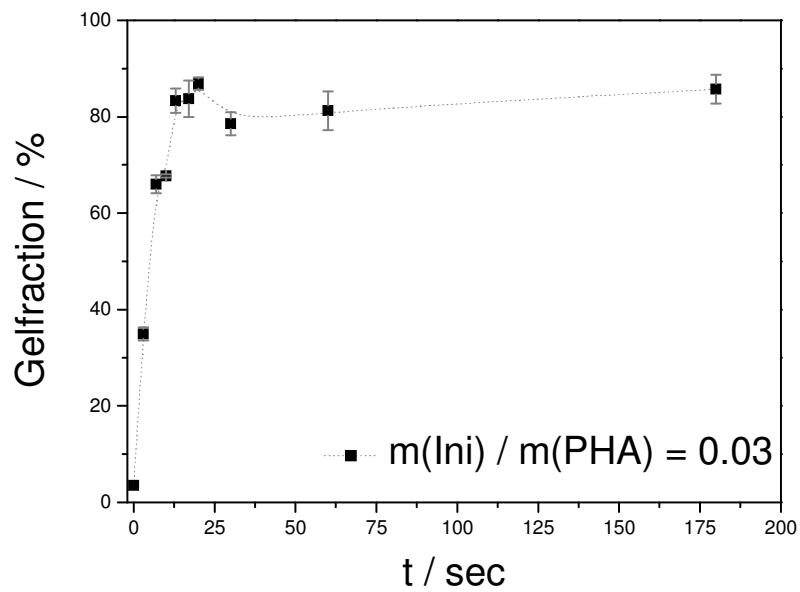
Fig 4-6:Photocrosslinking of PHA with 3 weight-% of bisazide. The insoluble fraction W is plotted as a function of the irradiation time.
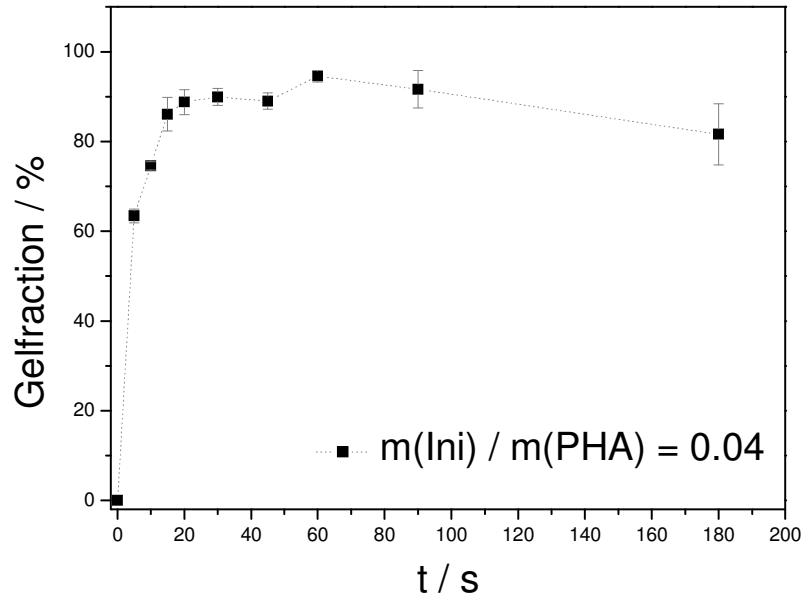
Fig 4-7:Photocrosslinking of PHA with 4 weight-% of bisazide. The insoluble fraction W is plotted as a function of the irradiation time.
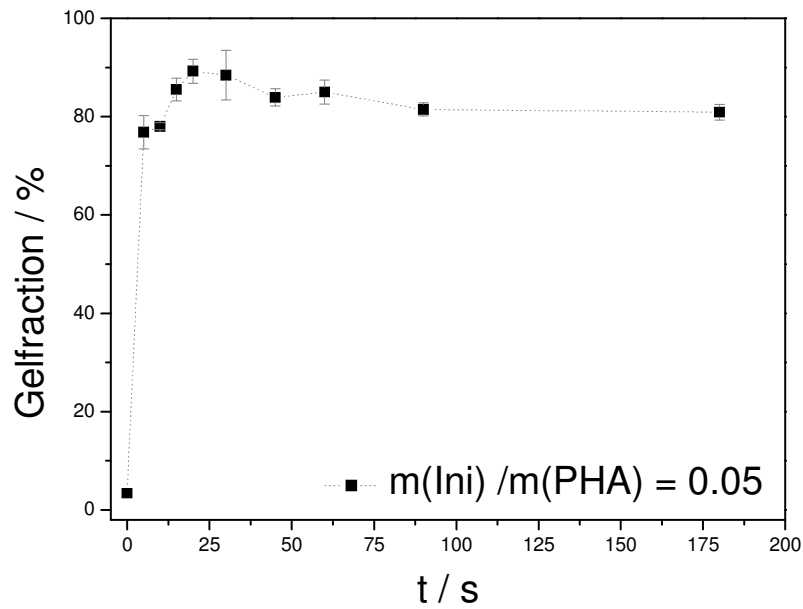
Fig 4-8:Photocrosslinking of PHA with 5 weight-% of bisazide. The insoluble fraction W is plotted as a function of the irradiation time.

To specify the results and the reactivity of the chosen systems also Charlsby-Pinner calculations have been done.

4.3.2 Charlesby-Pinner calculations

In systems in which the probabilities of cross-linking and scission are for all units independent of each other and constant, the following equation was derived (Charlesby and Pinner, 1958):[74][75]

$$s + \sqrt{s} = \frac{p}{q} + \frac{1}{P_n^0 \times q} \qquad (2)$$

where s is the soluble fraction of the polymer, P_n^0 is the average number polymerisation degree, q is the cross-linking density and p the scission density. Assumed that both processes have a constant rate, the following form is accessible:

$$s + \sqrt{s} = \frac{v_p}{v_q} + \frac{1}{v_q \times P_n^0} \times \frac{1}{t} \qquad (3)$$

$s + \sqrt{s}$ is determined experimentally. These data plotted as function of the reciprocal time (1/t) gives a linear correlation, the so called Charlesby-Pinner plot.
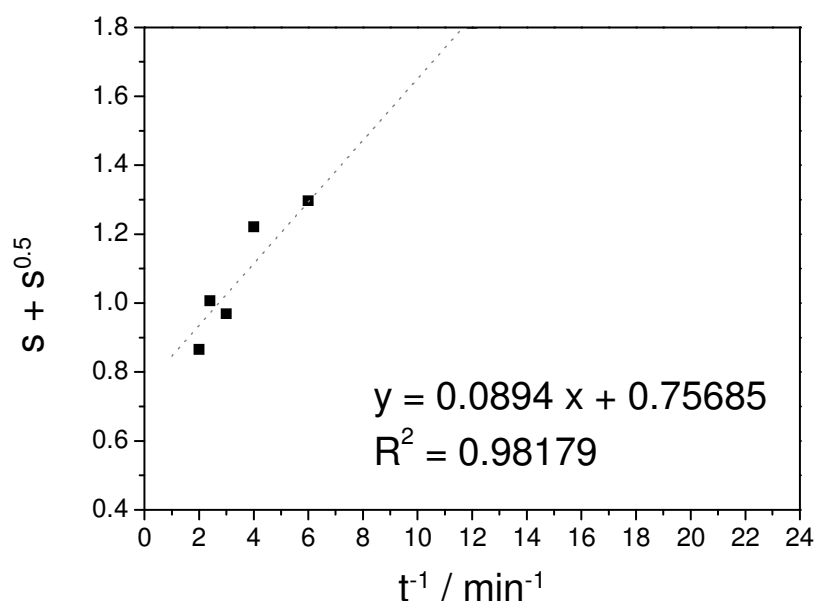
Fig 4-9: Charlsby-Pinner plot of samples with 1 wt-% bisazide

[74] Charlesby, A., Pinner, S.H., *Proceedings of the Royal Society of London. Series A, Mathematical and Physical Science* **1959**, *249*, (1258), 367-386.
[75] Ivan, B., Nagy, T.T., Kelen, T., Turcsányi, B., Tüdös, F., *Polymer Bulletin*, **1980**, *2*, 83-88.

$$y = 0.06772\,x + 0.6333$$
$$R^2 = 0.97459$$
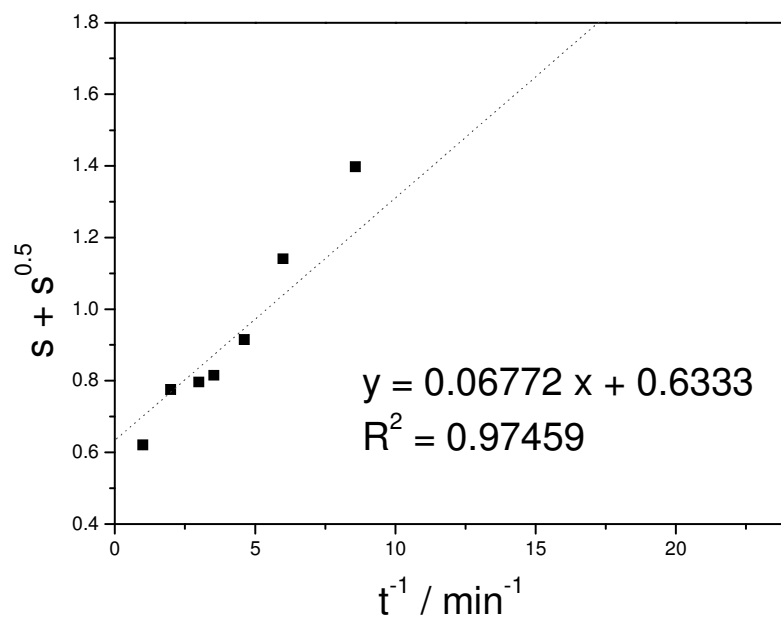
Fig 4-10: Charlsby-Pinner plot of samples with 2 wt-% bisazide

$$y = 0.05468\,x + 0.40107$$
$$R^2 = 0.967$$
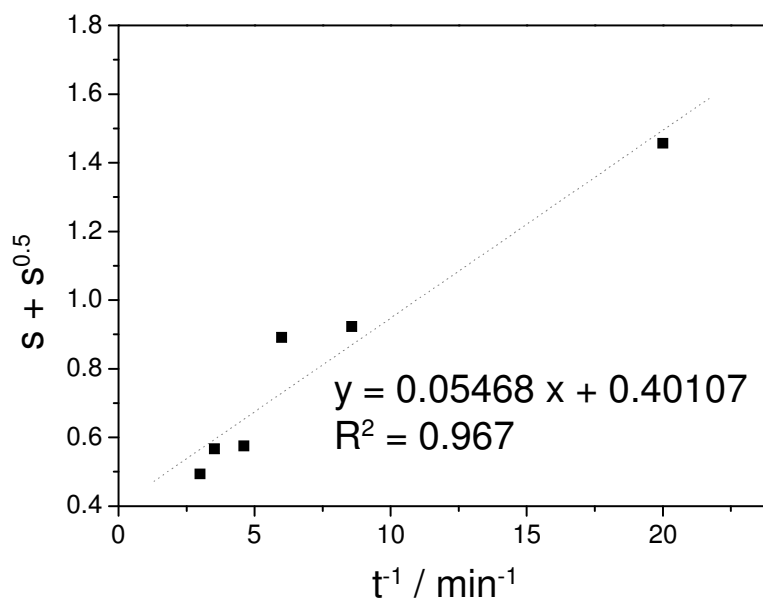
Fig 4-11: Charlsby-Pinner plot of samples with 3 wt-% bisazide
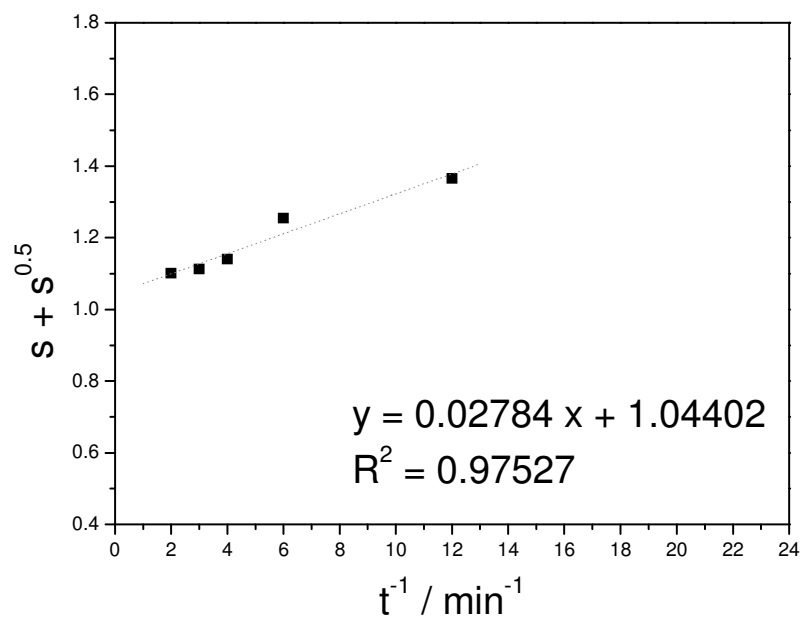
Fig 4-12: Charlsby-Pinner plot of samples with 4 wt-% bisazide
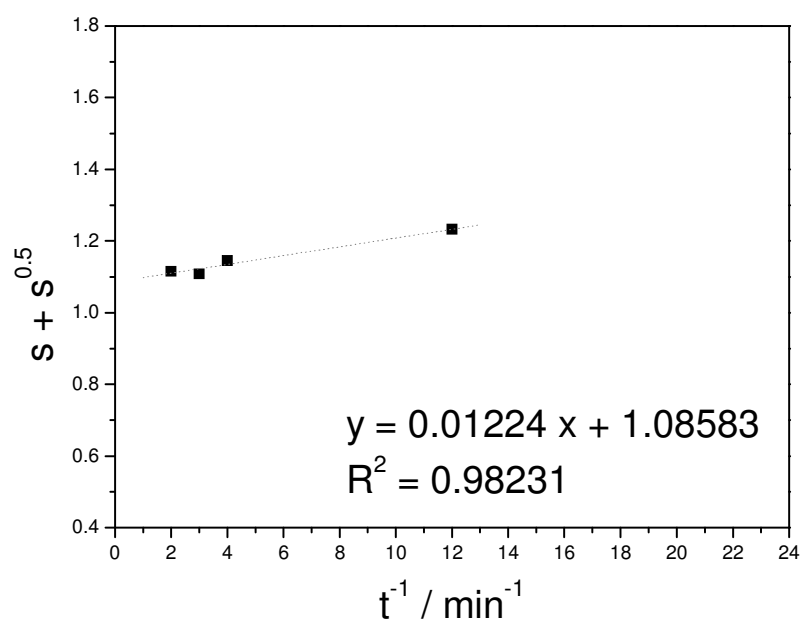
Fig 4-13: Charlsby-Pinner plot of samples with 5 wt-% bisazide

The following values in *table 1* have been calculated as shown in equations (3) above. For a better insight the ratio of v_q and v_p is shown in Fig 4-14. It can be seen that there is a minimum of the curve with 3 wt% of cross-linker. That means that the probability for the crosslinking is much higher than the probability for chain scissoring

and results in a ratio of v_q to v_p of 0.40. With higher concentrations of the bisazide the probability of chain scissoring increases enormously while the probability of crosslinking increases only slightly. The ratio of the experiment with 4 wt% of the crosslinking agent shows a ratio of even 1.04, so the probability of the scissoring is higher than that of the crosslinking step. That is why the maximum of the gelfraction of the 4-wt% sample is reached later than with lower concentrations. This theory gets proved by the experiments with 5 wt% where this trend proceeds.

Table 1: Concentrations of the crosslinking agent and the appending calculated values of q and p

m(Ini) : m(PHA)	v_q	v_p
0.01	0.00932	0.00705
0.02	0.01231	0.00779
0.03	0.01524	0.00611
0.04	0.02993	0.03125
0.05	0.06808	0.07393
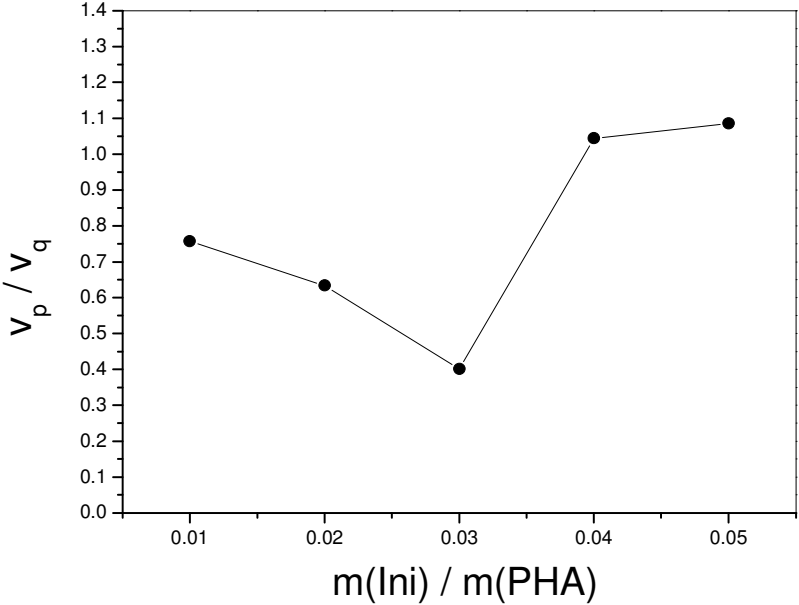
Fig 4-14: Ratio of q / p for the concentrations determined

4.3.3 Photolithography

After the successful proof for the ability of scl-PHAs to undergo photochemical crosslinking with a bisazide also the applicability for photolithographic uses was evaluated.

For this purpose the system investigated was used as a negative photoresist. The procedure is explained in detail above. The patterned image is shown in Fig 4-15.
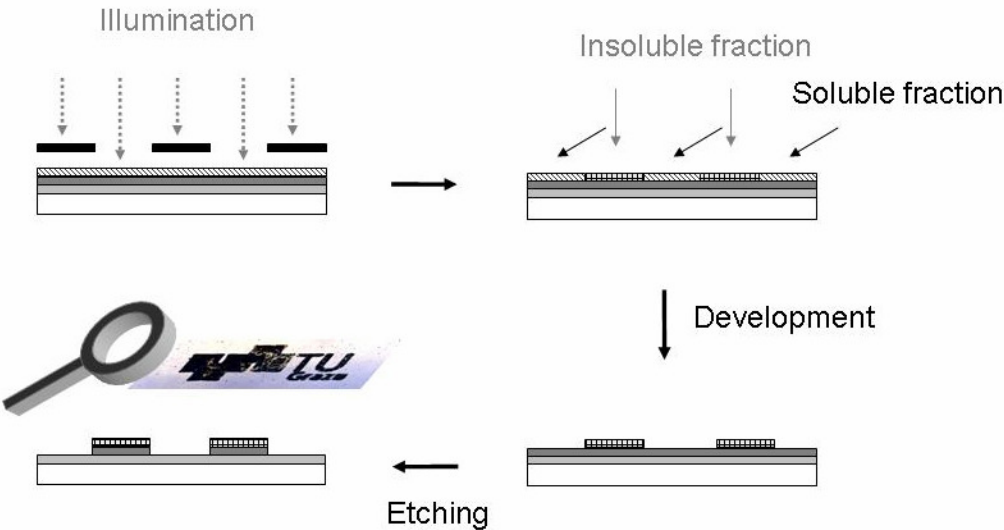
Fig 4-15: Scheme of the generation of the photolithographic imprint

4.4 Conclusion

In this work we introduce a new and promising strategy of crosslinking scl PHAs photochemically. Due to the straight forward and cost effective way of preparation of these PHAs they become attractive candidates for a broad variety of applications. The additional modification via photochemical crosslinking opens again new potential utilisations. It could be shown that the photochemical crosslinking of these scl PHAs with a bisazide as crosslinking agent is possible at all. Various concentrations of crosslinker have been tested and the appropriate gelfractions were determined. Further the optimal concentration of the crosslinker for this system was determined by Charlesby-Pinner calculations due to the ratio of probability of chain scissoring and crosslinking. Also the potential application as biodegradable photoresist was proven.

4.5 Acknowledgement

5. Thiol-ene reaction as tool for cross-linking of polynorbornenes and polymeric micelles

Abstract

The thiol-ene reaction is a established photoreaction of multifunctional thiols and olefines. Virtually any type of olefines will participate in a free radical reaction with the thiol. An advantage over many other photochemical reactions is that the reaction proceeds almost as rapidly in ambient conditions as in inert atmosphere.

In this work we introduce the UV-crosslinking of polynorbornenes made by ring opening metathesis polymerization making use of the residual double bond in the polymer backbone.

The crosslinking experiments were done in thin films and were followed by FTIR measurements, to proof the accessibility of double-bonds in the polymers for the addition of the thiols. As a result of these pre-experiments we created flexible and light transmitting films. To further increase the scope of this reaction, amphiphilic block copolymers were prepared and used to form block copolymer micelles in a selective solvent, which were subsequently crosslinked with pentaerythritol tetra(3-mercaptopropionate) (PETMP). FT-IR, DLS and SEM-measurements were used to prove the successful crosslinking and thus nanoparticle formation.

5.1. Introduction

Amphiphilic block copolymers have gained more and more attention in recent years. Due to their molecular structure they provide an efficient pathway to prepare controlled structures in the nanometer range. Applications of systems like these range from medicine to microelectronics.[76,77,78]

Living polymerizations are an ideal method to prepare well defined amphiphilic block copolymers. Ring Opening Metathesis Polymerisation (ROMP) provides a method for producing low polydispersity of these polymers without protecting group chemistry and with high flexibility concerning functional groups and/or end group fictionalization.[79] Due to the highly controlled molecular weight and length of the polymer chains also the architecture of the formed micelles can be well predicted.[80] For several applications it is necessary to stabilize these self-assembled structures. The most prominent methods for the covalent crosslinking of micelles are the incorporation of a polymerizable or a photo/UV crosslinkable group.[81,82,83,84]

Herein we introduce a crosslinking system for polynorbornenes and amphiphilic block copolynorbornenes without any additional synthetic effort and an exceeding convenient experimental set-up: the thiol-ene reaction. The thiol-ene photo reaction offers many advantages over traditional photopolymerisation and –crosslinking processes including versatility in types of enes and insensitivity versus oxygen.[85]

In this contribution we combine the versatility of ROM polymers with the non sensitive thiol-ene photo reaction. Due to these facts the scope of potential candidates and applications is broad.

We show the feasibility to crosslink diverse polynorbornenes via the double bond in the backbone of the polymer chain with a multifunctional thiol. Using this system lithographic structuring can be realized. Further we determine the sol and gel fraction

[76] Matyjazewski, K.; Gnanou, Y.; Leibler, L. "*Macromolecular Engineering. Precise Synthesis, Materials Properties, Applications*", Vol. 4: Applications; Wiley-VCH: Weinheim, **2007**.

[77] Lazzari, M.; Liu, G.; Lecommandoux, S.; "*Block Copolymers in Nanoscience*"; Wiley-VCH: Weinheim, **2006**.

[78] Förster, S.; Antonietti, M.; *Adv Mater* **1998**, *10*, 195-217.

[79] Slugovc, C.; *Macromolecular Rapid Communications* **2004**, *25*, 1283-1297.

[80] Stubenrauch, K.; Moitzi, C.; Fritz, G.; Glatter, O.; Trimmel, G.; Stelzer, F.; *Macromolecules* **2006**, *39*, 5865-5874.

[81] O'Reilly, R. K.; Hawker, C. J.;Wooley, K. L.; *Chem Soc Rev* **2006**, *35*, 1068-1083.

[82] Wilson, D. J.; Riess, G.; *Eur Polym J* **1988**, *24*, 617-621.

[83] Jiang, X.; Luo, S.; Armes, S. P.; Shi, W.; Liu, S.; *Macromolecules* **2006**, *39*, 5987-5994.

[84] Szczubialka, K.; Nowakowska, M.; *Polymer* **2003**, *44*, 5269-5274.

[85] Hoyle, C.E.; T. Y., Lee; T., Roper; Journal *of Polymer Science Part A: Polymer Chemistry* **2004**, *42*, 5301-5338.

of the built networks. Finally we stabilize self-assembling amphiphilic block co-polynorbornene micelles.

5.2. Experimental

5.2.1. Methods

Unless otherwise noted materials were obtained from commercial sources (Aldrich or Fluka) and were used without further purification. Solvents were purified and dried according to standard procedures and degassed before use. Reactions were carried out under inert atmosphere of argon using standard Schlenk techniques.

endo,*exo*-Bicyclo[2.2.1]hept-2-ene-5,6-dicarboxylic acid dimethyl ester was kindly provided by Orgentis Chemicals GmbH and further purified by distillation.
NMR spectroscopy was performed on a Bruker 300 MHz spectrometer. FT-IR Spectra were obtained with a Perkin Elmer Spectrum One.

Dynamic light scattering measurements were done on a Malvern ZetaSizer equipped with a 633 nm laser.

The number average molecular weight (M_n) as well as the polydispersity index (PDI) were determined by gel permeation chromatography against polystyrene standard with chloroform as solvent.

For UV-irradiation a polychromatic medium pressure mercury lamp from Heraeus was used with a rating of 45 mW/cm^2 and a mercury lamp (Novacure) from EFOS. The highest intensities are obtained at 365, 404 and 437 nm.

As crosslinking agent pentaerythritol tetra(3-mercaptopropionate) (PETMP) and as photoinitiator Lucirin TPO$^©$ were used.

5.2.2. Monomer synthesis

5.2.2.1. endo,exo-bicyclo[2.2.1]hept-5-ene-2,3-dicarboxylic acid dimethyl ester

The provided monomer was characterised by NMR:
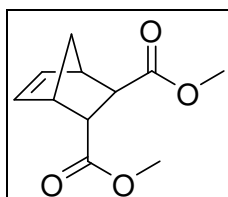
Fig 5-1: scheme of endo,exo-bicyclo[2.2.1]hept-5-ene-2,3-dicarboxylic acid dimethyl ester

^{1}H-NMR (δ, 20 °C, CDCl$_3$, 500 MHz): 6.27 (m, 1H, nb^6), 6.06 (m, 1H, nb^5), 3.71 (s, 3H, COOCH$_3$), 3.64 (s, 3H, COOCH$_3$), 3.37 (t, 1H, nb^3), 3.25 (b, 1H, nb^4), 3.12 (b, 1H, nb^1), 2.68 (dd, 1H, nb^7), 1.61 (d, 1H, nb^7), 1.45 (dd, 1H, nb^7).

^{13}C-NMR (δ, 20 °C, CDCl$_3$, 125 MHz): 174.9, 173.7 (2C, C=O), 137.6, 135.1 (2C, nb^{5,6}), 52.1, 51.8 (2C, CH$_3$), 47.7, 47.6, 47.3, 47.1 (4C, nb^{1,2,3,4}), 45.6 (1C, nb^7).

5.2.2.2. endo,exo-bicyclo[2.2.1]hept-5-ene-2,3-dicarboxylic acid, bis[2-[2-(2-ethoxyethoxy)ethoxy]ethyl] ester
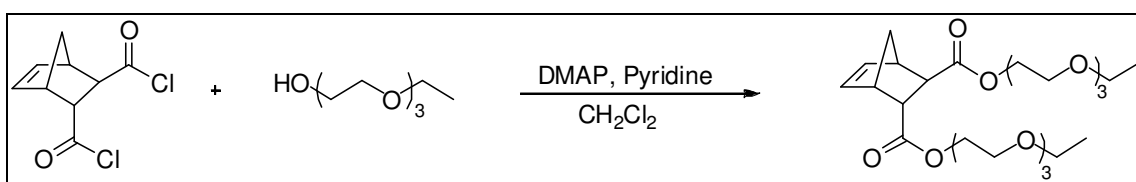
Fig 5-2 Scheme of the reaction to obtain the hydrophilic monomer endo,exo-bicyclo[2.2.1]hept-5-ene-2,3-dicarboxylic acid, bis[2-[2-(2-ethoxyethoxy) ethoxy]ethyl] ester

endo,exo-5-Norbornene-2,3-dicarbonyl chloride (0.75 mL, 4.56 mmol, 1 eq) was diluted with dry CH$_2$Cl$_2$ (20 mL). Then, di(ethyleneglycol)monoethyl ether (1.37 mL, 10.0 mmol, 2.2 eq) and 4-dimethylaminopyridine (DMAP; 0.0278 g, 0.23 mmol, 0.05 eq) were added. The reaction mixture was cooled with an ice bath and pyridine (0.93 mL, 11.4 mmol, 2.5 eq) was added drop wise. A clear solution with a purple precipitate appeared. Then the mixture was stirred for 24 h at room temperature. The reaction was monitored by TLC (Cy:EE = 1:2; detection: UV/VIS, 2% KMnO$_4$ solution, R$_f$: 0.5).

The white precipitate was removed by filtration and the organic layer was extracted with 10% HCl (4x 200 mL). The organic layer was dried over Na$_2$SO$_4$ and the solvent was removed under reduced pressure. Purification was done by column chromatography (silica, Cy:EE = 1:2). Yield: 1360 mg (72 %) colourless oil.

^{1}H-NMR (δ, 20°C, CDCl$_3$, 500 MHz): 6.26 (m, 1H, nb^6), 6.08 (m, 1H, nb^5), 4.33-4.10 (m, 4H, COOCH$_2$), 3.71–3.51 (m, 24H, CH$_2$), 3.43 (t, 1H, nb^3), 3.28 (bs, 1H, nb^4), 3.14 (bs, 1H, nb^1), 2.73 (dd, 1H, nb^2), 1.61, 1.44 (d, 2H, nb^{7a,b}), 1.21 (t, 6H, CH$_3$).

^{13}C-NMR (δ, 20°C, CDCl$_3$, 125 MHz): 174.3, 173.2 (2C, C=O), 137.5, 135.1 (2C, nb^{5,6}), 70.6, 69.8, 69.1 (10C, CH$_2$), 66.7 (2C, *C*H$_2$CH$_3$), 63.9, 63.6 (2C, COO*C*H$_2$), 47.9 (1C, nb^3), 47.7 (1C, nb^1), 47.2 (1C, nb^7), 47.1 (1C, nb^2), 45.8 (1C, nb^4), 15.1 (2C, CH$_3$).

5.2.2.3. exo,endo-2-(tert-butylamino)ethyl Bicyclo[2.2.1]hept-5-ene-2-carboxylate, Mo (1)

exo,endo-2-(*tert*-butylamino)ethyl-bicyclo[2.2.1]hept-5-ene-2-carboxylate hydrochloride [Mo(1)·HCl] (M = 273.15 g·mol^{-1}; 73.22 mmol, 1 eq.) was dissolved in 200 mL CH$_2$Cl$_{2(abs.)}$. Na$_2$CO$_3$·H$_2$O (M = 124.01 g·mol^{-1}; 293.53 mmol, 4 eq.) and Na$_2$SO$_4$ (M = 142.04 g·mol^{-1}; 175.73 mmol, 2 eq.) were added and the suspension was stirred for 24 hours at room temperature. After 24 hours, the mixture was filtered through a funnel. The recovered filtrate's solvent was evaporated under vacuum. The thus-obtained liquid is redissolved in cold *n*-pentane, filtered and concentrated under vacuum. The procedure should be repeated twice. The colorless liquid is dried under vacuum. Yield: 16.16 g (93%) R$_f$ ≈ 0.4 (MeOH).

MS: m/z = 237.2 (M$^+$)

^{1}H-NMR (CDCl$_3$): δ (ppm) = 6.19-5.91 (m, 2.00 H, H5,H6), 4.11 (m, 2.01 H, H9), 3.11-2.76 (2 s,1 m, 2.91 H, H1, H2, H4), 2.77 (m, 2.05 H, H10), 1.89 (dd, 1.04 H, H3), 1.43-1.37 (bs, 3.08 H, H3,H7), 1.28 (bs, 0.97 H, NH), 1.10 (s, 9.16 H, H12).

FT-IR (CaF$_2$): 3324, 3063, 2968, 2869, 1735, 1448, 1362, 1336, 1186, 1110 cm^{-1}.

5.2.2.4. exo,endo-n-dodecyl Bicyclo[2.2.1]hept-5-ene-2-carboxylate, Mo (2)

Freshly cracked and cooled cyclopentadiene (M = 66.1 g·mol^{-1}; 98.03 mmol, 2 eq.) and 20 mL CH$_2$Cl$_{2 (abs.)}$ were added to a stirring flask. Lauryl acrylate (M = 240.38

g·mol^{-1}; 49.05 mmol, 1 eq.) was added dropwise during 10 min. The reaction was stirred for 24 h at 40 °C. After full consumption of the lauryl acrylate (monitored by TLC), the crude product was purified by column chromatography (SiO$_2$, cyclohexane/ethyl acetate 10:1). The colorless liquid was dried under vacuum. Yield: 12.18 g (81 %), R$_f \approx$ 0.27 (CH:EE=30:1)

MS: m/z = 306.6 (M$^+$)

^{1}H-NMR (CDCl$_3$): δ (ppm) = 6.20-5.93 (dd, 2.00 H, H5,H6), 4.05 (m, 1.99 H, H9), 3.20 (bs, 0.83 H, H1), 3.03 (bs, 0.16 H, H1), 2.94-2.90 (m, 1.81 H, H2,H4), 2.19 (m, 0.19 H, H2), 1.89 (m, 1.00 H, H3), 1.65-1.52 (m, 2.05 H, H10), 1.43-1.26 (m, 21.16 H, H3,H7,H3, H11-H19), 0.88 (t, 3.02 H, H20) For the allocation numbering, please see Fig 5-3.

FT-IR (CaF$_2$): 3063, 2925, 2855, 1736, 1466, 1335, 1175, 1110 cm^{-1}.
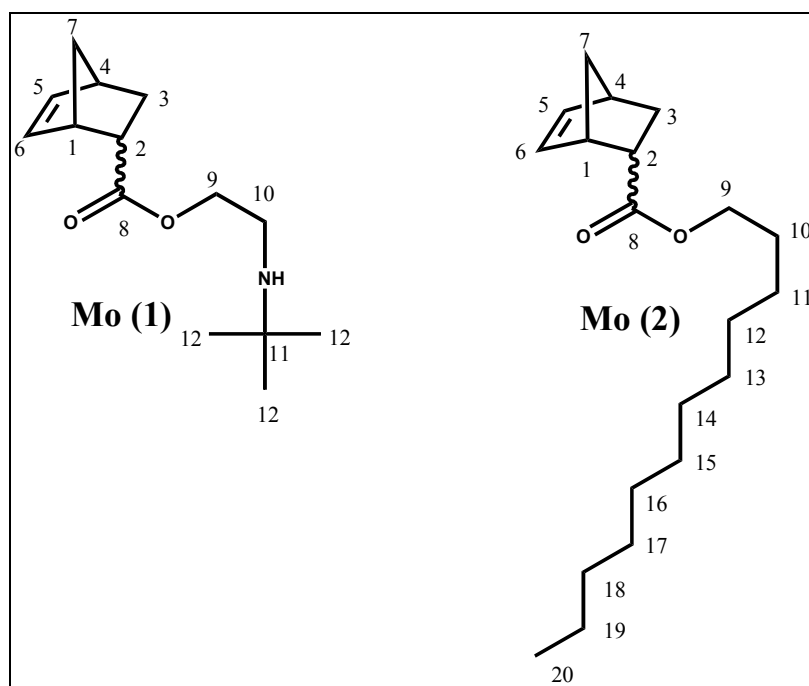
Fig 5-3: scheme of the to monomers exo,endo-2-(tert-butylamino)ethyl Bicyclo[2.2.1]hept-5-ene-2-carboxylate, Mo (1) and exo,endo-n-dodecyl Bicyclo[2.2.1]hept-5-ene-2-carboxylate, Mo (2)

5.2.3. Homopolymer synthesis

5.2.3.1. Homopolymer synthesis for endo,exo-bicyclo[2.2.1]hept-5-ene-2,3-dicarboxylic acid dimethyl ester

To a solution of endo,exo-bicyclo[2.2.1]hept-5-ene-2,3-dicarboxylic acid dimethyl ester (660.0 mg, 1,32 mmol, 300 eq) in dry CH$_2$Cl$_2$ (5 mL), a solution of the

initiator (H₂IMes)(pyridine)(Cl)₂Ru=Ind [$C_{15}H_{10}$ = Indenyliden (Ind)], 3.13 mg, 0.0043 mmol, 1 eq] in dry CH_2Cl_2 (1 mL) was added. After consumption of the monomer, monitored by TLC (Cy:EE = 1:5; detection: UV/VIS, 2% KMnO₄ solution, R_f: 0.0), the reaction was terminated with ethylvinyl ether (100 μL, excess) and stirred for 15 min at room temperature. The polymer was purified by repeated precipitation of CH_2Cl_2 solutions (1 mL) of the polymer into cold *n*-pentane. Yield: 81% brown, gluey solid.

^1H NMR (CDCl₃): δ = 7.30–7.11 (bs, 10H, Ph), 5.53–4.79 (bm, 8H, -CH=CH, OCH₂Ph), 3.53–3.09 (bm, 10H, CH₂OCH₃), 3.08–2.79, 2.76–2.48, 2.32–2.02, 2.02–1.14 (bm, 12H, cp).
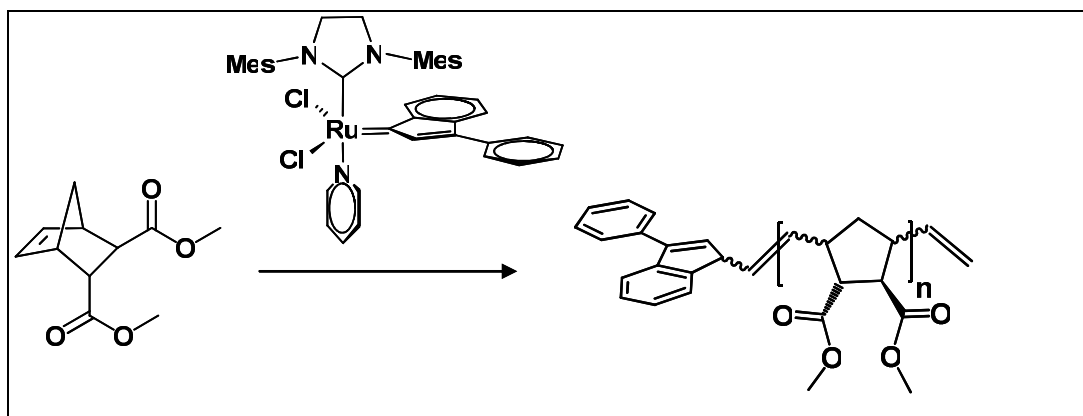
Fig 5-4: ROM Polymeristion of the homopolymer

5.2.3.2. Homopolymer synthesis for exo,endo-2-(tert-butylamino)ethyl Bicyclo[2.2.1]hept-5-ene-2-carboxylate

The polymerizations were performed under inert gas atmosphere in the glove box. For the synthesis of the homopolymers, Mo (1) (237.34 g·mol⁻¹, 2 g; 8.43 mmol; 600 eq.) was dissolved in $CH_2Cl_{2(abs.)}$. For the polymerizations, the initiator (25.75 mg, 0.035 mmol, 1 eq.) was dissolved in a small amount of $CH_2Cl_{2(abs.)}$ and added to the solution, upon which its color changed from green to brown. The reaction mixture was stirred at 250 rpm at room temperature. After full conversion of the monomers (monitoring by TLC), an excess of ethyl vinyl ether (1 mL) was added to quench the reaction and to remove the catalyst from the polymer. The polymer was dissolved in dichloromethane, precipitated twice in cold ethanol or *n*-pentane (depending on precipitation tests) and once in water (using THF as solvent in the latter case) to eliminate water soluble constituents.
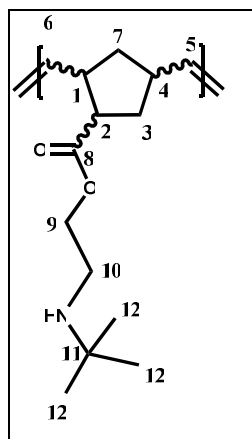
¹H-NMR (CDCl₃):

δ (ppm) = 5.32 (m, 2.00 H, H5,H6), 4.11 (t, 1.99 H, H9), 3.23-2.21 (m,s, 5.07 H, H1, H2, H4, H10), 2.15-1.38 (s,m, 5.18 H, H3, H7, NH), 1.09 (t, 9.02 H, H12)

FT-IR (CaF₂): 3320, 2962, 2866, 1730, 1447, 1362, 1174, 972 cm⁻¹

Fig 5-5: scheme of exo,endo-2-(tert-butylamino)ethyl Bicyclo[2.2.1]hept-5-ene-2-carboxylate

5.2.4. Blockcopolymers

5.2.4.1. endo,exo-bicyclo[2.2.1]hept-5-ene-2,3-dicarboxylic acid, bis[2-[2-(2-ethoxyethoxy)ethoxy]ethyl] ester and endo,exo-bicyclo[2.2.1]hept-5-ene-2,3-dicarboxylic acid dimethyl ester

To a solution of *endo*,*exo*-bicyclo[2.2.1]hept-5-ene- 2,3-dicarboxylic acid dimethyl ester (30 eq) in dry CH_2Cl_2 a solution of the initiator $(H_2IMes)(pyridine)_2(Cl)_2Ru=Ind$ [$C_{15}H_{10}$ = Indenyliden (Ind)] (1 eq) in dry CH_2Cl_2 was added. After consumption of the monomer, as monitored by TLC (Cy/EE 5:1, R_f = 0.0), *endo*,*exo*-bicyclo[2.2.1]hept-5-ene- 2,3-dicarboxylic acid, bis[2-[2-(2-ethoxyethoxy) ethoxy]ethyl] ester (70 eq) was added. After finished polymerization, monitored by TLC (Cy/EE 1:5, R_f = 0.0), the reaction was terminated with ethylvinyl ether (100µL, excess) and stirred for 15 min at room temperature. The polymer was purified by repeated precipitation of CH_2Cl_2 solutions of the polymer into *n*-pentane. The product was obtained as a light brown, gluey solid.
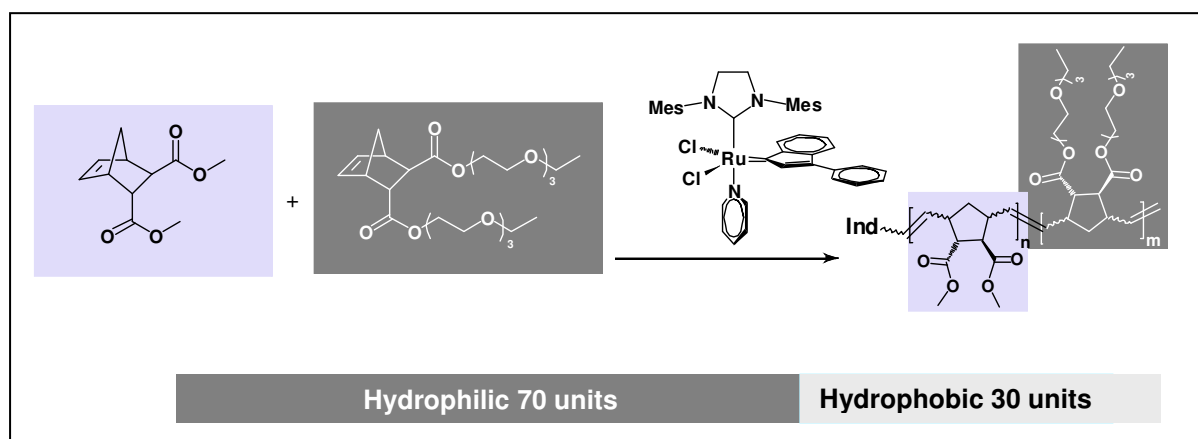
Fig 5-6: Scheme of the block-copolymer synthesis and the ratio of hydrophilic and hydrophobic units
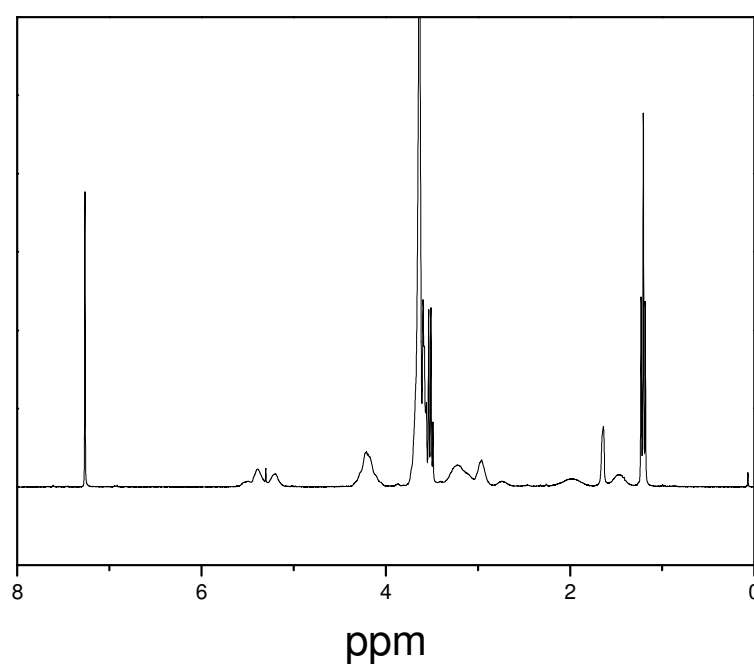
Fig 5-7: ^{1}H spectrum of the block-co-polynorbornene

^{1}H-NMR (δ, 20 °C, CDCl$_3$, 500 MHz): 5.63-5.08 (m, 2H, CH=CH), 4.34-3.98 (m, 3H, COOCH$_2$) 3.76–3.44 (m, 18H, OCH$_2$, 1.5H COOCH$_3$), 3.38-2.83 (m, 4H, cp$^{1, 2, 3, 5}$), 2.23–1.33 (m, 2H, cp^4), 1.26-1.09 (m, 4.5H, CH$_3$).

FT-IR(film on CaF$_2$, cm^{-1}): 2967-2869 (m), 1732 (s, $v_{C=O}$), 1645 (m), 1444 (w), 1382 (w), 1357 (w), 1259 (w), 1177 (w), 1110 (s).

M_n= 44200, PDI = 1.1.

5.2.4.2. exo,endo-2-(tert-butylamino)ethyl Bicyclo[2.2.1]hept-5-ene-
2-carboxylate and exo,endo-n-dodecyl Bicyclo[2.2.1]hept-5-
ene-2-carboxylate

For the copolymers poly (1_x-co-2_{600-x}), Mo (1) (237.34 g·mol^{-1}, 1.00/2.51/4.01 g; 4.21/10.57/16.90 mmol; x = 120/300/480 eq.) and Mo (2) (306.48 g·mol^{-1}, 5.17/3.23/1.31 g; 16.86/10.53/4.27 mmol; 600-x eq.) were dissolved in CH$_2$Cl$_{2\ (abs.)}$.
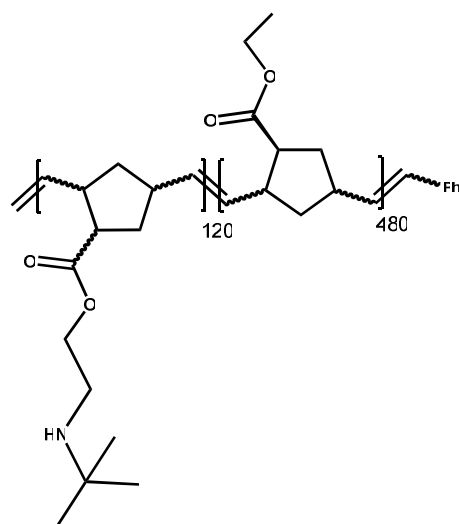
^{1}H-NMR (CDCl$_3$):

δ (ppm) = 5.64-4.98 (m, 2.00 H, H5,H6 $^{Mo(1),Mo(2)}$), 4.48-3.68 (m, 1.96 H, H9 $^{Mo(1),Mo(2)}$), 3.23-2.38 (bs, 3.45 H, H1,H2,H4 $^{Mo(1),Mo(2)}$, overlay H10 $^{Mo(1)}$), 2.19-1.51 (bs,m, 4.66 H, H3,H7 $^{Mo(1),Mo(2)}$, overlay H10 $^{Mo(2)}$), 1.49-1.25 (s, 14.58 H, NH $^{Mo(1)}$, H11-H19 $^{Mo(2)}$), 1.09 (s, 1.83 H, H12 $^{Mo(1)}$), 0.88 (t, 2.42, H20 $^{Mo(2)}$)

Fig 5-8: scheme of the copolymer

FT-IR (CaF$_2$): 3348, 2957, 2919, 2857, 1732, 1460, 1363, 1170, 965 cm^{-1}.

For the polymerization the procedure was carried out as described in chapter 5.2.2.3.

5.2.5. Determination of the gelfraction of thin films

Thin films were obtained via spin coating of solutions of polymers in CH$_2$Cl$_2$onto CaF$_2$ plates. The films were illuminated and afterwards developed in CH$_2$Cl$_2$. The comparison of FT-IR spectra after the illumination and after the development allows conclusions of the sol fraction: due to the crosslinking the polymer network becomes insoluble and the remaining film detected in the FT-IR spectra equates to the sol fraction. Unless otherwise noted, the peak of the C=O stretching vibration (about 1735 cm^{-1}) of the polynorbornene esters has been used as reference band for these evaluations.

5.2.6. Micellisation of the block-co-polymer

Three different block-copolymer micelle solutions in H_2O were prepared as follows: one part with the block-copolymer without any additional chemicals, one part with the block-copolymer an additional photo initiator and finally a part with the polymer, the photo initiator and the crosslinking agent.

The Polymer was readily dispersed in water and equilibrated for 12 hours.
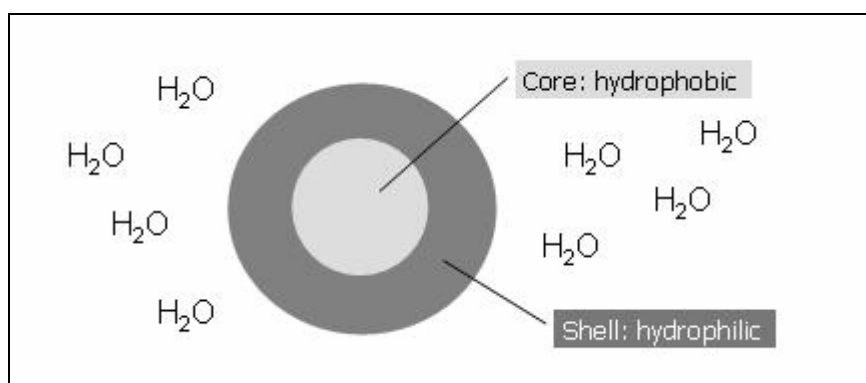
Fig 5-9: Micellisation of the block-copolymer in water

5.3. Results and discussion

5.3.1. Pre-test for the crosslinking of polynorbornenes

5.3.1.1. Crosslinking of endo,exo-Bicyclo[2.2.1]hept-2-ene- 5,6-dicarboxylic acid dimethylester homopolymers

The first approach for the crosslinking of the polymers was to proof the ability of the double bonds in the backbone of the polymers for the thiol-ene reaction as proposed in Fig 5-10.
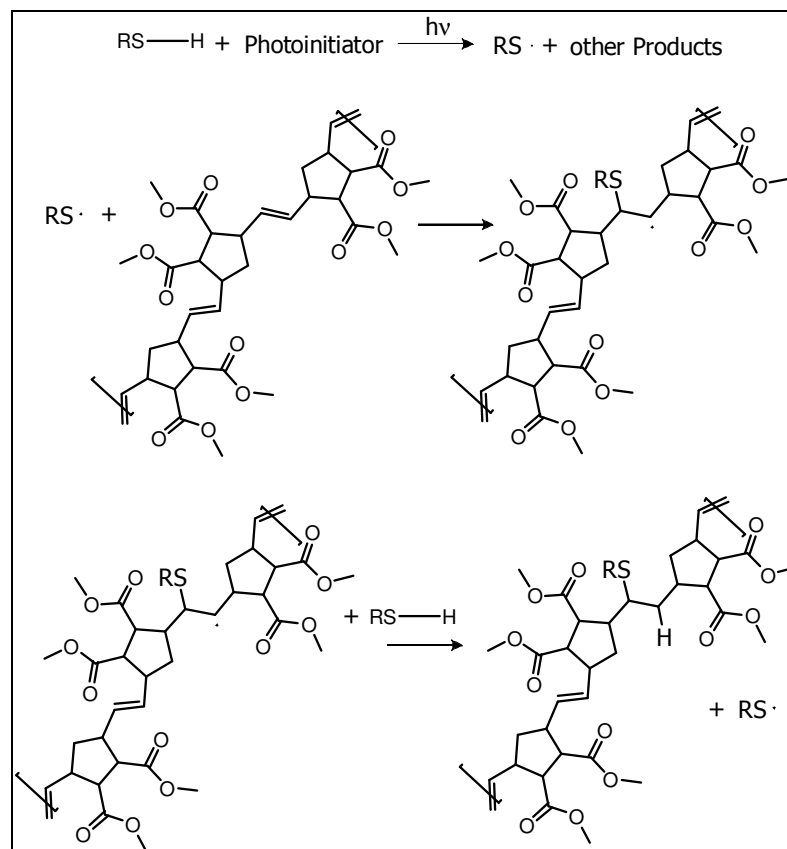
Fig 5-10: Scheme of the thiol-ene reaction a polynorbornenedimethylester

The thiol used in the following experiments is a tetrathiol called pentaerythritol tetra(3-mercaptopropionate).
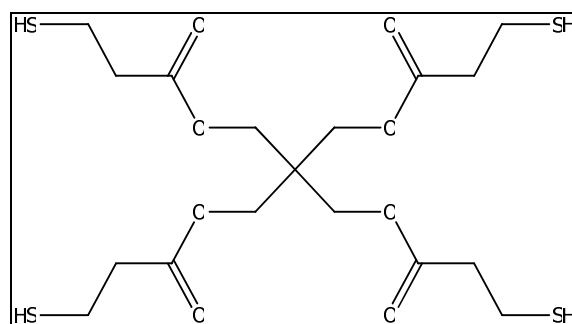
Fig 5-11: Pentaerythritol tetra(3-mercaptopropionate)

The cross-linking pre-testing was done with the homopolymer *endo,exo*-bicyclo[2.2.1]hept-5-ene- 2,3-dicarboxylic acid dimethyl ester with an average of 300 monomerunits per polymer chain.
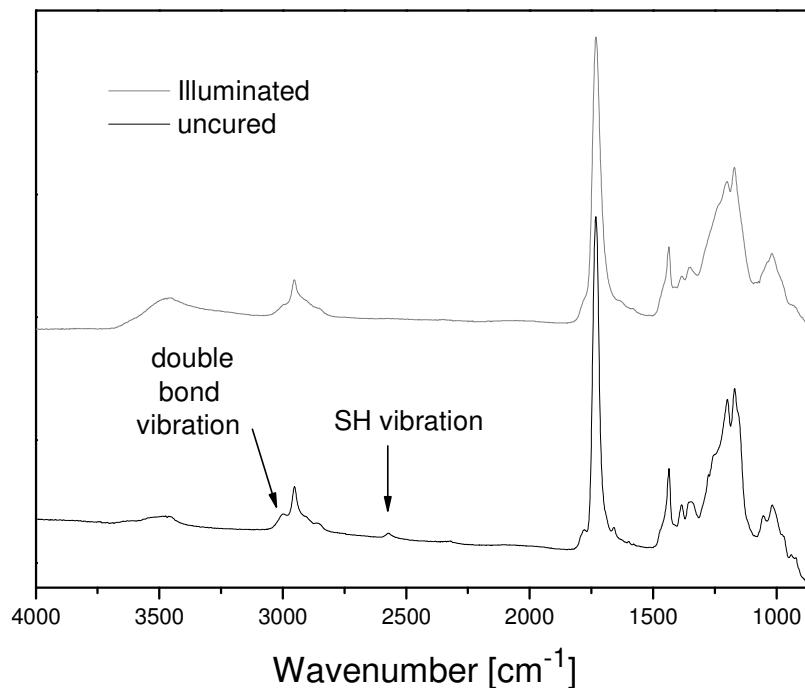
Fig 5-12: Comparison of the IR-spectra before and after illumination of the polynorbornene dimethylester with benzophenone as photoinitiator

In Fig 5-12 the FTIR-spectra of an unilluminated and illuminated sample of the reaction mixture of the polymer, the tetra-thiol and benzophenone as photoinitiator are shown. In the spectrum of the untreated composite some differences to the illuminated one can be seen: at 3002 cm^{-1} a small peak can be observed which can be assigned to the stretching vibration of the hydrogen in the =C*H*- group. This band gets diminished after illumination as well as the peak at 975 cm^{-1} which is dedicated to the deformation vibration of the same group. The band at 2572 cm^{-1} belongs to the S*H* stretching vibration and disappears completely after the treatment.

For optimisation of the reaction various photoinitiators (shown in Fig 5-13) has been tested with this polymer and the crosslinker showed above.

Irgacure 250

Darocur

Irgacure 2959

Benzopehenone

Lucirin TPO

2,6-bis(4-azidobenzylidene)-

4-methylcyclohexanone
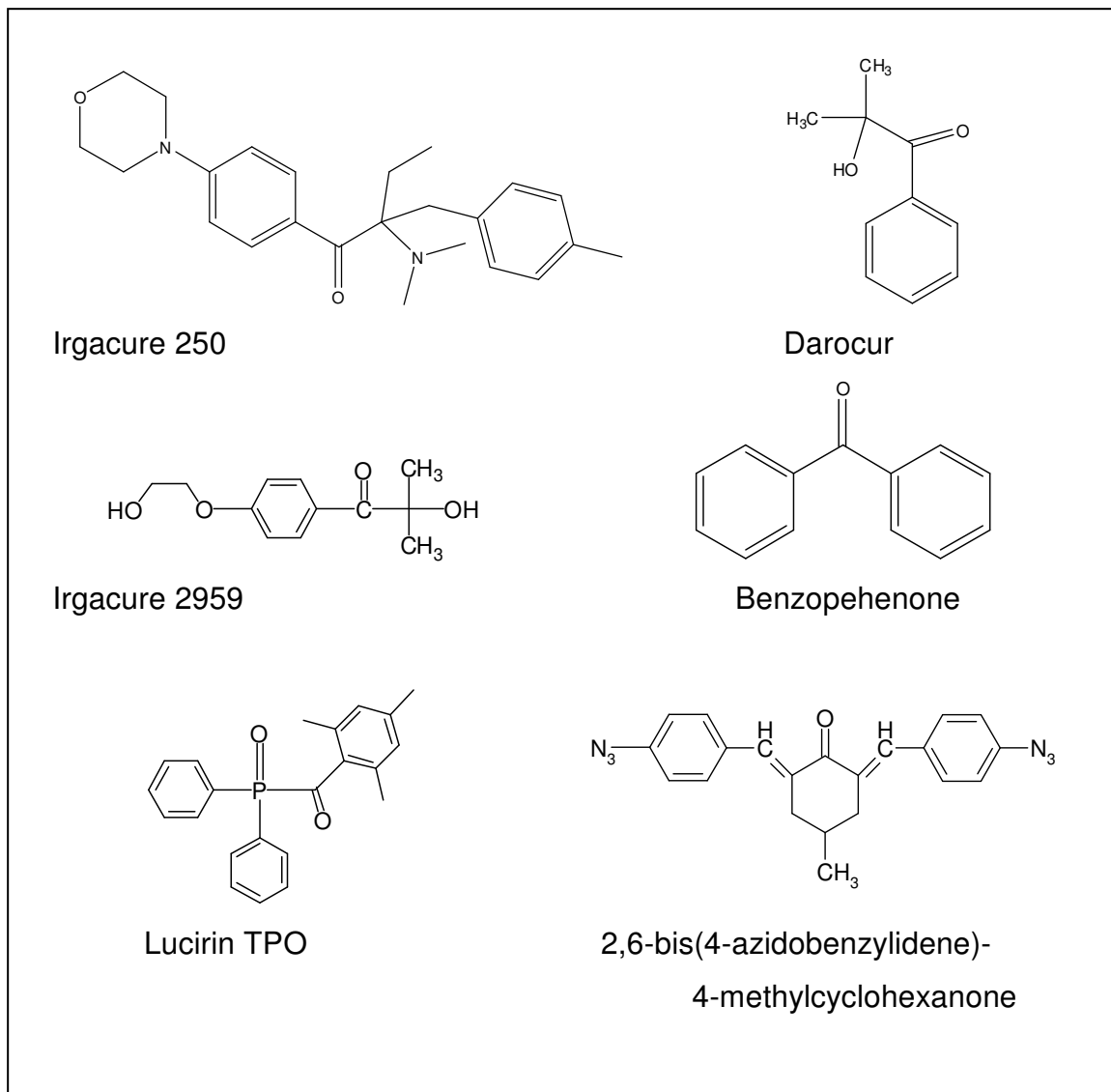
Fig 5-13: Overview of the photoinitiators tested
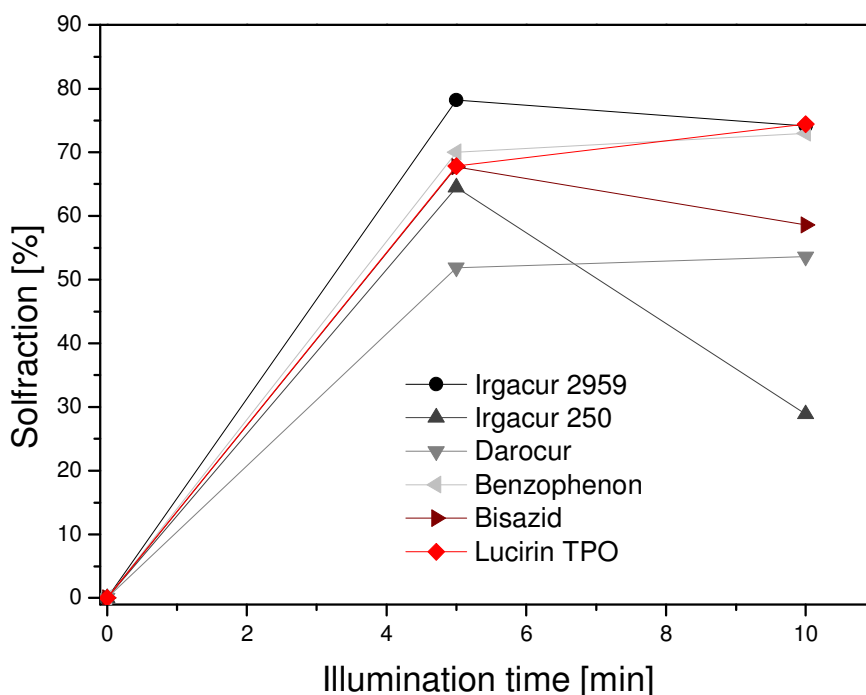
Fig 5-14: Generation of the sol-fraction depending on the illumination duration and the photoinitiator

The ratio of double bonds to thiol-groups in the film was 4:1 and 5 wt% of the photoinitiator was added.

After spin-coating the samples were measured by means of FT-IR, illuminated for different durations (0, 5, 10 minutes) and developed for at least 15 minutes in dichloromethane. The illumination and the progress of the thiol-ene reaction were monitored by FT-IR-spectroscopy, as described above. In the diagram above the solfractions of the polymers after illumination are shown. The highest solfraction reaches the photoinitiator Irgacur 2959 but because of the better mixing and an easier handling with a liquid photoinitiator Lucirin TPO was chosen for further experiments.

5.3.2. NMR study of norbornene oligomeres

In a series of experiments with norbornene oligomers the ability of the double bonds of the backbone to undergo the thiol-ene reaction was investigated by NMR (nuclear magnetic resonance) spectroscopy. The oligomers were synthesized the same way like the polymers accept of the fact that the ratio of catalyst to monomer

was much lower: the oligomers consist of only ten monomer units per molecule catalyst (compared to three hundred in the polymer synthesis). Butyl-3-mercaptopropionate was used as thiol component and Lucirin TPO® as photoinitiator.
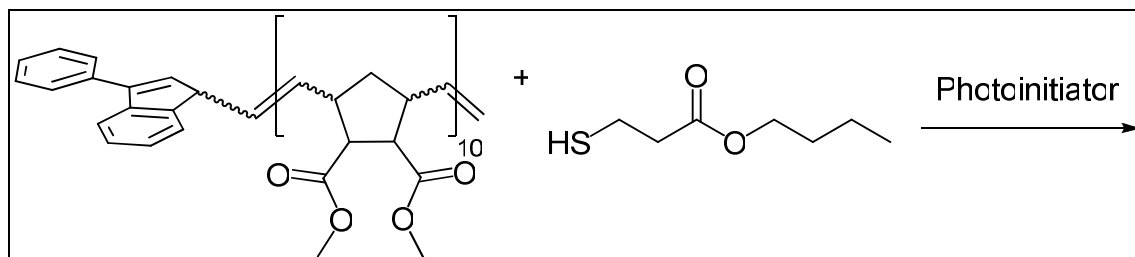
Fig 5-15: scheme of the components of the thiol-ene reaction

Now it was interesting to see if the double bonds react with the thiol and if the sterical hindrance due to the side chains of the oligomers influences the reactivity.

In solution no thiol-ene reaction could be observed. Finally, with elongated illumination duration in the solid state the following results were obtained:
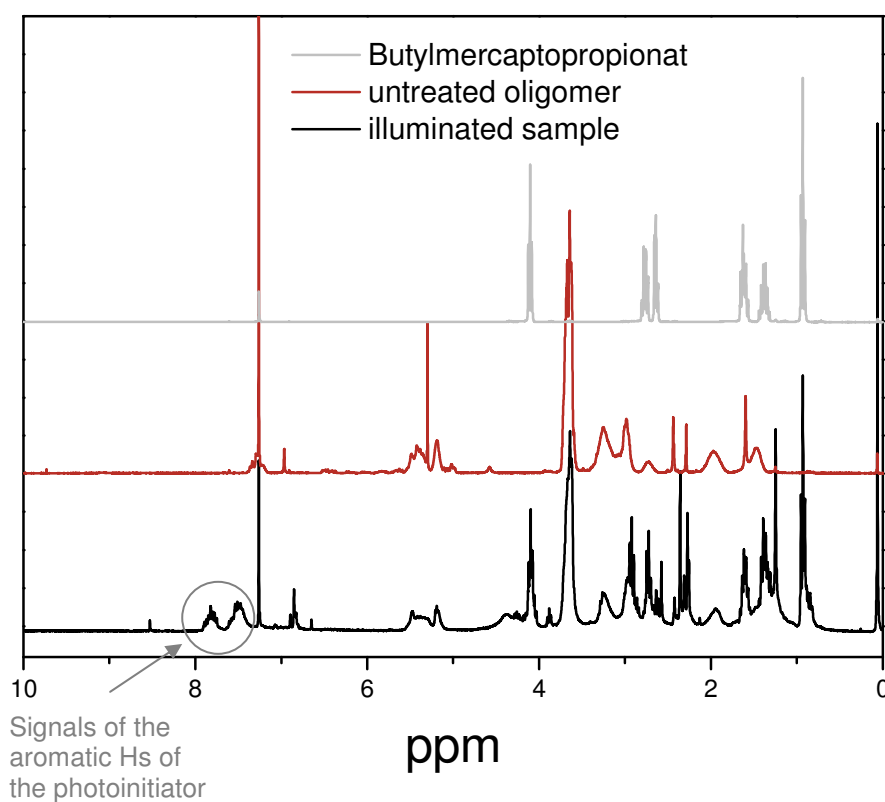
Fig 5-16: Comparison of the NMR spectra of the thiol component, the oligomeric polynorbornene and the illuminated mixture of both with the additional photoinitiator lucirin TPO.

Butyl-3-mercaptopropionate:

^{1}H-NMR: (δ, 20 ℃, CDCl$_3$, 500 MHz): 4.106 (t, $^3J_{HH}$ = 7 Hz, 2H, CH$_2$, -OC(=O)-CH_2), 2.808-1.732 (m, 2H, CH$_2$, -S-CH_2-), 2.639 (t, $^3J_{HH}$ = 6.058 Hz, 2H, CH$_2$, -C(=O)O-CH_2), 1.661 – 1.567 (m, 2H and 1H, CH$_2$ and SH, -C(=O)-O-C-CH_2- and SH), 1.440-1.317 (m, 2H, CH$_2$, CH_2-CH$_3$), 0.929 (t, $^3J_{HH}$ = 7.573 Hz, 3H, CH_3)

Oligomer:

^{1}H-NMR: (δ, 20 ℃, CDCl$_3$, 500 MHz): 7.33–7.16 (m, 5H, Ph), 6.51–6.37 (m, 1H, CH-Ph), 6.25–5.85(m, 1.5H, CH=CH, CH=CH$_2$), 5.53–5.14 (m, 20.5H, CH=CH-Oligomer), 5.10–4.98 (m, 2H, CH=CH$_2$), 3.75–3.55 (m, 60H, O-CH$_3$), 3.38–2.61 (m, 40H, cp^{1,2,3,5}),2.09–1.38 (m, 20H, cp^4).
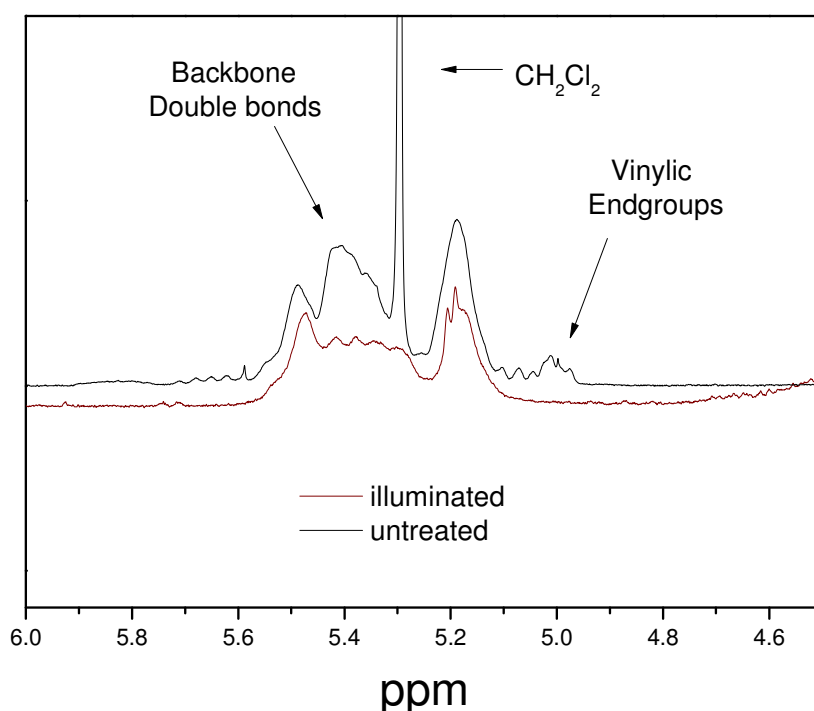
Fig 5-17: Section of the NMR spectra shown above: the comparison of the untreated oligomer and of the illuminated oligomer (including the Butyl-3-mercaptopropionate and Lucirin TPO as photoinitiator).

In the NMR spectra in Fig 5-16 the thiol component Butyl-3-mercaptopropionate, the Oligomer of the used Norbornene and the combination of both with the photoinitiator after an illumination time of 10 minutes is shown. For a better

illustration of the reaction investigated the range from 6.0 ppm to 4.5 ppm is shown in Fig 5-17.

The peak of the proton in the –SH group at 1.6 ppm overlaps with another peak of the Butyl-3-mercaptopropionate and with a peak of the oligomer. The decrease of the integral of this peak after the illumination allows the assumption that the S-H bond gets broken due to the illumination.

It can be easily seen that the vinylic groups disappear completely after the treatment. Further the peak at 5.4 ppm decreases which can be an indication for the consumption of the double bonds in the backbone of the oligomer.

With these first NMR-investigations we showed that the thiol-ene reaction is a possible tool for the photochemical modification of polynorbornenes.

5.3.3. Crosslinking of thin films

In the next series of cross-linking experiments the intensity of the UV-lamp was varied as well as the concentration of the cross-linking agent. For this purpose the Novacure-UV-lamp was used in a distance of 7 cm to the samples. The intensities of the lamp used were 5000 mW/cm^2 and 10000 mW/cm^2 respectively.

The ratio of double bonds to thiol-groups in the film was 4:1 and 2:1 respectively. 5 wt% of the photo initiator Lucirin TPO$^{©}$ were added.
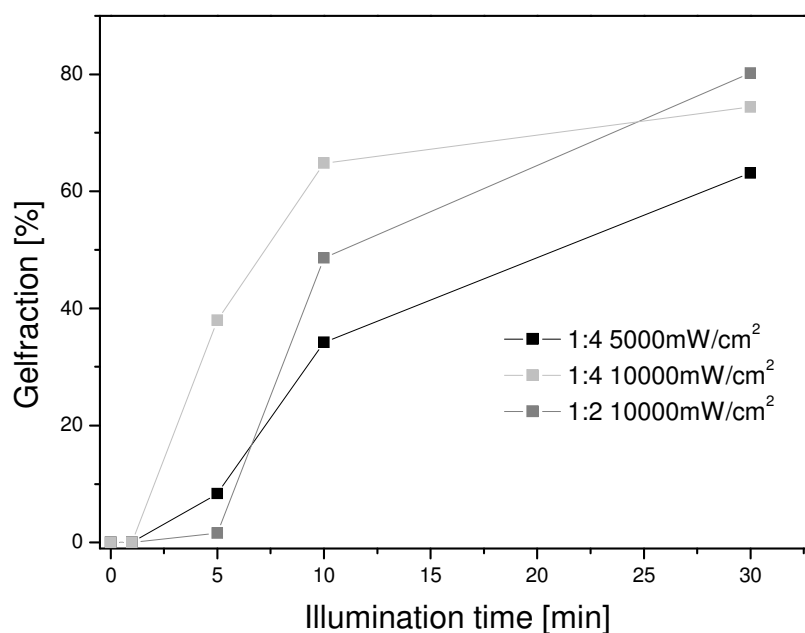
Fig 5-18: Gelfraction of the cross-linked dimethylesterpolynorbornene with various PETMP concentrations and intensities

In Fig 5-18 the Gel-fraction of the cross-linked polynorbornendimethylester is plotted against the time of irradiation. It can be seen that the onset of the photo reaction takes more than one minute with this lamp under the chosen conditions. Further it is shown that the enhanced intensity of the lamp leads to an accelerated cross-linking reaction and a higher insoluble fraction. The doubled concentration of the thiol in the reaction mixture does not lead to a shorter onset time of the reaction. In the first 10 minutes the gel-fractions are lower than the composition with a ratio of 1:4. Not until 30 minutes of illumination the higher thiol concentration shows advancement. A possible explanation could be that the generated tetrathiol-radicals react first with each other and so the cross-linking reaction with the polymer occurs later. In this way the high gel-fraction after 30 minutes irradiation duration is not a discrepancy.
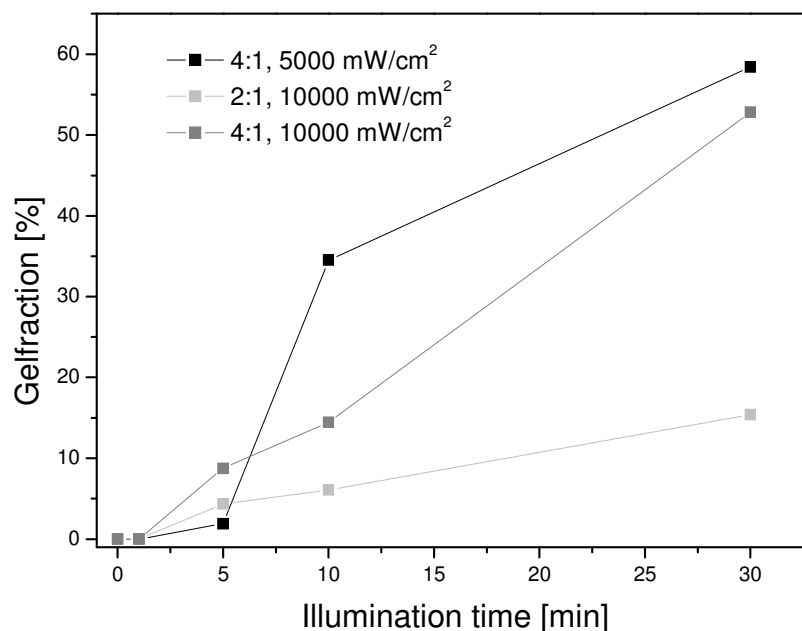
Fig 5-19: Gelfraction of the cross-linked Polymoter with various PETMP concentrations and intensities

In figure Fig 5-19 polynorbornene *tert*-aminobutylester has been treated as the polynorbornene dimethyl ester before. Also in this series of experiments the onset of the photoreaction takes more than one minute. Contrary to expectations the ratio of thiol to doublebond equivalent is 4:1 with a lower intensity of 5000 mW/cm^2 shows the highest gelfraction after 10 and 30 minutes. In comparison to the *endo,exo*-bicyclo[2.2.1]hept-5-ene- 2,3-dicarboxylic acid dimethyl ester the polynorbornene tert.-aminobutylester is (in terms of sterical properties) more demanding for the cross-linking reaction due to the bulky side chains of the polymer. That results generally in lower gelfractions: the maximum value achives almost 60% instead of 80% in the first experiment series. So it is explicable that the higher tetrathiol concentration leads to a low gelfraction: provided that the generated thiol radicals react first with each other and build kind of midsize aggregates, the crosslinking step with the polymer chains is not possible anymore. The backbone of the polymers is shielded by the sidechains and the double bonds cannot react with the – now - more voluminous crosslinking reagent.

- 74 -

The higher intensity of the lamp with the same concentration of crosslinker leads in the initial phase of the illumination to a higher gelfraction as expected but falls behind at longer curing durations. It suggests itself that this phenomenon has a similar background like in the case before.

Also free standing films up to 500-750 micrometers have been prepared with both polymers. The cross-linked polymer swells in the surrounding of the solvent which is used for the development whereas the uncured samples are dissolved completely.

Fig 5-20: picture of the crosslinked swollen polynorbornene tert-aminobutylester sample in dichlormethane (right) and the empty left glass substrate of the uncured sample

After drying of the samples the mechanical properties of the material are similar to those of elastomers. During longer storing periods the material is hardenenig.

This system is adaptive for various homo-polymers and as well assessable to photo-lithographic structures. The polymeric substrates have been coated with a scraper with a solution of dichloromethane and polynorbornenes with different functional groups (e.g. methylester or glycolether) and illuminated with a mask for 10 minutes. The developing step in dichloromethane took 15 min.

The thickness of the coatings ranged between 20 and 25 micrometers.
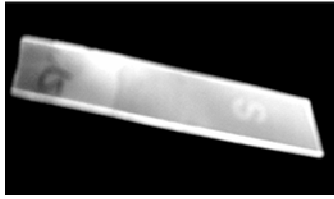
Fig 5-21: Lithographic images in two different polynorbornenes (the glycol derivative above and the diethylester below)

Table 1: Contact angles of the used polynorbornene derivatives

Contact angle	Glycolether	Methylester
Water	30.3°± 0.7	66.5°± 0.3
Diiodomethane	115.2°± 1.1	51.3°± 0.8

With contact angle measurements the properties of the different norbornene derivatives in terms of surface energy are shown.
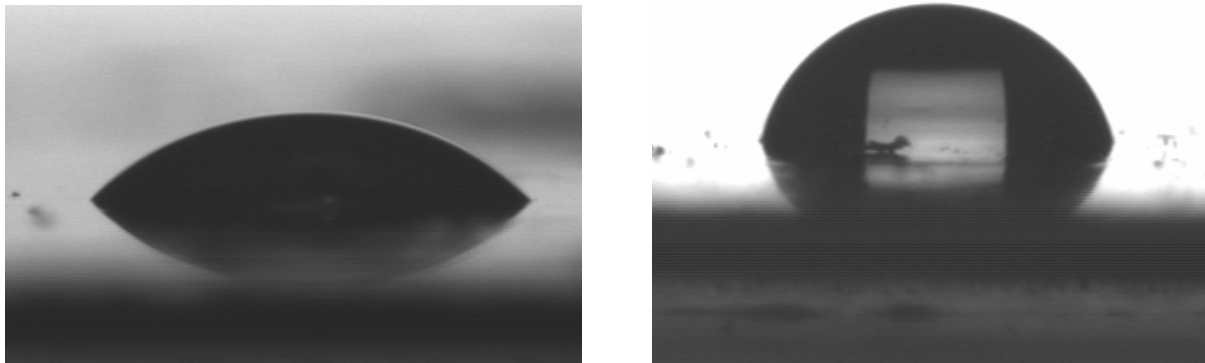
Fig 5-22: Contactangle measurement of water on the glycol (left) and the dimethylester (right) norbornenes
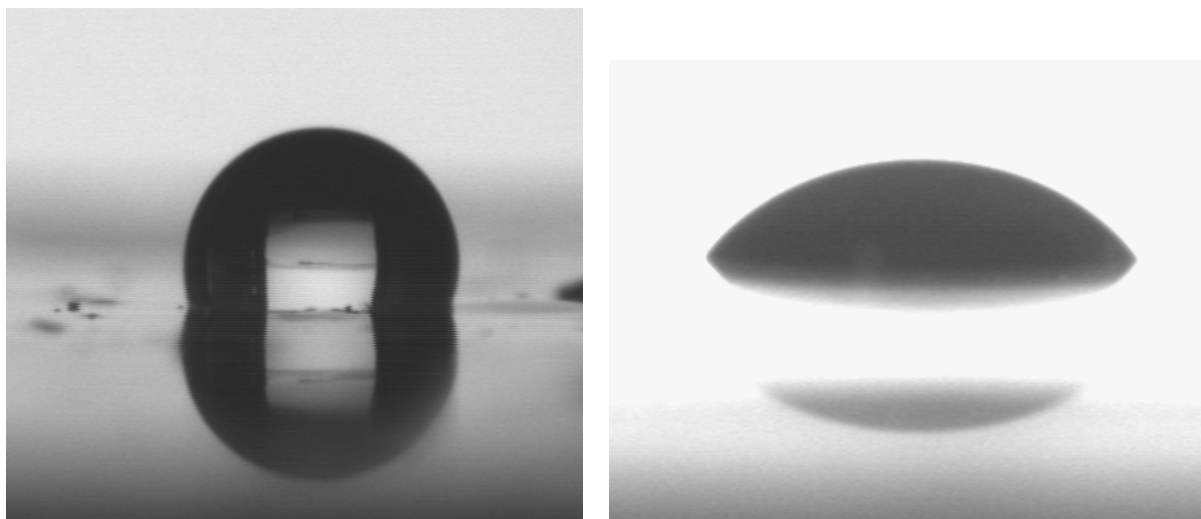
Fig 5-23: Contactangle with diiodomethane on the glycol (left) and the dimethylester (right) norbornenes

In the pictures of the contactangle measurements it can be easily seen that water as the polar liquid gives a higher contact angle on the nonpolar dimethylester derivative and a lower angle on the polar glycol derivative. Vice versa is the situation with the diiodomethane. The properties of the side chains influence the properties of the polymer.

5.3.4. Crosslinking of the block copolymer

The illumination and the progress of the thiol-ene reaction were monitored by FT-IR-spectroscopy, as described in sections above. The micelles were diluted, the crosslinking agent and the photo initiator were added and the sample was equilibrated for 12 hours. The solutions were drop coated on CaF_2.

The thiol peak of the pentaerythritol tetra(3-mercaptopropionate) corresponds to the peak at 2567 cm^{-1} and is significant because in this region of the spectrum no other peaks are expected. The break-up of S-H bonding occurs very fast as seen in the experiments in thin film. After one minute of illumination the peak at 2567 cm^{-1} disappears completely.

The peaks of the double bonds are ambiguous since they overlap with other vibrations of the block copolymer and could not be used for monitoring the cross-linking reaction.
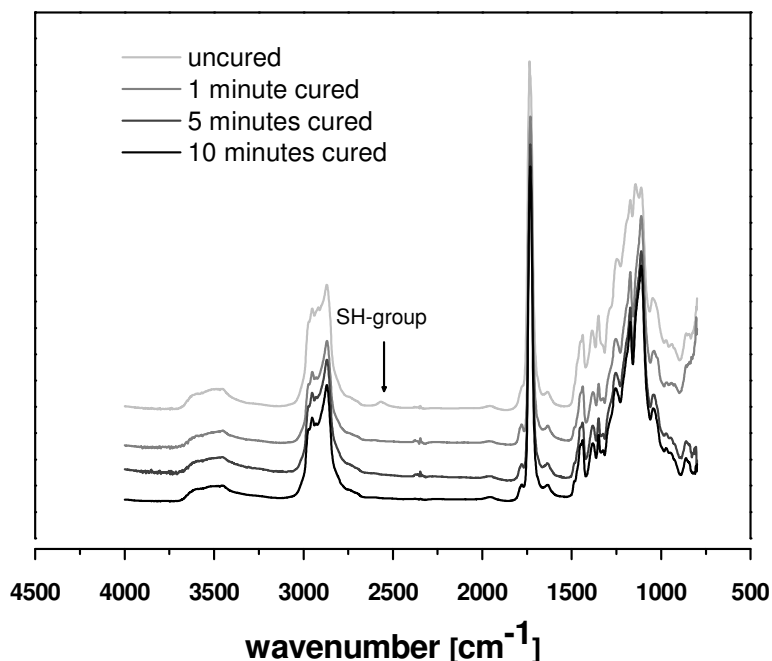
Fig 5-24: FT-IR spectra of the block-copolymers after various illumination times

As a consequence an indirect proof for successful crosslinking was chosen. The micellar solutions were prepared with additional crosslinking agent and photo initiator and after illumination of the sample and drying they were solved in an unselective solvent. In DLS measurements the effect of the treatment could be seen as in the results listed in section 5.3.5.1.

5.3.5. Detection of the micelles

5.3.5.1. Dynamic Light Scattering measurements

Dynamic light scattering (DLS) measurements were done after the dilution of the block copolymers in water in presence of the thiol and the photo initiator and equilibration for 12 hours. The measurements in water before illumination show the behavior of the micelles in water. The polynorbornene chosen forms micelles with an average diameter of 32.7 nm. Accordingly the samples have been illuminated. To verify the successful crosslinking reaction the water was evaporated and the residue

was solved in an unselective solvent (CH_2Cl_2). As expected there was no signal detectable in the non illuminated sample.

Table 2: Diameter of the micelles non illuminated and after various illumination durations in different solvents

Illumination duration	In water before illumination	In CH$_2$Cl$_2$	In water redispersed
0 min	32.7 nm	No signal	43.8 nm
1 min	-	32.7 and 106 nm	43.8 nm
5 min	-	78.8 nm	32.7 nm
10 min	-	78.8 nm	50.7 nm

The denoted values are the maxima of the distributions shown in the diagram below.
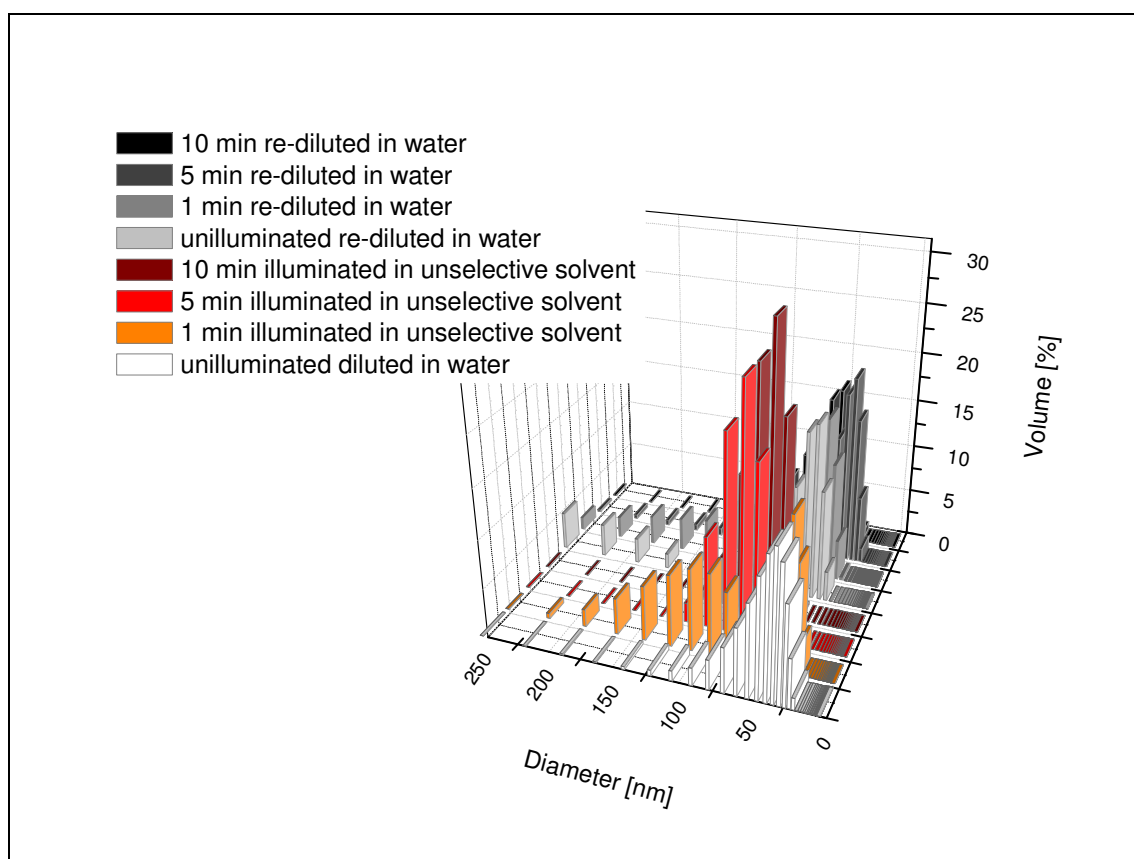
Fig 5-25: Graphic overview of diameters of the micelles in different solvents and various illumination times

As expected, the illuminated samples behave in a different manner than the untreated samples do. In fact it was possible to measure nano particles in the anticipated range, which was not possible for the untreated samples. It was expected

that the diameter will change in the unselective solvent because of the change of the polarity. The measured difference in diameter was Δ = 46.1 nm.

In the following the return to the initial solvent showed that on one hand the enlargement in CH₂Cl₂ was in fact only an effect caused by the polarity of the solvent and on the other hand that the illumination did not change the diameter of the micelles significantly. As well the untreated sample showed the micelle formation in water again.

5.3.5.2. Scanning Electron Microscopy measurements

For further investigations Scanning Electron Microscopy (SEM) measurements were done. It was necessary to pre-treat the samples by filtering the suspension (25 nm diameter) and sputtering the samples with gold and palladium.
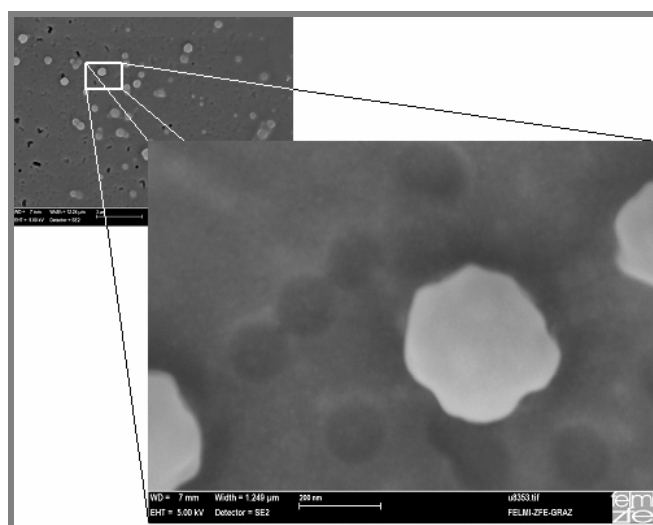
Fig 5-26: SEM picture of the micelles crosslinked in a ratio of 1:4 = thiol: double bond

In the picture above it is shown that the amphiphilic block-copolymers were successfully crosslinked. The diameter of the micelles shown is about 200 nm, thus larger as detected in the DLS measurements. This can be attributed to the pre-treating and the conditions in the ultra high vacuum or to the phenomenon called "super micelle". In the latter case the micelles aggregate and fuse in a slow step to build bigger micelles in various diameters. In the picture above it seem to be a narrow distribution. But in experiments with a high excess of crosslinking agent (PETMP) the size distribution of the micelles is broader. Some of the micelles seem to "start the fusion" in the moment the SEM picture was taken.
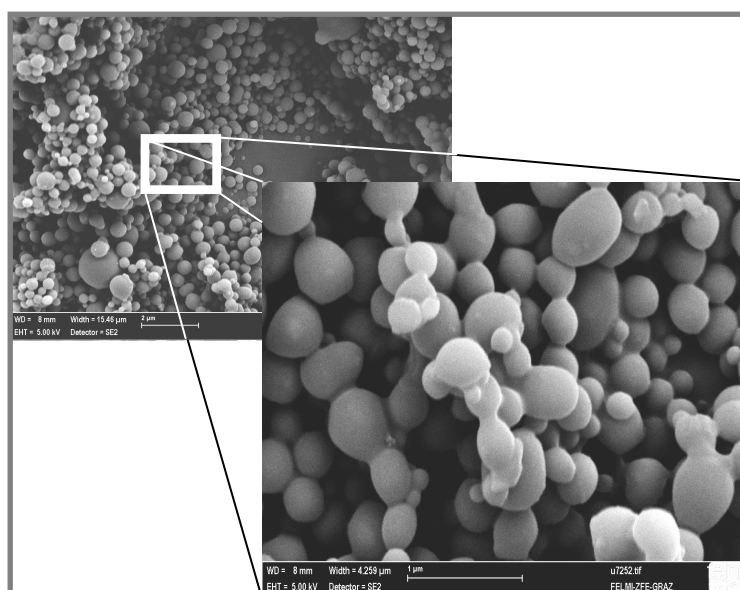
Fig 5-27: SEM picture of the micelles crosslinked in a ratio of 2:1 = thiol : double bond

A further explanation of this phenomenon could be the so called lower critical solution temperature effect, which is typical for polymers bearing oligo(ethyleneoxide) groups in the side chain.[86,87]

In this case, the polymer is dissolved at lower temperatures and precipitates at a certain temperature and above. This effect is entropy driven: at lower temperatures the water-soluble ethylene-oxide chains interact with the water molecules. At higher temperatures this interaction is not preferred anymore and the water-water hydrogen bonding is formed. The entropy is elevated and compensates the enthalpic effect of the new order and so the polymer precipitates.
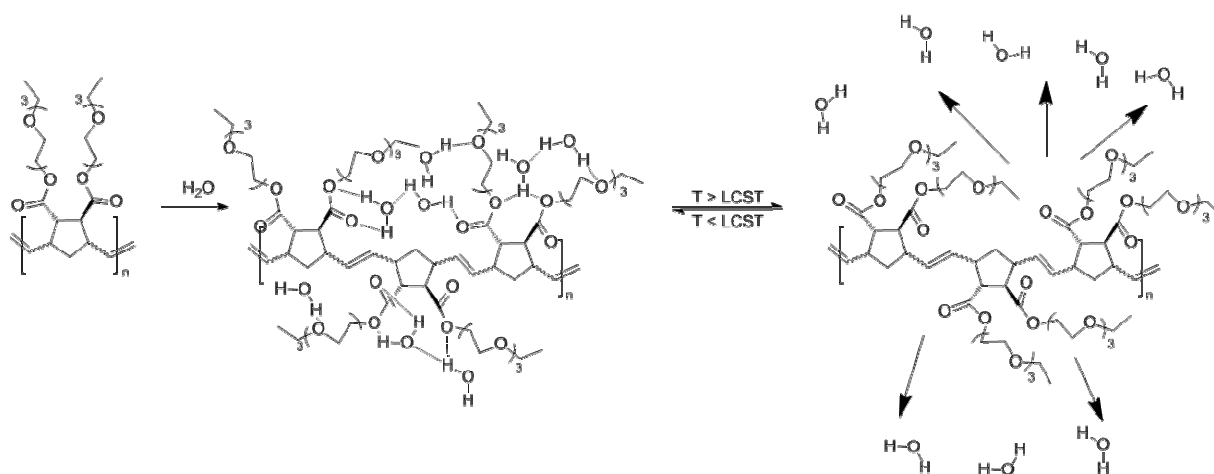
Fig 5-28: Lower critical solution temperature effect on polynorbornenes with oligo(ethyleneglycol) side chains [88]

[86] Lutz, J.-F. J. *Polym. Sci. Part A: Polym. Chem.* **2008**, *46,* 3459-3470.
[87] Smith, G. D.; Bedrov, D. J. *Phys. Chem.: Part B* **2003**, *107* (14), 3095-3097.

Keeping this effect in mind, a plausible argumentation is that due to the illumination and hence the resulting heat of this treatment, the temperature of the sample elevates above the LCST. From this point of view the collapsed cross-linked micelles are a consequence of the precipitation of the polymer.

5.4.   Conclusion

Herein, the synthesis and characterization of amphiphilic block copolymers by ROMP using functionalized norbornenes was presented. We showed the successful crosslinking of homo- and block-copolynorbornenes via the thiol-ene reaction. We proofed the ability of the double bonds of the polynorbornene-backbone to undergo this reaction. Moreover it is possible to use this system for lithographic applications. Furthermore it was demonstrated that the formed nano particles can be dispersed in an unselective solvent. We found a way to obtain micelles in the nanometer range with low synthetic effort. The photoreaction we chose is non-sensitive to ambient conditions and the setup of the experiment is simple and convenient.

5.5.   Acknowledgement

---

[88] Diplomarbeit, Thomas Bauer, *The Thermo Responsive Behaviour of Glycol Functionalized ROM Polymers*, University of Technology, **2008**.

6. Photochemical crosslinking of Polyoxazolines

Abstract

Polyoxazoline are an intensively studied kind of polymers. Because of their diversity and their fast production via microwave irradiation their applications are versatile. In this work we focus on copolymers of different oxazoline monomers and on special modifications to crosslink these polymers photo chemically. Therefore we synthesized 2-(3'-butenyl)-2-xazoline as counterpart for multifunctional thiols in the network building thiol-ene-reaction. Further 2-undecyl-2-oxazoline has been synthesized and co-polymerized with water-soluble 2-oxazolines. So amphiphilic polymers were generated, which form micelles in aqueous solutions.

6.1.　Introduction

Microwave assisted synthesis draw the attention to a broad variety of applications because of a significant acceleration, concomitant with an increased yield and an improved purity of the targeted product.[89,90,91] The influence of microwave irradiation on chemical reactions is of great interest in virtually every field of chemistry. In recent years also microwave assisted polymerizations were investigated.[92] In this chapter we focus on the living cationic ring-opening polymerization of 2-oxazolines. Since 1966[93,94] 2-oxazolines are intensively studied because of the large number of different substituted monomers available[95] and the potential applications. Wiesbrock et al.[96] published in 2005 a milestone for the polymerization of 2-ethyl-2-oxazoline: they decreased the reaction time from 6 h under standard conditions down to one minute under microwave irradiation which yields an acceleration factor of 400. In further experiments they could show this phenomenon not only for the 2-ethyl-2-oxazoline but also for other derivatives like 2-methyl, 2-nonyl and 2-phenyl-2-oxazoline with similar promising results.[89] Further investigations focused on the synthesis of di- and triblock copolymers. The applications of the copolymers are versatile: from drug delivery to surface modifications via thin films or polymers with lower critical solution temperature[97,98,99]. In this chapter we focus also on copolymers. First the synthesis of two monomers is shown than a statistical microwave assisted polymerization and finally a block copolymerization (as well microwave assisted).

The target of the polymerizations is to receive modified amphiphilic block-copolymers which can self-assembly in water and form micelles. The next step is a photochemical crosslinking step to preserve this special arrangement not only in

[89] Wiesbrock, F.; Hoogenboom, R., Leenen, M.A.M., Meier, M.A.R., Schubert, U.S., *Macromolecules* **2005**, *38*, 5025-5034.
[90] Adams, D., *Nature* (London) **2003**, *421*, 571-572.
[91] Kappe, C., Stadler A., *Microwaves in Organic Synthesis*; Loupy, A., Ed.; Wiley-VCH: Weinheim, Germany; **2002**; pp 405-433.
[92] Wiesbrock F. Hoogenboom, R.; Schubert, U. S, *Macromol. Rapid Commun.* **2004**, *25*, 1739-1765.
[93] Tomalia, D. A., J. Polym. Sci. 1966, 4, 2253–2265.
[94] Seelinger, W. Sheetz, D.P., *Angew. Chem.* **1966**, *5*, 875-888.
[95] Kempe, K., Lobert M., Hoogenboom, R., Schubert, U.S., *J. Comb. Chem.* **2009**, *11*, 274-280.
[96] Wiesbrock F., Hoogenboom, R., Abeln, C.H., Schubert, U.S., *Macromol. Rapid Commun* **2004**, *25*, 1895-1899.
[97] Hoeppener, S., Wiesbrock, F.; Hoogenboom, R.; Thijs, H. M. L.;. Schubert, U. S. *Macromol. Rapid Commun* **2006**, *27*, 405-411.
[98] Adams, N., Schubert, U. S., *Advanced Drug Delivery Reviews* **2007**, *59*, 1504-1520.
[99] Huber, S., Jordan, R., *Colloid Polym Sci* **2008**, *286*, 395-402.

water as solvent but also in unselective solvents.[100,101] As photochemical crosslinking reaction the thiol-ene reaction was chosen because of the tolerance versus oxygen and the flexibility: Virtually any double bond can react with the multifunctional thiol which is used as crosslinking agent.[102] The thiol-ene reaction has been already used in conjunction with polyoxazolines having a double bond in the side chain of the polymer as click chemistry for polyoxazolines.[103] Here, we introduce this reaction as tool for crosslinking the polymer.

6.2. Experimental

All chemicals used in the following were obtained from Sigma-Aldrich and used without further purification unless otherwise noted.

6.2.1. Monomer Synthesis

6.2.1.1. 2-(3'-Butenyl)-2-oxazoline[104]
6.2.1.1.1. N-Succinimidyl-4-pentenoate

16,36 mL 4-pentenoic acid were solved in 800 mL dichloromethane. Afterwards 29,39 g N-Hydroxysuccinimide and 39,62 g dicyclohexylcarbodiimide (DCC) were added. The solution was stirred at room temperature overnight. A milky white solution was obtained. After evaporating the solvent under vacuum the residual was extracted in a mixture of diethyl ether and distilled water (3:1 v/v). For a complete remove of the DCC the part of water was enhanced and sodium chloride was added stepwise. The organic phase was dried over sodium sulfate. The residual solvent was evaporated under vacuum.

30.85 g (0.156 mol) N-Succinimidyl-4-pentenoate were obtained as light yellow solid (98% of the theoretical yield).

[100] Binder, W., Gruber, H., *Macromol. Chem. Phys.* **2000**, *201*, 949-957.

[101] Huang, H., Hoogenboom, R., Leenen, M.A.M., Guillet, P., Jonas, A.M., Schubert, U.S., Gohy, J.-F., *J. Am. Chem. Soc.* **2006**, *128*, 3784–3788.

[102] Hoyle, C.E., Lee, T.Y., Rope, T., *Journal of Polymer Science Part A: Polymer Chemistry* **2004**, *42*, 5301-5338.

[103] Gress, A., Smarsly, B., Schlaad, H., *Macromol. Rapid Commun.* **2008**, *29*, 304-308.

[104] Gress A., Völkel, A., Schlaad, H., *Macromolecules* **2007**, *40* (22) 7928-7933.
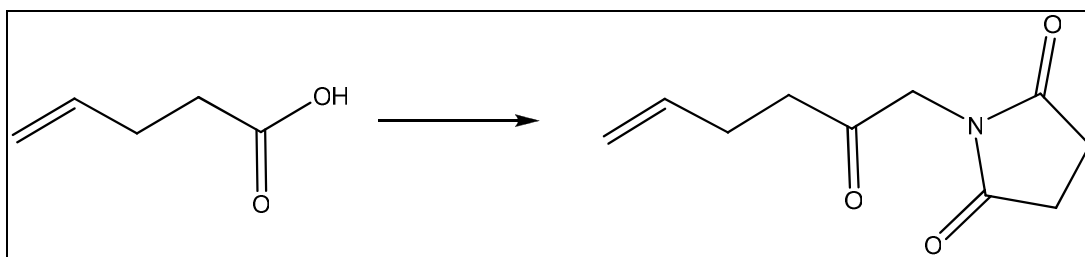
Fig 6-1: Reactionscheme of the synthesis of N-Succinimidyl-4-pentenoate
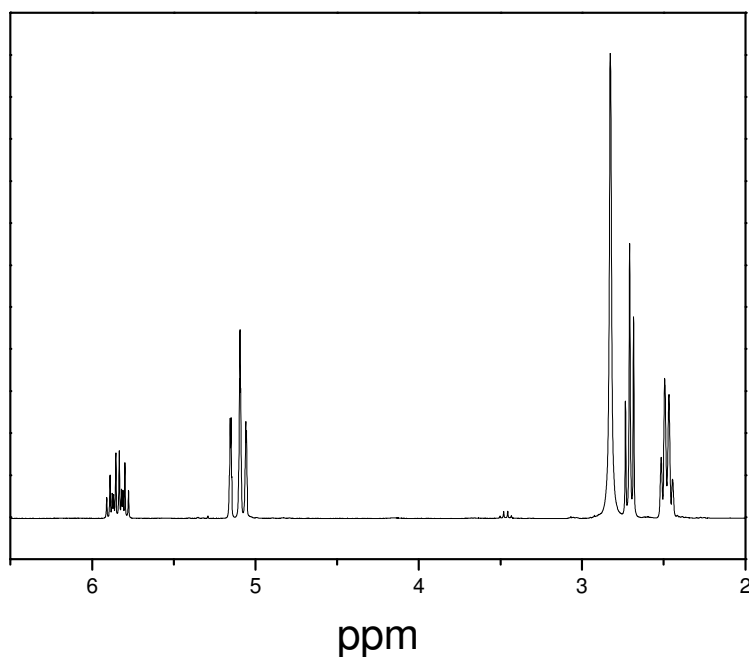
Fig 6-2: NMR-spectrum of N-Succinimidyl-4-pentenoate

^{1}H-NMR (δ, 20°C, CDCl$_3$, 300 MHz): 5.910-5.776 (m 1H, CH$_2$=CH-), 5.070 (t, 2H, CH_2=CH, ^{3}J$_{HH}$ = 11.738 Hz), 2.803 (s, 4H, -CH$_2$-CH$_2$-$_{succ.}$), 2.686 (t, 2H, C(=O)-CH_2, ^{3}J$_{HH}$ = 7.951), 2.515-2.445 (m 2H, =CH-CH_2-)

6.2.1.1.2. N-(2-Chlorethyl)-4-pentene amide

N-Succinimidyl-4-pentenoate (30.85 g) was dissolved in 800 mL dichloromethane. While stirring the solution a mixture of 36.29 g 2-Chlorethylamine hydrochloride and 12.55 g Sodium hydroxide in 300 mL of distilled water was added drop wise. The reaction solution consisted of two phases and was stirred at room temperature overnight. Afterwards the organic phase was separated and washed two times with distilled water and then dried over sodium sulfate. The solvent was now evaporated under vacuum. 23.00 g (0.156 mol) of N-(2-Chlorethyl)-4-pentene amide as light yellow liquid were obtained (100% of the theoretical yield).
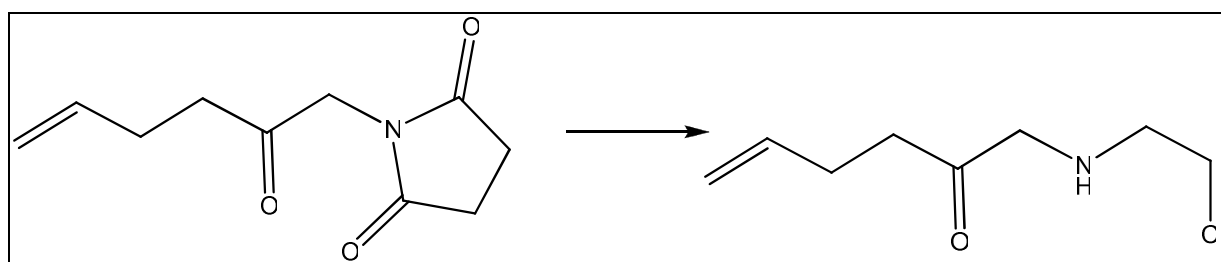
Fig 6-3: Reaction scheme of the synthesis of N-(2-Chlorethyl)-4-pentene
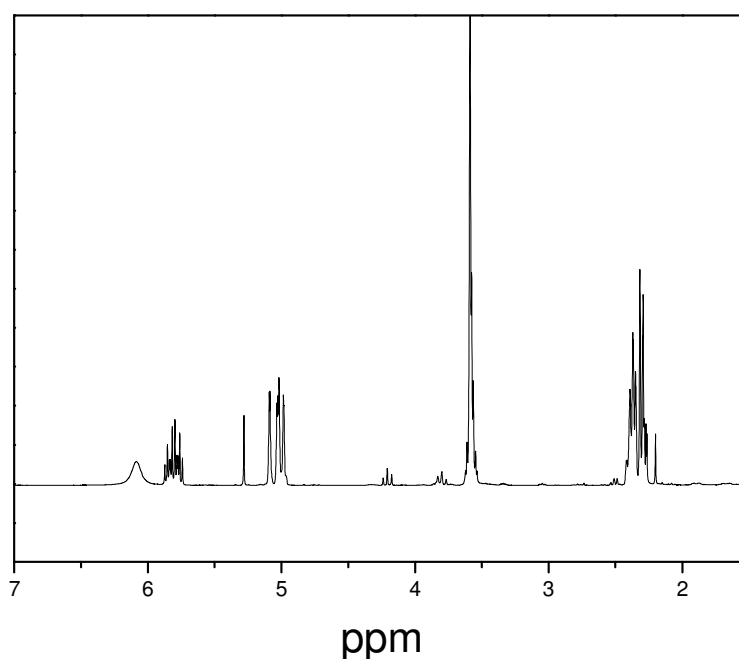
Fig 6-4: NMR spectrum of N-(2-Chlorethyl)-4-pentene

^{1}H-NMR (δ, 20 °C, CDCl$_3$, 300 MHz): 6.087 (s, 1H, NH), 6.087-5.743 (m, 1H, =CH-), 5.094-4.988 (m, 2H, CH$_2$=), 3.614-3.550 (m, 4H, NH-C$_2$$H_4$-Cl), 2.417-2.202 (m, 4H, -C$_2$$H_4$-(C=O)-)

6.2.1.1.3. 2-(3'-Butenyl)-2-oxazolin

In this reaction step it was necessary to work anhydrous and so the equipment was baked out before use and all steps were done inert atmosphere. To a solution of 23.00 g N-(2-Chloroethyl)-4-pentene amide in 100 mL dichloromehtane a mixture of 8.75 g potassium hydroxide in 75 mL dichloromethane was added drop wise. After 10 minutes a white precipitate of potassium chloride could be observed. The reaction

mixture was stirred overnight at 70°C. Afterwards the salt was filtered and the residual solution was concentrated to several mL. This mixture was now distilled under water-jet vacuum. At a bath temperature of 120°C and a head temperaute of 56°C the product evaporates abrupt. 10.51 g (0.084 mol) 2-(3'-Butenyl)-2-oxazolin were obtained after distillation as light yellow liquid (54% of the theoretical yield).

.
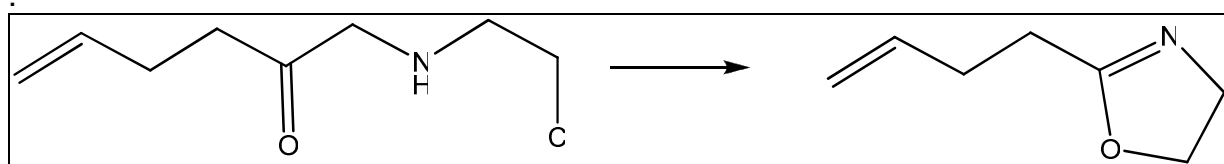
Fig 6-5: Reaction scheme of the synthesis of 2-(3'-Butenyl)-2-oxazolin
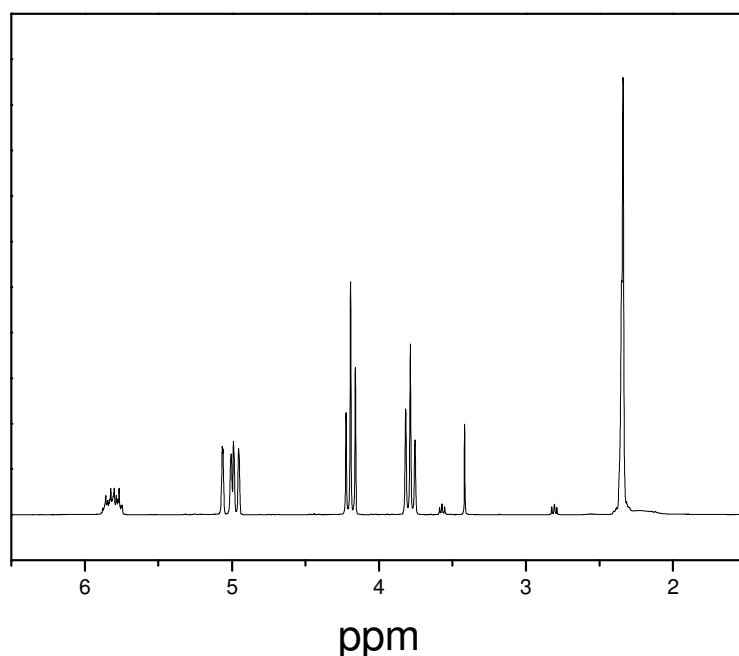
Fig 6-6: NMR spectum of 2-(3'-Butenyl)-2-oxazolin

^{1}H-NMR (δ, 20°C, CDCl$_3$, 300 MHz): 5.882-5.750 (m, 1H, CH$_2$=CH-), 5.070-4.959 (m, 2H, CH_2=), 4.196 (t, 2H, -O-CH_2-$_{oxaz.}$, ^{3}J$_{HH}$ = 9.844 Hz), 3.790 (t, 2H, CH_2-N=, ^{3}J$_{HH}$ = 9.466 Hz), 2.344 (s, 4H, C$_2$H$_4$-Oxaz.)

6.2.1.2. 2-Undecyl-2-oxazoline[95]

For the synthesis of 2-Undecyl-2-oxazoline 97 g (0.53 mol) of Dodencanenitrile was mixed with 32.29 mL (0.53 mol) Ethanolamine and 2.94 g (13.4 mmol) Zinc

acetate dehydrate and heated up to 180 °C under argon atmosphere. The reaction mixture was stirred at this temperature for 4 hours. Subsequently, the reaction mixture was cooled down to ambient temperature and 100 mL of dichloromethane was added. The organic phase was washed with water and with brine several times and dried over MgSO$_4$. After filtration and removing the solvent under reduced pressure the brownish yellow product was purified by distillation. Yield: 24.6 g (25.5 % of the theoretical yield).
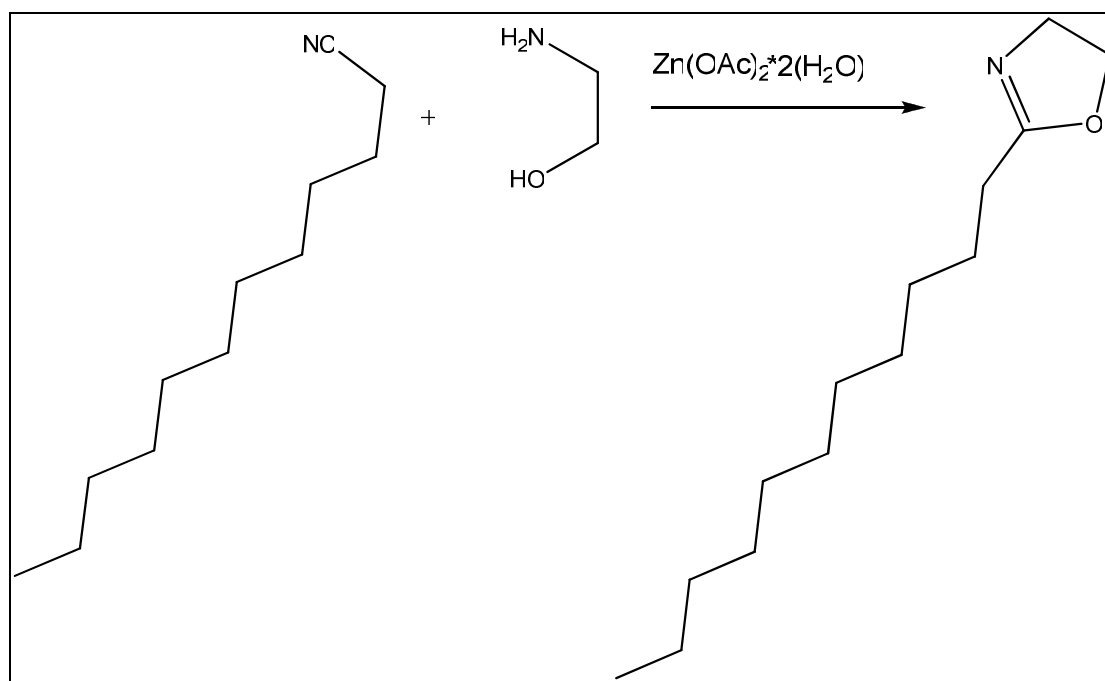
Fig 6-7: Reaction scheme of the synthesis of Undecyl-2-oxazoline
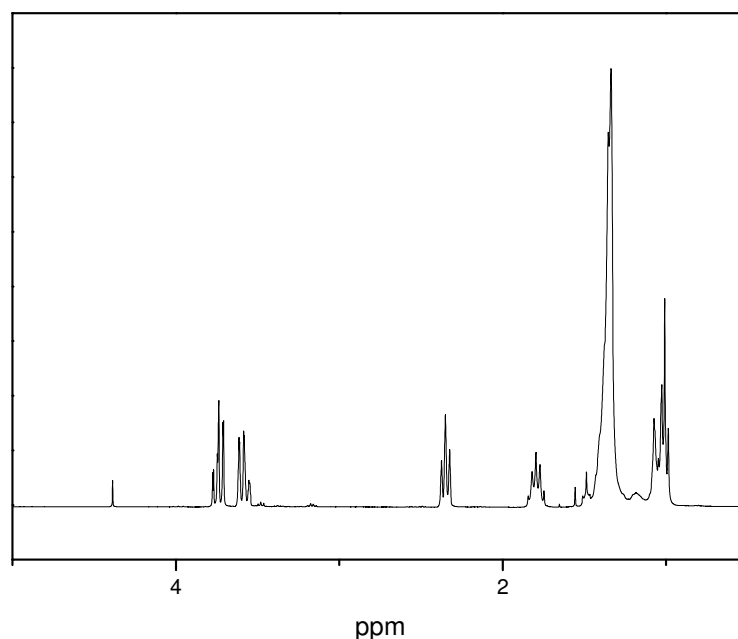
Fig 6-8: NMR spectrum of Undecyl-2-oxazoline

^{1}H-NMR (δ, 20°C, CDCl$_3$, 300 MHz): 3.742 (t, 2H, N-CH_2-$_{Oxaz.}$, ^{3}J$_{HH}$= 8.898 Hz), 3.589 (t, 2H,CH_2-O-$_{Oxaz.}$, ^{3}J$_{HH}$= 9.087 Hz), 2.354 (t, 2H, -CH_2-Oxaz., ^{3}J$_{HH}$= 7.573Hz), 1.750-1.848 (m, 2H, Oxaz.-CH$_2$-CH_2-), 1.341 (s, 16H, C$_8$H$_{16}$-CH$_3$), 1.012 (t, 3H, -CH_3, ^{3}J$_{HH}$= 6.815 Hz)

6.2.2. Microwave assisted polymerization

In general the microwave assisted polymerization of oxazolines was performed in dried dichloromethane and with methyl tosylate as initiator. The cationic ring opening polymerization starts with the formation of a cationic oxazolinium species. The C-O bond is weakened and propagation occurs by the nucleophilic attack of a second monomer.[105] The general polymerization process is shown in Fig 6-9 by using 2-Ethyl-2-oxazoline.

---

[105] Hoogenboom, R., Moore, B.C., Schubert, U.S., *Polymeric Materials: Schience & Engineering* **2005**, *93*, 894-895.
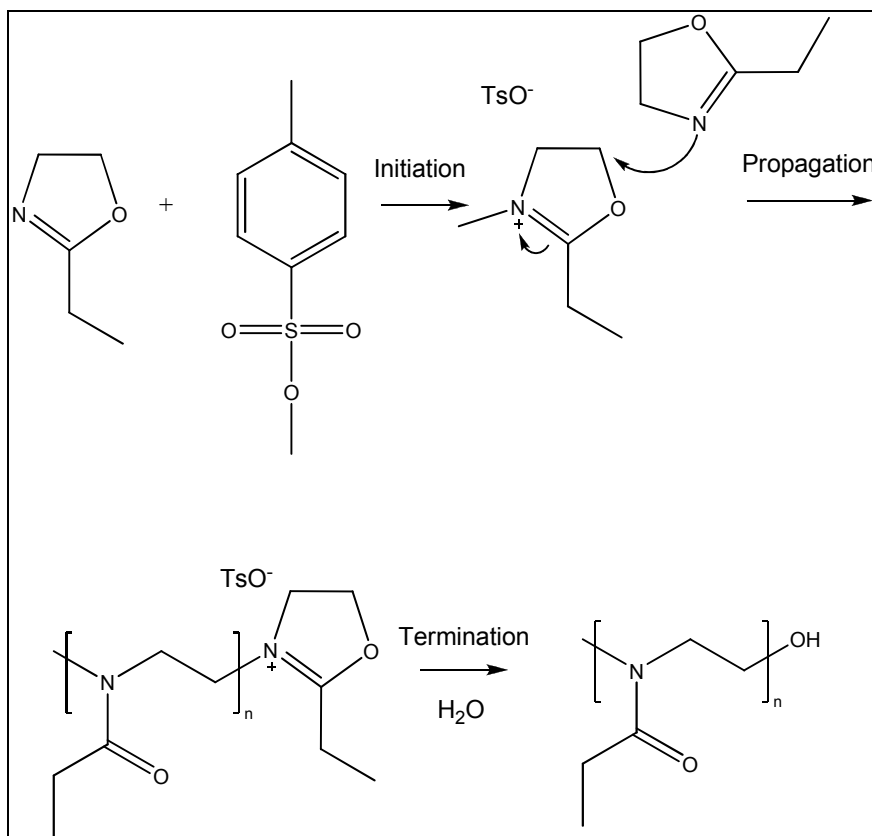
Fig 6-9: Scheme of the cationic ring opening polymerization of 2-Ethyl-2-oxalzoline

6.2.2.1. Copolymeristations
6.2.2.1.1. Statistical Copolymer

For copolymerisation 2.5 g (0.025 mol) of freshly distilled 2-Ethyl-2-oxazoline and 0.353 g (0.003 mol) 2-(3'-Butenyl)-2-oxazoline were dissolved in 7 mL dry dichloromethane under inert gas conditions. As initiator for the polymerisation 0.038 g (0.2 mmol) Methyltosylate were added. Due to these initial weights the the ratio of the polymer chains is 2-Ethyl-2-oxazoline : 2-(3'-Butenyl)-2-oxazoline = 9 :1 in a 4 molar solution. The polymerisation was carried out in a microwave oven (Biotage, Initiator Eight) at 140 °C for 20 minutes.
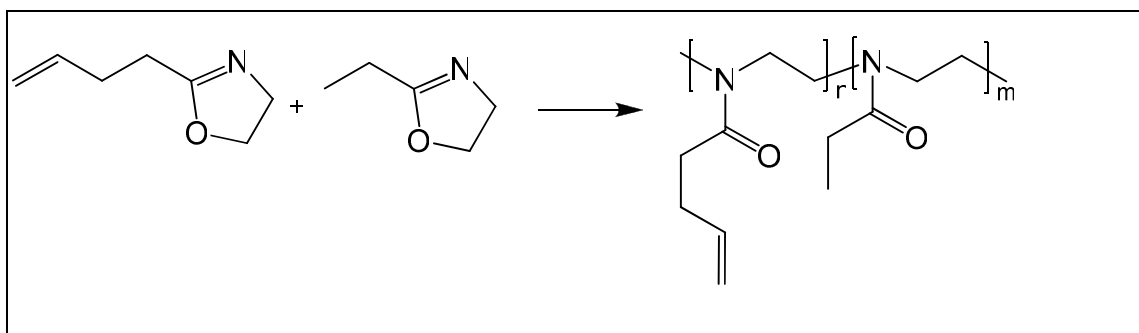
Fig 6-10: Scheme of the copolymerization of 2-Ethyl-2-oxazoline and 2-(3'-Butenyl)-2-oxazoline

After the polymerization the solvent was evaporated under vacuum and the liquid light yellow product was obtained.
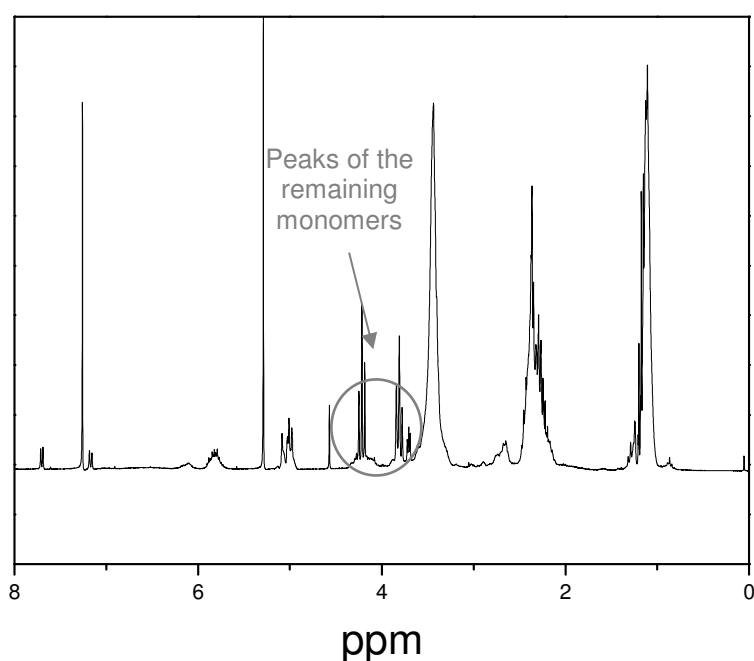
Fig 6-11: NMR spectrum of the statistical copolyoxazoline

^{1}H-NMR (δ, 20 °C, CDCl$_3$, 300 MHz): 1.200-1.108 (m, 3H, Methyl of Ethyloxa.), 2.479 – 2.145 (m, 2H, Methylene of Ethyloxa. and 4H of Methylene of Butenyloxa.), 3.691 – 3.289 (m, 8H of the backbone of the polymer), 5.980 – 5.290 (m, 1H, CH$_2$=CH- of Butenyloxa.), 5.090 – 4.980 (m, 2H, CH_2= of Butenyloxa.)

Out of this spectrum it could be seen that the ratio of the two used monomers in fact is not 9 : 1 like proposed but 8 : 1. Probably the 2-Ethyl-2-oxazoline monomer was not fully availible for polymerisation because of sidereactions during storage.

For the tri-co-polymer a statistical polymer like in 6.2.2.1.1 was synthesized in the ratio of 0.8 g (80 equivalents) of 2-Ethyl-2-oxazoline and 99.3 mg (10 equivalents) of 2-(3'-butenyl)-2-oxazoline. Afterwards 0.18 g (10 equivalents) of 2-Undecyl-2-oxazoline in 0.2 mL dry dichloromethane was added under inert gas conditions. The polymerization was done as before in a microwave oven at 140°C for 20 minutes.
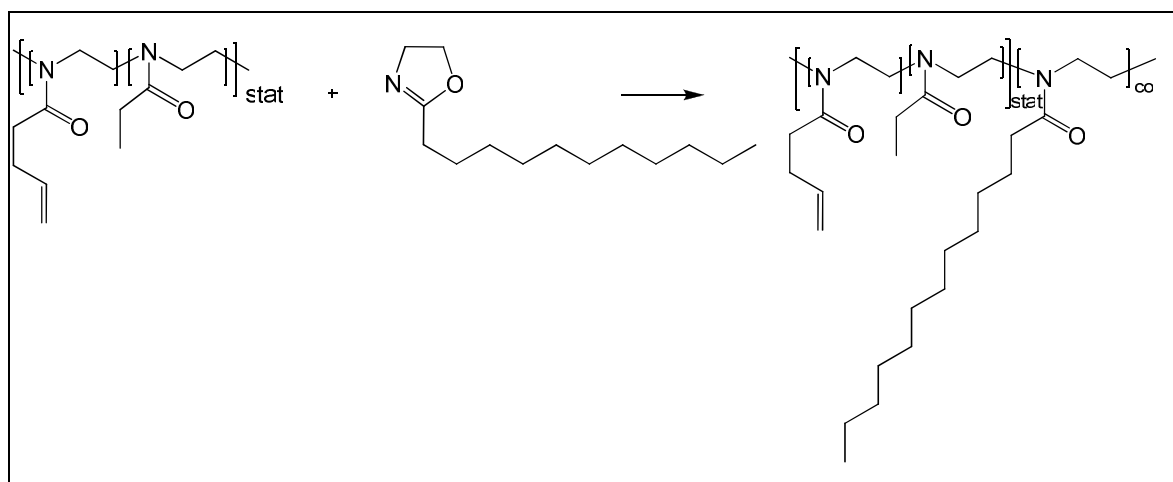
Fig 6-12: Scheme of the copolymerization of the statistical block-copolymer consisting of 2-Ethyl-2-oxazoline and 2-(3'-Butenyl)-2-oxazoline units with 2-Undecyl-2-oxazoline
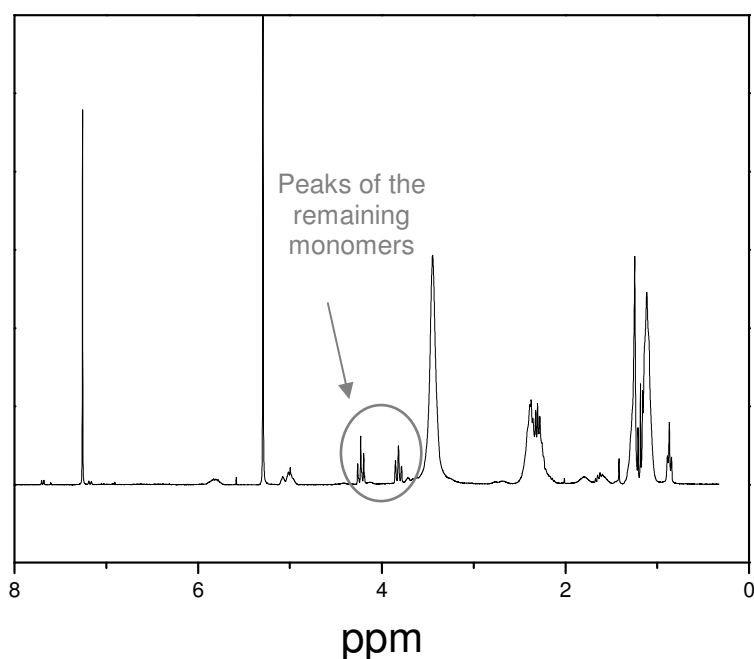
Fig 6-13: NMR spectrum of the block copolyoxazoline

^{1}H-NMR (δ, 20°C, CDCl$_3$, 300 MHz): 0.870 (t, 3H, ^{3}J$_{HH}$ = 7.951 Hz, Methyl of Undecyloxa.), 1.160-1.100 (m, 3H, Methyl of Ethyloxa.), 1.235 – 1.210 (m, 18H Methylene of Undecyloxa.), 2.386 – 2.149 (m, 2H, Methylene of Ethyloxa., 4H of Methylene of Butenyloxa. and 2H of Undecyloxa.), 3.820 – 3.204 (m, 12H of the backbone of the polymer), 5.093 – 4.969 (m, 2H, C*H$_2$*= of Butenyloxa.) 5.872 – 5.781 (m, 1H, CH$_2$=C*H-* of Butenyloxa.)

Also in this spectrum it could be seen that about ten equivalents of the 2-Ethyl-2-oxazoline did not react and stayed as monomer in the solution. The reason is presuambly the same as mentioned above.

6.2.3. Photochemical cross-linking

For cross-linking the thiol-ene reaction was chosen. Therefore 0.516 g (8.5 equivalents) of the statistical copolymer consisting of Ethyl-2-oxazoline and 2-(3'-Butenyl)-2-oxazolin in the ratio 9:1 were dissolves in dry dichloromethane. Afterwards 0.059 g (1 equivalent) Pentaerythrit-tetrakis-(3-mercapto-propionate) (PETMP) and 0.029 g (5 wt%) Lucirin TPO were added. This solution was spin coated on CaF$_2$ plates and subsequently the plates were illuminated with a medium-pressure mercury lamp for various irradiation times (0, 1, 2, 5, 10 minutes). FTIR-spectra of the samples were collected and afterwards the polymer layers were developed in dichloromethane for about 15 minutes. After drying another series of FTIR spectra of the samples were collected. From the difference in absorbance at the C=O band at 1637 cm^{-1} the residual film thickness was calculated.

6.3.   Results and discussion

6.3.1. Photochemical cross-linking

The statistical copolymers consisting of 2-(3'-Butenyl)-2-oxazoline and 2-Ethyl-2-oxazoline units and the effect of illumination of them were investigated with FTIR spectroscopy. In Fig 6-14 the spectra of the polymer before treatment, after illumination and after development are shown. The intensities of the developed sample are lower because of the lower concentration of the polymer on the CaF$_2$

plate after this washing step. In the untreated sample the peak at 912 cm^{-1} is presumably the end standing double bond of the side chain of 2-(3'-Butenyl)-2-oxazoline units which vanishes after illumination.
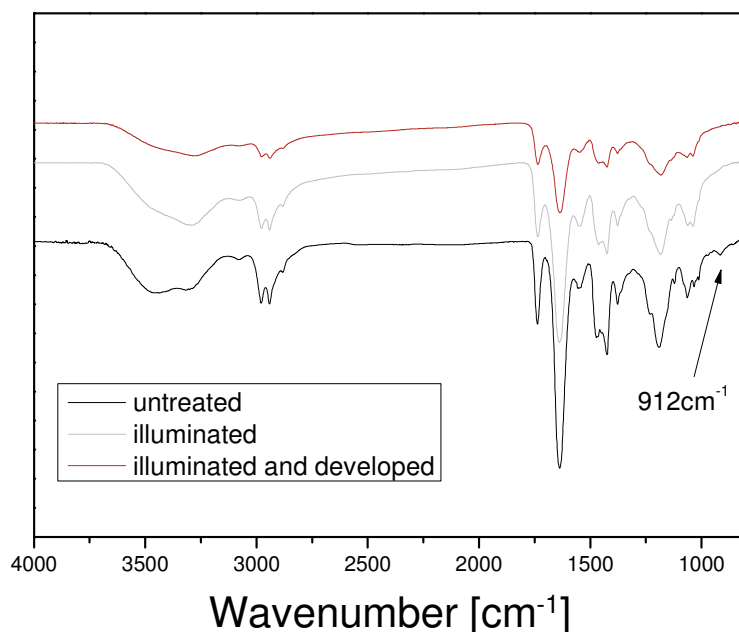
Fig 6-14: FTIR-spectra of the Copolymer of Butenyl- and Ethyloxazolin untreated, illuminated and developed

The determination of the soluble and gel fraction of this copolymer after various illumination times and various concentrations of cross-linker are shown in Fig 6-15. The photoreaction was carried out with one thiol unit per double bond available in the polymer chain and two thiol units per double bond. The higher concentration of cross-linker led to more than 60% gelfraction after two minutes and reached almost 70% after 10 minutes. The lower concentration seemed to be too diluted for high gel fractions. The maximum in this series were 45% gelfraction after 10 minutes illumination duration. It is probable that these results can be further improved with higher concentrations of 2-(3'-Butenyl)-2-oxazoline units in the polymer chain.
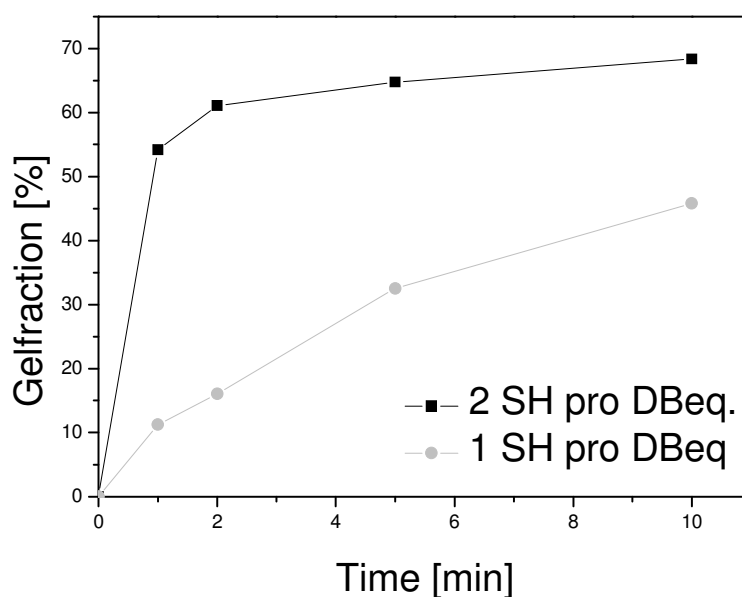
Fig 6-15: Gelfraction of crosslinked polymer with various concentration of the multifunctional thiol

6.3.2. Micellisation of the block-co-polymer:

Block-stat[poly(2-ethyl-2-oxazoline)-co-poly-2-(3'-butenyl-2-oxazoline)]-co-poly(2-undecyl-2-oxazoline) was solved in distilled water in a concentration of 5 mg/mL. After equilibration of 24 hours the amphiphilic polymer formed micelles as shown in Fig 6-17. The hydrophobic part of the block-copolymer built a core and the hydrophilic block the shell of the micelle in aqueous solution.

Hydrophilic 80 Units   Hydrophobic 10 Units
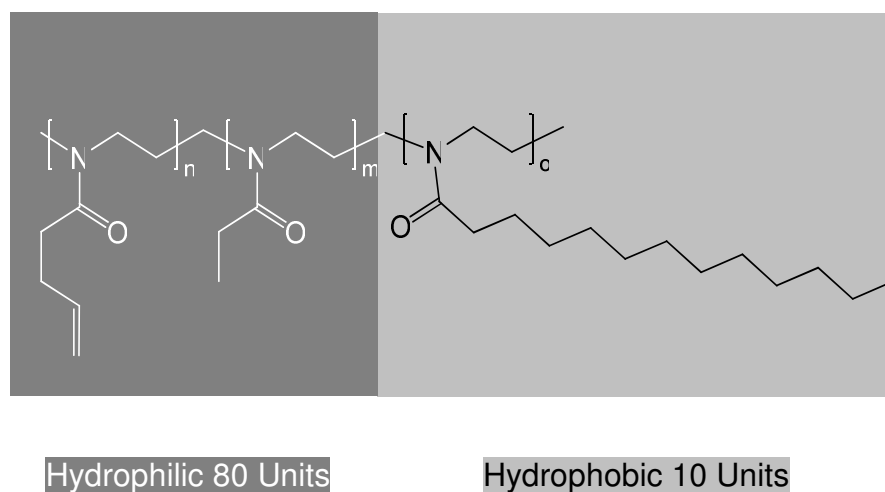
Fig 6-16: Amphiphilic copolymer with hydrophilic and hydrophobic blocks
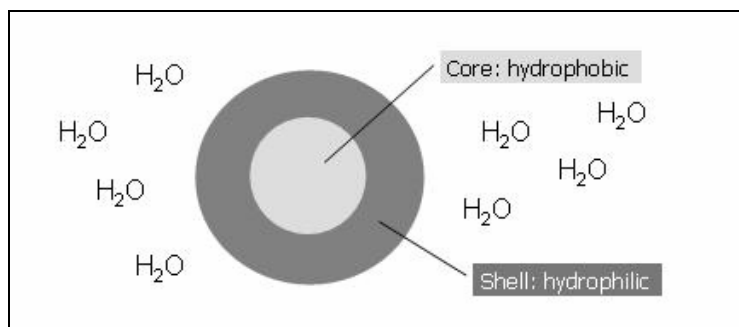
Fig 6-17: Micellformation of the copolymer in water

The aqueous solution was measured by dynamic light scattering (DLS) to determine the average diameter of the formed micelles. In Fig 6-18 it can be seen that the diameter of the bigger part of the particles was around 15 nm and for a small part a diameter of 35 nm was determined.
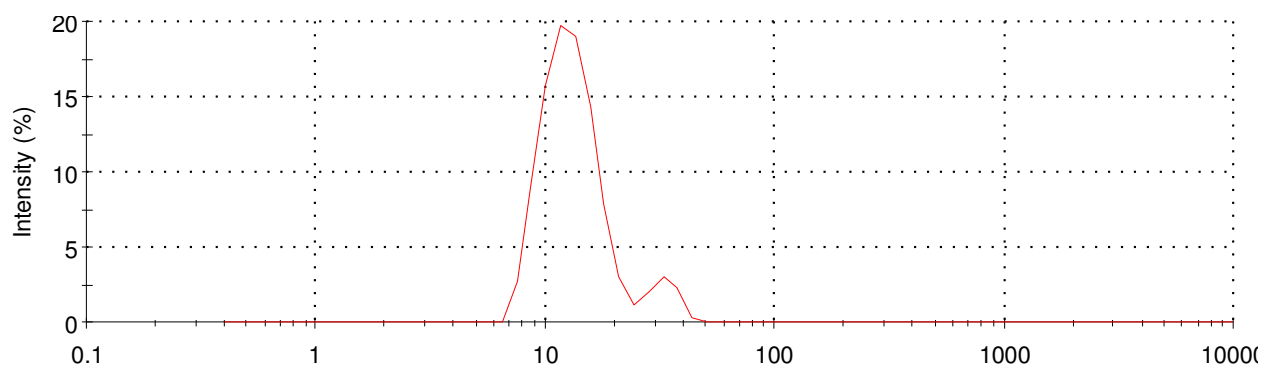
Fig 6-18: DLS measurement of the micelles formed

The crosslinking of the micelles like described in 6.3.1 was not successful until now. The main challenge is the combination of the crosslinker PETMP and the polymer. A method of resolution could be the mixing of the polymer with the crosslinking agent and the photo initiator before the micellisation step in water.

6.4. Conclusion

In this work we present the synthesis of oxazoline monomers and following copolymers. Not only the first approach to synthesise a polyoxazoline with crosslinkable goups in the side chain was successful but also the following

cross-linking step too. The gelfractions determined reached values up to 70 % with two thiol units per double bond.

The synthesis of Block-stat[poly(2-ethyl-2-oxazoline)-co-poly-2-(3'-butenyl-2-oxazoline)]-co-poly(2-undecyl-2-oxazoline) was effective. Micelles had been formed in water as solvent and the diameter was determined by DLS measurements. The crosslinking of the micelles was not carried out successful until jet.

6.5. Acknowledgement

7. Outlook

In this work photochemical crosslinking was used as tool to achieve different targets in various projects.

The successful crosslinking of polyethylene oxide with benzophenone leads to a material with enhanced mechanical properties and also as composite with the chosen ionic liquid and the conducting salt, this improvement was obtained without a decrease of the ion conductivity. The upper limit for the ratio of ionic liquid in this system (without losing mechanical stability) is not reached yet and consequently the ion conductivity of the composite. Furthermore, the compatibility of this electrolyte material with diverse electrode materials should be tested in half cells.

The photocrosslinking of short chain length polyhydroxy alkanoates opens up new applications for this class of polymers. The advantage of the cost effective and simple production of scl-PHAs and the biodegradability of these polyesters make them very attractive candidates for many applications. With a modification, which leads to higher flexibility and better mechanical properties, the spectrum of applications can be broadened further. Crosslinking either photochemical or thermal is a promising approach to achieve these targets, by reducing the crystallinity and enhancing the flexibility. The homopolymeres of polyhydroxy butyrates as well as the copolymers of hydroxyl butyrates and hydroxyl valerates have the potential to replace common polymers e.g. polyethylene or polypropylene.

The successful modification of the norbornene oligomers with thiols leads to many possibilities: modifications of polynorbornenes with monofunctional thiols are possible and also crosslinking with multifunctional thiols. The crosslinking of thin films as well as the crosslinking of self assembled structures, out of amphiphilic block-co-polymers were shown. The high variability of the polynorbornenes offer many applications itself. The new possibilities of modification via the thiol-ene reaction broaden this spectrum of applications even more.

The synthesis of oxazoline monomers and following the microwave assisted polymerization were a successful approach to synthesise amphiphilic block-co-

polymers. Also in this case the thiol-ene reaction was chosen for further modifications. The crosslinking step in thin films of these polymers is possible and can be optimised by varying the ratio of thiol groups and double bonds in this system. The crosslinking of the self assembled micelles should be possible but has to be improved by varying the crosslinking agent or the solvent in use.

8. Appendix

8.1.   List of figures

8.2. List of tables

8.3. Curriculum vitae

Date of birth	4. january 1982
Place of birth	Leoben

EDUCATION

Since 12.2006	dissertation at the Institute for Chemistry and Technology of Materials, University of Technology Graz Title: Photochemical cross-linking as tool for
tailoring	properties of polymers
03.10.2006	**2. Diploma exam**
12.2005 - 10.2006	diploma thesis at the Institute of Physical and Theoretical Chemistry, University of Technology Graz Title: One-electron-reductions of pharmacological active anthraquinone derivatives Grade: excellent
04.2005	**1. Diploma exam**
10.2000	Beginning to study technical chemistry at the University of Technology Graz

School career

2000	Matura at Bundesgymnasium Leoben II
1992 - 2000	BG/BRG Leoben II
1988 - 1992	Elementary school Leoben Stadt

CAREER PROGRESSION

Scientific employee

seit 01.2008	Junior researcher at the Polymer Competence Center Leoben (PCCL) in collaboration with the University of Technology Graz and the industrial partner AT&S
	Lab assistant within the framework of semester students
12.2006-12.2007	Junior researcher at the University of Technology Graz at the Institut for Chemistry and Technology of Materials, within the framework of the project of the European Union, called „Ionic Liquid Lithium BATTeries" (ILLIBATT)

Internships

07-09.2005	Internship at the Schering AG, Berlin at the department of chemical engineering and development
02.2004	Internship at the Institute of Organic Chemistry at the University of Technology Graz

8.4.   List of publications

Papers in peer reviewed journals

2009

Schmuck, M.; Balducci, A.; Rupp, B.; Kern, W.; Passerini, S.; Winter, M.:

Alloying of electrodeposited silicon with lithium-a principal study of applicability as anode material for lithium ion batteries. - in: Journal of solid state electrochemistry (2009)

Lux, S.; Schmuck, M.; Rupp, B.; Kern, W.; Appetecchi, G.; Passerini, S.; Winter, M.; Balducci, A.:

Mixtures of Ionic Liquids in Combination with Graphite Electrodes: The Role of Li-salts. - in: ECS transactions 16 (2009) 35, S. 45 – 49.

2008

Lev-Soldman, V.; Mester, B.; Ben-Aroya, N.; Hanoch, T.; Rupp, B.; Stanoeva, T.; Gescheidt-Demner, G.; Seger, R.; Koch, Y.; Weiner, L.; Fridkin, M.:
Conjugates of Gonadotropin Releasing Hormone (GnRH) with Carminic Acid: Synthesis, Generation of Reactive Oxygen Species (ROS) and Biological Evaluation. - in: Bioorganic & medicinal chemistry 16 (2008) 14, S. 6789 – 6798.

Balducci, A.; Schmuck, M.; Kern, W.; Rupp, B.; Passerini, S.; Winter, M.:
Ionic Liquids as Electrolyte in Lithium Ion Batteries: In Situ FTIRs Studies on the Use of Electrolyte Additives. - in: ECS transactions 11 (2008) 29 , S. 109 - 114

Rupp, B.; Schmuck, M.; Balducci, A.; Winter, M.; Kern, W.:
Polymer Electrolyte for Lithium Batteries based on Photochemically Crosslinked Poly(ethylene oxide) and Ionic Liquid. - in: European polymer journal (2008), S. 2986 – 2990.

Proceedings

2009

Rupp, B.; Bauer, T.; Slugovc, C.:
Thiol-ene reaction as tool for crosslinking of polynorbornene micelles in the nanoscale. - in: Proceeding of the International Society for Optical Engineering (2009), S. 73930Y0 - 73930Y9, Nanophotonic Materials ; 6

Oral presentations

2009

Hecke, A.; Kelly, A.; Kreutzwiesner, E.; Rupp, B.; Stelzer, F.; Wiesbrock, F.:
Microwave-Assisted Synthesis and Characterization of 2-Oxazoline-Based Hydrogels. - in: 11th Pacific Polymer Conference. Cairns am: 06.12.2009

2008

Wiesbrock, F.; Rupp, B.; Kreutzwiesner, E.; Stelzer, F.:

Poly(2-oxazoline)-based Hydrogels. - in: 3. Wiener Biomaterialsymposium. Wien am: 19.11.2008

2007

Balducci, A.; Schmuck, M.; Kern, W.; Rupp, B.; Winter, M.:

Ionic Liquids as electrolyte in lithium batteries: in situ FTIR studies on the use of electrolyte additives. - in: The Electrochemical Society, 212th Meeting. Washington am: 07.10.2007

Poster presentations

2009

Rupp, B.; Bauer, T.; Wiesbrock, F.; Slugovc, C.:

Thiol-ene Reactions as Tool for Crosslinking of Polymeric Micelles. - in: European Polymer Congress (epf'09). Graz am: 12.07.

Hecke, A.; Kreutzwiesner, E.; Rupp, B.; Stelzer, F.; Wiesbrock, F.:

Microwave-Assisted Synthesis and Characterization of 2-Oxazoline-Based Hydrogels. - in: European Polymer Congress EPF09. Graz, Austria am: 12.07.

Ebner, C.; Rupp, B.; Fasl, H.; Koller, M.; Braunegg, G.; Stelzer, F.; Wiesbrock, F.:

Injection Moulding of Short-Chain-Length Poly(hydroxyalkanoate)s. - in: 11th Pacific Polymer Conference. Cairns, Australien am: 06.12.

2008

Rupp, B.; Bauer, T.; Slugovc, C.:

Thiol-ene Reaction as Tool for UV-Induced Crosslinking of Ring Opening Metathesis Polymers. - in: XXII IUPAC Symposium on Photochemistry 2008. Goethenburg am: 28.07.

Rupp, B.; Schmuck, M.; Kern, W.:

PEO based polymer electrolytes for lithium ion batteries. - in: 1st Joint Austrian & Slovenian Polymer Meeting ASPM 2008 and 9th Austrian Polymer Meeting. Graz am: 26.03.

Rupp, B.; Bauer, T.; Slugovc, C.:

New Strategies of UV-Induced Crosslinking of Ring Opening Metathesis Blockcopolymers and Micelles. - in: 2nd European Chemistry Congress. Turin am: 16.09.

Schmuck, M.; Balducci, A.; Rupp, B.; Lux, S. F.; Passerini, S.; Winter, M.:

Alloying of Electrodeposited Silicon with Lithium for the use as Anode Material in Lithium Ion Batteries. - in: 9th ABA, Advanced Batteries and Accumulators. Brno am: 29.06.

2006

Rupp, B.; Gescheidt-Demner, G.; Weiner, . L.:

Peptide-bonded anthraquinone derivatives – one-electron reductions. - in: 1st European Chemistry Congress. Budapest, Ungarn am: 27.07.